

POLITECNICO DI TORINO

Corso di Laurea magistrale in Ingegneria Energetica

Innovazione nella Produzione di Energia

Tesi di Laurea Magistrale

**Decarbonisation of an industrial plant
in the food sector**



Supervisor

Pierluigi Leone

Candidate

Paola Mattioli

A.A. 2017/2018

“Look wide, and even when you think you are looking wide - look wider still.”

Robert Baden-Powell

Abstract

Focusing on GHG emission reduction in the industrial sector, until now several steps have been taken by concentrating on process efficiency, thermal recovery from waste, cutting energy losses. However, in order to reach more significant results in fighting climate change, a new approach to the problem is needed.

The present analysis tries to answer the need to find solutions that apply to industrial realities and help to reach the target of emission reduction. Thus, a decarbonization pathway has been structured for an industrial plant in the food sector that includes a series of actions to be implemented both in the short and medium-long term with a view to minimizing the environmental impact of energy supply.

The key points of this study are:

- a technological scouting of applications aimed at reducing carbon dioxide emissions associated with energy supply in industrial food sector;
- a study technical feasibility for the installation of such applications, emphasizing critical issues linked to the operational aspects and the production activity of the plant;
- an economic evaluation of the investments including considerations on commodities and CO₂ allowances price scenarios as well as possible incentives related to the interventions.

Nell'ambito della riduzione delle emissioni di gas serra nel settore industriale, varie azioni sono state finora realizzate con un particolare focus sull'aumento dell'efficienza di processo, il recupero termico e l'eliminazione delle perdite energetiche. Tuttavia, per raggiungere maggiori risultati nella lotta al cambiamento climatico, è necessario un nuovo approccio al problema.

La presente analisi cerca di rispondere all'esigenza di soluzioni per supportare le realtà industriali nel loro percorso volto alla riduzione delle emissioni. Pertanto, considerando il caso concreto di uno stabilimento nel settore alimentare, è stato strutturato un percorso di de-carbonizzazione che include una serie di azioni da attuare sia a breve che a medio-lungo termine, nell'ottica di minimizzare l'impatto ambientale correlato all'approvvigionamento energetico.

I punti chiave di questo studio sono:

- scouting tecnologico di applicazioni volte a ridurre le emissioni di anidride carbonica legate all'approvvigionamento energetico di stabilimento;
- studio di fattibilità tecnica relativo all'installazione di tali applicazioni;
- valutazione economica degli investimenti, comprese considerazioni sugli scenari dei prezzi delle commodities, delle quote di CO₂ ed eventuali incentivi relativi agli interventi.

Sommario

Chapter I: Introduction	11
1.1 Climate change as a GHG emission concentration rise consequence	11
1.2 Mitigation pathways	15
1.3 Regulatory framework.....	16
1.4 EU Emission Trading System and white certificates market.....	17
1.4.1 Phase 1 (2005-2007)	19
1.4.2 Phase 2 (2008-2012)	19
1.4.3 Phase 3 (2013-2020)	19
1.4.4 Phase 4 (2021-2030)	19
1.5 Energy efficiency and white certificates	20
1.6 CO ₂ price.....	20
1.7 Italian energy framework.....	22
1.8 Industrial sector as main actor in fighting climate change.....	22
Chapter II: Case study description.....	24
2.1 Productive processes: pasta processing	24
2.2 Industrial Plant Energy requirements.....	26
2.2.1 Thermal needs.....	26
2.2.2 Electric Energy needs	28
2.3 Today plant emissions	29
Chapter III: Technological scouting.....	31
3.1 Thermal Energy from RES.....	31
3.1.1 Solar Collectors	33
3.1.2 Solar Thermal concentrator.....	35
3.2 Electric Energy from RES.....	37
3.2.1 PV technology	39
3.3 Waste to Energy	42
3.3.1 Biogas in boiler.....	46
3.3.2 Biogas in ICE CHP	46
3.3.3 Biogas in SOFC CHP	48
3.3.4 Biogas Upgrading	50
3.4 Power and Waste to Fuel.....	53
3.5 Shifting Thermal towards Electric	56
3.4.1 Heat Pumps for thermal recovery	56
3.4.2 Electro-heat technologies	61

3.6 Carbon Capture and Utilization.....	65
3.6.1 POST COMBUSTION	66
3.6.2 PRE-COMBUSTION CC.....	67
3.6.3 OXY-FUEL COMBUSTION CC.....	68
3.6.4 Separation technologies	69
3.6.5 Comparison of different combustion technologies for CO ₂ capture.....	71
3.6.6 CO ₂ utilization	72
Chapter IV: Economics and technical results	74
4.1 Price assumptions	74
4.2 Discriminating Indexes.....	74
4.2.1 LCOC.....	74
4.2.2 Unit price per ton of CO ₂	75
4.2.3 Payback time	76
4.3 Results for the individual solutions.....	77
4.3.1 Thermal Energy from RES.....	77
4.3.2 Electric energy from RES	82
4.3.3 Waste to Energy.....	85
4.3.4 Power and Waste to Fuel	95
4.3.5 Shifting Thermal towards electric.....	99
4.3.6 Carbon Capture	105
Chapter V: Optimal combinations and sensitivity analysis.....	108
5.1 Today optimal combination.....	108
5.1.1 Selection criteria.....	108
5.1.2 Survey of results	110
5.1.3 Best decarbonized-scenario.....	112
5.1.4 Alternative combinations.....	114
5.2 Future scenarios and sensitivity analysis	117
5.2.1 Uniform increase in prices	117
5.2.2 Uniform decrease in prices	118
5.2.3 CO ₂ price increase	118
Chapter VI: Conclusions.....	121
Bibliography	122

List of figures

Figure 1: average Annual Global Temperature anomaly relative to 1901-2000.....	11
Figure 2: CO ₂ atmospheric concentration based on NOAA ESR DATA	12
Figure 3: Annual mole fraction increase based on NOAA ESR DATA.....	13
Figure 4: GHG Emission Pathways 2000-2100: All AR5 Scenarios.....	15
Figure 5: Key technologies for reducing CO ₂ emissions under the BLUE Map scenario ..	16
Figure 6: Historical trend of volumes and prices of the first chained annual futures (Dec-AA) of EUA and CER on ICE. Period from April 2005 to September 2018.....	21
Figure 7: Performance of EUA prices on the primary market in the first three trimesters of 2018.....	21
Figure 8: Total share of gross final consumption covered by RES.....	22
Figure 9: Greenhouse gas emissions by economic sectors [7]	23
Figure 10: Main steps in pasta production [22]	25
Figure 11: Plant thermal needs.....	27
Figure 12: yearly profile of thermal power for high temperature final uses.....	27
Figure 13: yearly profile of thermal power for 80° C final uses.....	28
Figure 14: Plant electrical needs	28
Figure 15: electric power profile.....	29
Figure 16: Heat Consumption per sector [TJ] from IEA[26].....	31
Figure 17: Heat requirements by temperature range in different industry sectors.....	32
Figure 18: Solar collectors and working temperatures for different applications [25] ..	33
Figure 19: Flat Plate Solar collector structure	34
Figure 20: Collector efficiency.....	35
Figure 21: CSP technology families	36
Figure 22: Linear Fresnel Reflector.....	37
Figure 23: 2017 National mix for the production of electricity in Italy	37
Figure 24: Global cumulative growth of PV capacity.....	38
Figure 25: Structure of a PV panel.....	39
Figure 26: PV system losses	41
Figure 27: process of organic matter degradation during anaerobic digestion	42
Figure 28: Theoretical analysis of AD technology	43
Figure 29: Evolution of primary energy biogas production in the EU[33]	44
Figure 30: biogas utilization pathways.....	45

Figure 31: comparison between traditional power plant and CHP system.....	46
Figure 32: CHP internal combustion engine	47
Figure 33: datasheet for the model JMS612_J612, General Electric [34].....	47
Figure 34: CH ₄ SOFC schematic functioning	49
Figure 35: SOFC based CHP	49
Figure 36: SOFC example datasheet [35]	50
Figure 37: biomethane production [36].....	50
Figure 38: biogas upgrading process and possible utilization pathways.....	51
Figure 39: Cost for biogas upgrading for methane [37]	53
Figure 40: Power and Waste to Fuel scheme[38]	54
Figure 41: Power and Waste to Fuel main steps.....	55
Figure 42: schematic demonstration of Methanation system based on a real project[38]	55
Figure 43: Simple Schematic of Mechanically Driven Heat Pump [39].....	57
Figure 44: Technical market potential of process heat in Europe accessible with industrial heat pumps distributed by temperature and industrial sector [31]	58
Figure 45: Commercially available industrial HTHPs sorted by maximum heat sink temperature [40]	59
Figure 46: Schematic diagram of an Open Cycle Mechanical HP	60
Figure 47: COP curve.....	61
Figure 48: Carbon Capture different pathways	65
Figure 49: schematic representation of post- combustion CC [43]	66
Figure 50: absorption process [43]	67
Figure 51: schematic representation of pre-combustion CC [43]	68
Figure 52: schematic representation of oxy-combustion CC [35].....	69
Figure 53: Carbon capture and Utilisation	73
Figure 54: TVP Solar MT-Power Specifications.....	77
Figure 55: Thermal Energy produced	78
Figure 56: Technical data of CS6K Canadian panel [51]	82
Figure 57: Average daily solar Irradiance	83
Figure 58: schematic representation of an AD system example.....	85
Figure 59: thermal load duration curve	92
Figure 60: electric load duration curve.....	92

Figure 61: one stage Heat Pump configuration100

Figure 62: Heat Pump performance [56]101

Figure 63: two stage Heat Pump configuration.....103

Figure 64: solutions ordered with ascending cost per ton of CO₂ avoided.....109

Figure 65: Technical solutions ordered with ascending PB110

Figure 66: Cumulative of CAPEX for the optimal configuration.....113

Figure 67: Saving and emission reduction potential of the best decarbonization pathway
.....113

Figure 68: second decarbonization pathway.....116

Figure 69: Saving and emission reduction potential of the best decarbonization pathway
.....116

Figure 70: CO₂ trend according to ENGIE forecast.....119

Figure 71: extended EU ETS trend from ENGIE forecast.....119

List of tables

Table 1: GHG properties	13
Table 2: Plant energy needs	26
Table 3: Plant emissions to date	30
Table 4: flowrate and mass composition of waste streams	44
Table 5: Electro-Heat technologies.....	62
Table 6: Comparison of different separation technologies	70
Table 7: Advantages and disadvantages of the different CO ₂ capture technologies	71
Table 8: Cost comparison for different capture processes. Costs include CO ₂ compression to 110 bar but excluding storage and transportation costs.....	72
Table 9: economic data for solar collectors	79
Table 10: CSP example	79
Table 11: Solar Energy on a horizontal plane	80
Table 12: economics of CSP	80
Table 13: costs and savings for Thermal Energy from RES Technology.....	81
Table 14: Thermal energy from RES indexes	82
Table 15: Monthly Solar Energy	84
Table 16: economics of a PV plant.....	84
Table 17: costs and savings for Electric Energy from RES Technology	84
Table 18: Electric energy from RES indexes	85
Table 19: Anaerobic Digestion system investment costs	86
Table 20: biogas cost.....	86
Table 21: costs and savings for Biogas in Boiler case	87
Table 22: J620 data [53]	88
Table 23: J612 data [34]	88
Table 24: CAPEX for biogas in ICE CHP.....	88
Table 25: costs and savings for Biogas in ICE CHP case	89
Table 26: C60 Datasheet.....	90
Table 27: costs and savings for Biogas in SOFC CHP case	91
Table 28: CHP data from datasheet.....	92
Table 29: CAPEX of biogas upgrading	93
Table 30: 15 MW CHP scenario.....	93

Table 31: OPEX of biomethane in CHP scenario.....	94
Table 32: costs and savings for Biogas Upgrading case	95
Table 33: Waste to Energy indexes	95
Table 34: Power and Waste to Fuel dimensioning.....	95
Table 35: Electrolyser efficiency	96
Table 36: Synthetic CH ₄ production	96
Table 37: CH ₄ on-site production.....	96
Table 38: Power and Waste to Fuel OPEX	98
Table 39: costs and savings for Power and Waste to Fuel case.....	99
Table 40: Power and Waste to Fuel indexes	99
Table 41: 90°C simulation results.....	102
Table 42: 160°C simulation results	104
Table 43: costs and savings for Shifting Thermal to Electricity Technologies.....	104
Table 44: Shifting Thermal towards Electric indexes	105
Table 45: Carbon Capture results	107
Table 46: costs and savings for Carbon Capture	107
Table 47: Carbon Capture indexes.....	107
Table 48: cost per ton of CO ₂ avoided	108
Table 49: Technical solutions ordered with ascending PB.....	109
Table 50: optimal decarbonization pathway results.....	112
Table 51: Best decarbonized scenario.....	114
Table 52: second decarbonization pathway results	115
Table 53: second decarbonized scenario	117
Table 54: Third decarbonized scenario	117
Table 55: +20% scenario	118
Table 56: -20% scenario.....	118
Table 57: 2022 and 2040 scenario according to Engie's forecast for CO ₂	119

Chapter I: Introduction

1.1 Climate change as a GHG emission concentration rise consequence

In the last decades the average global temperature across land and ocean surface areas has been rising year by year, reaching in 2017 a value of 0.84°C above the 20th century average of 13.9°C, according to the *Global Climate Report for Annual 2017* [1]. The same report also states that since 1880 the yearly global land and ocean temperature has increased at an average rate of 0.07°C per decade. However, the rate of increase has doubled starting from 1980.

In the following graph (Figure 1: average Annual Global Temperature anomaly relative to 1901-2000), built on NOAA Global Time Series [2], the average annual temperature anomaly is shown, relative to a common 1901-2000 base period.

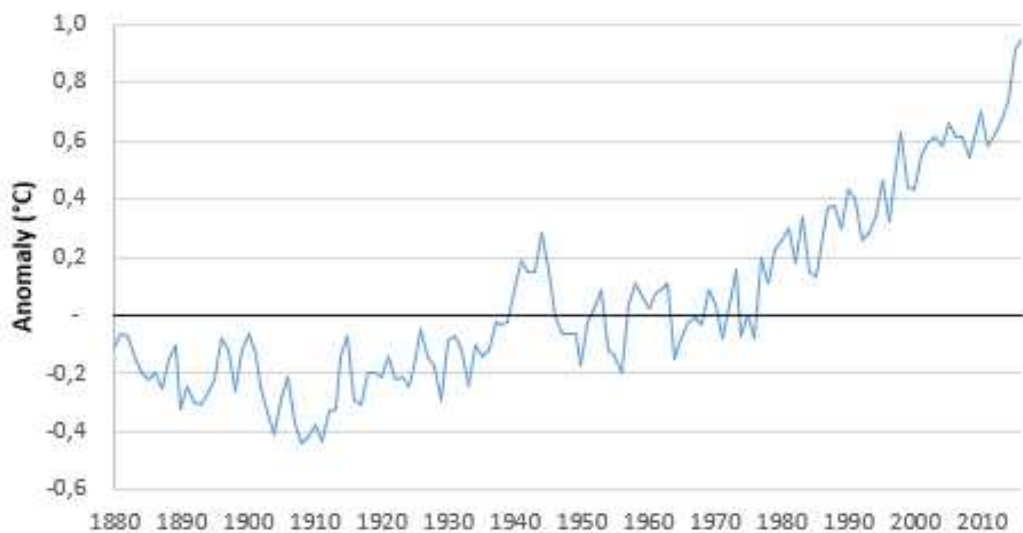


Figure 1: average Annual Global Temperature anomaly relative to 1901-2000

This temperature rise phenomenon, the so-called Global Warming, has been recognized by the scientific world as associated to the Greenhouse Gases (GHG) emissions increase. The presence of a high concentration of these gases in atmosphere has a negative impact on Earth's average temperature, trapping the sun's heat and therefore modifying the Earth temperature to restore planetary energy balance.

Many of the GHG gases, considered responsible for the Climate Change, are naturally present in atmosphere. By absorbing the infrared energy radiated from the Earth and radiating it back to the Earth surface, they made life on Earth possible. Without this natural greenhouse effect, Earth's average annual temperature would be around -18°C, instead of close to 15°C. However human activity associated to the burning of fossil fuels, the clearing of land for agriculture, industry, and other human activities has rapidly increased their concentrations.

If no limits were set, temperature rise would produce an important climate change, involving dramatic consequences in the global environment and socio-economic

prosperity. As a result, the international community has recognized the risks associated to this scenario imposing the threshold limit of increase of 2°C above the temperature in pre-industrial times.

The main gases that contribute to the greenhouse effect are: water vapor, carbon dioxide (CO₂), methane (CH₄), nitrous oxide (N₂O), chlorofluorocarbons (CFCs). CFCs have a stronger effect in heat absorption, because of their chemical properties.

However, the imposed limit on GHG concentration to cut down Global warming mainly focuses on CO₂ emissions reduction. This is due to the fact that carbon dioxide is the gas produced to a greater extent by human activities, being responsible for 64% of man-made global warming. In fact, even if it is released through natural processes such as respiration and volcano eruptions, a great increase in CO₂ atmospheric concentration occurs as a result of deforestation, land use changes, and massive fossil fuel burning.

According to the *State of the Climate in 2017* [3] from NOAA and the American Meteorological Society, global atmospheric carbon dioxide was 405.0 ppm in 2017, 60% higher than 1990 levels (the reference year for the Kyoto Protocol), as in Figure 2: CO₂ atmospheric concentration based on NOAA ESR DATA.

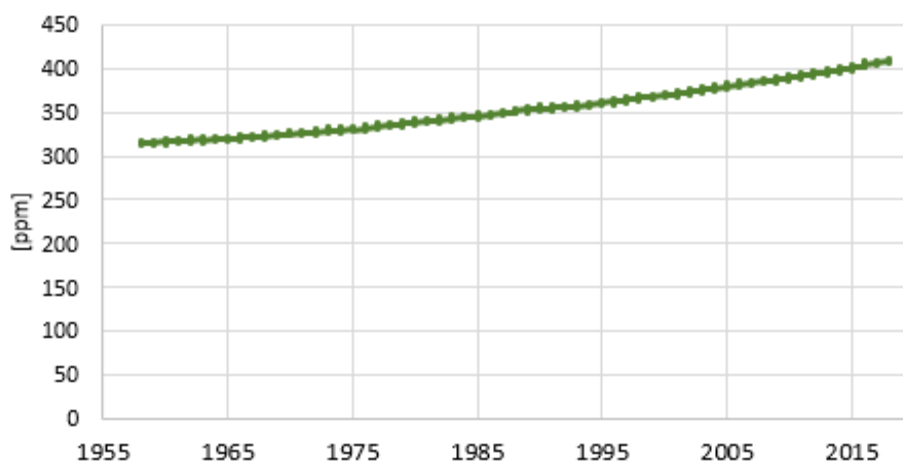


Figure 2: CO₂ atmospheric concentration based on NOAA ESR DATA

Moreover, the annual rate of increase in CO₂ concentration over the past 6 decades is about 100 times faster than previous natural increases. CO₂ atmospheric concentration in the last 60 years is shown in Figure 3: Annual mole fraction increase based on NOAA ESR DATA

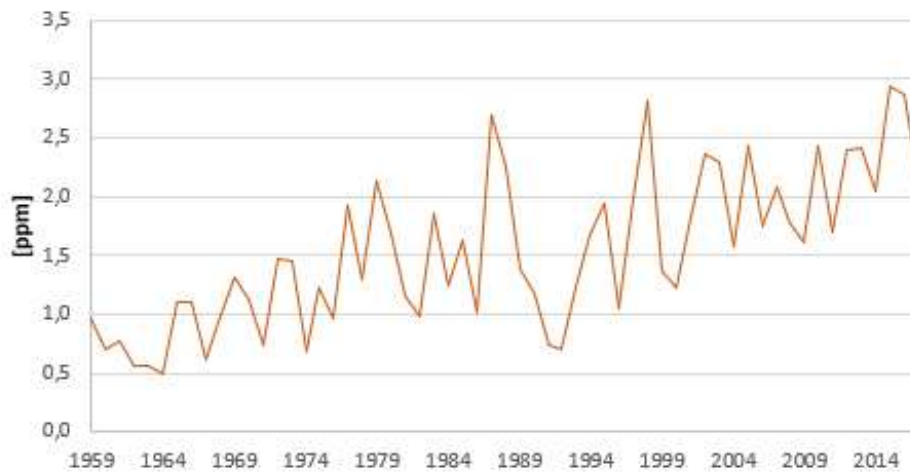


Figure 3: Annual mole fraction increase based on NOAA ESR DATA

As well as methane and nitrous oxide, carbon dioxide is a long-lived greenhouse gas (LLGHG) since it is chemically stable and persists in the atmosphere over time scales of a decade to centuries or longer, with a long-term influence on climate.

In the Table 1 the comparison between different GHG is shown, considering various parameters: Pre-1750 tropospheric concentration, recent tropospheric concentration, Global Warming Potential, atmospheric lifetime, increased radiative forcing.

Table 1: GHG properties

Gas	Pre-1750 tropospheric concentration ¹	Recent tropospheric concentration ²	GWP ³ (100-yr time horizon)	Atmospheric lifetime ⁴ (years)	Increased radiative forcing ⁵ (W/m ²)
Concentrations in parts per million (ppm)					
Carbon dioxide (CO ₂)	~280	399.5	1	~ 100-300	1.94
Concentrations in parts per billion (ppb)					
Methane (CH ₄)	722	1834	28	12.4	0.50
Nitrous oxide (N ₂ O)	270	328	265	121	0.20
Tropospheric ozone (O ₃)	237	337	n.a.	hours-days	0.40
Concentrations in parts per trillion (ppt)					
CFC-11 (CCl ₃ F)	Zero	232	4,660	45	0.060

1. Preindustrial (1750) concentrations of CO₂, CH₄, N₂O are taken from Chapter 8.3.2 of IPCC (2013)[4]. Preindustrial and recent O₃ amounts are taken from Chapter 8.2.3.1 of IPCC (2013).[4]
2. over a specific 12-month period for all gases except ozone (O₃), for which a current tropospheric total amount has been more broadly estimated (IPCC, 2013)[4]. The CO₂ concentration given is the average for year 2015, taken from the National Oceanic and Atmospheric Administration, Earth System Research Laboratory[5]. CH₄ concentration is the average of preliminary monthly concentrations, taken from[6].
3. Taken from [4];
4. Taken from Table 8.A.1 in IPCC (2013)[4];
5. Taken from Table 8.6 in IPCC(2013)[4];

The Global Warming Potential (GWP) is a parameter used to estimate the radiative effects of emissions of various greenhouse gases, integrated over a specified time horizon, relative to an equal mass of CO₂ emissions. The GWP with respect to CO₂ is calculated using the formula:

$$GWP_i = \frac{\int_{TR}^{TH} a_i c_i (t) dt}{\int_{TR}^{TH} a_{CO_2} c_{CO_2} (t) dt}$$

Where:

- a: instantaneous radiative forcing due to the release of a unit mass of trace gas, i, into the atmosphere, at time TR;
- c: amount of that unit mass remaining in the atmosphere at time, t, after its release;
- TH: end time for calculation, considering a specific time horizon (100 years in this case) starting from TR;

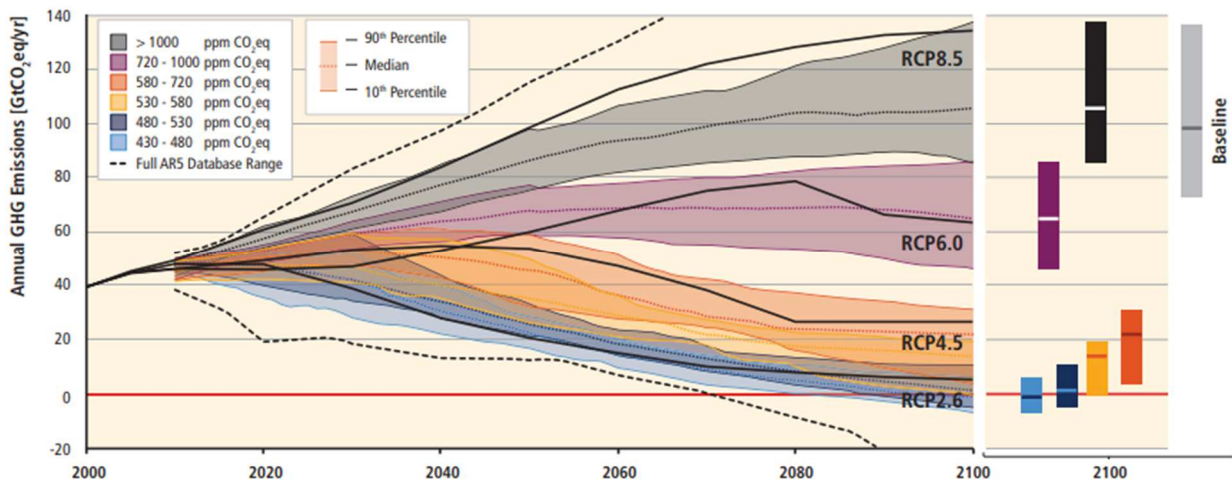
Atmospheric lifetime represents the average time that a molecule resides in the atmosphere before it is removed by chemical reaction or deposition, in other words the time that it takes for the concentrations of that gas in the atmosphere to return to natural levels after the human-caused emission of a gas. The estimation of this parameter in CO₂ case is complicated by temporary removal processes which store carbon in the biosphere before it is returned to the atmosphere as CO₂ via respiration or as combustion product. Although this evaluation necessitates complex modelling of the decay curve, most estimates fall in the 100-300-year range.

Radiative Forcing is defined in the eighth chapter of IPCC *Climate Change 2014* [4] as “Change in net downward radiative flux at the tropopause after allowing for stratospheric temperatures to readjust to radiative equilibrium, while holding surface and tropo-spheric temperatures and state variables fixed at the unperturbed values” and is used in order to evaluate and compare the strength of the various mechanisms affecting the Earth’s radiation balance that cause climate change. Positive radiative forcing means Earth receives more incoming energy from sunlight than it radiates back to space, resulting in global warming. On the contrary, negative radiative forcing means that Earth loses more energy to space than it receives from the sun, which produces cooling. As the main cause of Radiative Forcing is the change in GHG atmospheric concentration, this parameter is used to quantify the warming potential associated to each of these gases. In the previous table values for increased radiative forcing are reported, based on the 2015 and 1750 concentrations.

Considering the mentioned parameters, the carbon dioxide results to be the gas with the higher contribution to Global Warming, for its very high concentration in atmosphere and its long permanence.

1.2 Mitigation pathways

In order to understand risks associated to GHG concentration increase and how to mitigate this phenomenon, the Intergovernmental Panel on Climate Change (IPCC), the leading international body committed with climate change, assessed options intended to reach a certain level of mitigation. These actions are aimed at limiting or preventing GHG emissions and enhancing activities that remove them from the atmosphere.



Several scenarios for 2100 have been studied, with a range of technological and behavioural options, with different characteristics and implications for sustainable development, from which different levels of mitigation are obtained.

In the following graph, taken from Fifth Assessment Report (AR5) [7], Representative Concentration Pathways (RCPs) are tracked. RCPs are four GHG concentration trajectories describing respective possible climate scenarios, and their probability to happen depends on emission change over the years to come. Their names are due to possible ranges of radiative forcing values in the year 2100 compared to pre-industrial values (+2.6, +4.5, +6.0, and +8.5 W/m², respectively).

Figure 4: GHG Emission Pathways 2000-2100: All AR5 Scenarios

The blue curve is representative of the scenario that is estimated to keep global temperature rise below the set limit. In fact, in AR5 it is stated that:

“mitigation scenarios in which it is likely that the temperature change caused by anthropogenic GHG emissions can be kept to less than 2°C relative to pre-industrial levels are characterized by atmospheric concentrations in 2100 of about 450ppm CO₂eq.”

This means that to limit the rise of the global average temperature to 2 °C by 2050, CO₂ emissions should be reduced by at least 50% compared to 2000 levels.

However, to make this scenario possible, great efforts have to be done. Thus, the International Energy Agency (IEA) published the *Energy Technology Perspectives 2010* (ETP 2010) [8] in which the possible impact of energy innovation on climate change is highlighted.

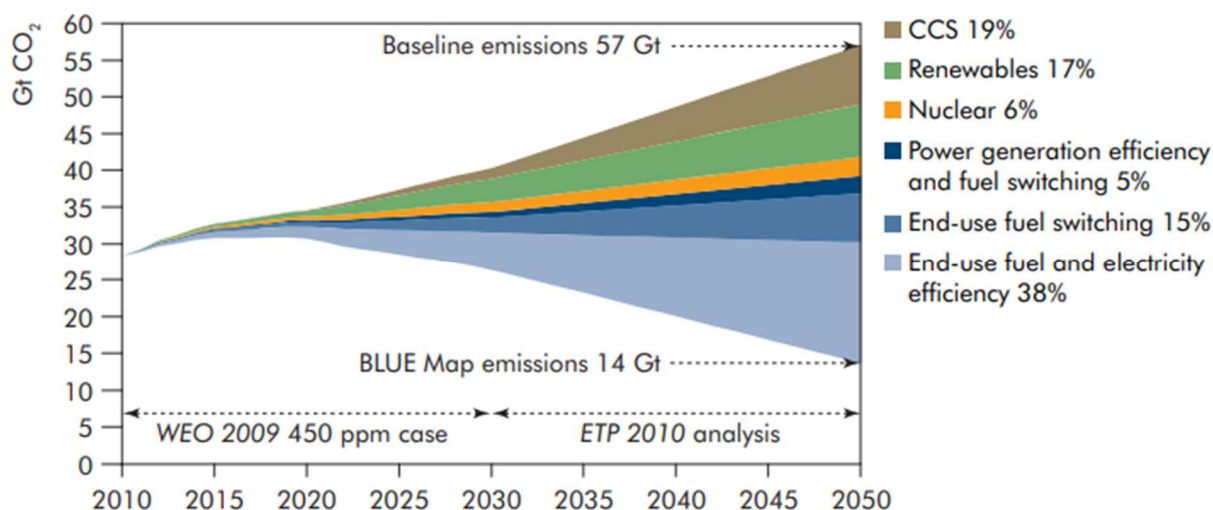


Figure 5: Key technologies for reducing CO₂ emissions under the BLUE Map scenario

The ETP 2010 Baseline scenario assumes that governments introduce no new energy and climate policies: it is characterized by a continuous growth of CO₂ atmospheric emission, with a 2050 value of 57 Gtons per year. On the opposite, the Blue Map scenario is designed with the goal of halving global energy-related CO₂ emissions by 2050 (compared to 2005 levels), with a 2050 value of the yearly emitted CO₂ equal to 14 Gtons. The least cost actions to achieve that goal are considered, through the development of existing and new low-carbon technologies. Only by combining these various technological solutions the COP21 goal would be feasible.

The included interventions are needed both in the power sector and in end-use sectors, since an equal effort in emission reduction need to be done. According to IEA prevision, an important role within the end-use sectors must be played through energy efficiency actions, accounting for around 38% in the emission reduction.

In the Blue Map scenario, the increased use of renewable energy accounts for 17% of the total emissions reduction, while nuclear energy accounts for 6%. Another important technological solution considered in *ETP 2017* is the Carbon Capture and Storage (CCS). CCS could be applied in power generation, fuel transformation and industry, accounting for 19% of the total emissions reduction, while fuel switching to less carbon-intensive fuels.

1.3 Regulatory framework

Starting from the *United Nation Convention on Climate Change* (UNCCC) held in Rio de Janeiro from 3 to 14 June 1992, the average global temperature rise has been recognized as a serious environmental problem. Even without scientific evidence, Climate Change was declared to be linked to GHG atmosphere concentration and the importance of mitigation actions became evident. Thus, the ultimate objective of the Convention was to stabilize GHG concentrations “at a level that would prevent dangerous anthropogenic interference with the climate system”[9].

Five years later, on 11 December 1997, the Kyoto Protocol operationalizes the intent of the Convention by committing industrialized countries to reduce GHG emissions in accordance with agreed targets. The main point of the Kyoto protocol was based on *“common but differentiated responsibility and respective capabilities”* [10]. Heavier burden was so placed on developed countries, recognized largely responsible for GHG emission high level: binding emission reduction targets were set for 36 industrialized countries and the European Union. The overall result of the eventual achievement of these targets would be an average 5 per cent emission reduction compared to 1990 levels over the five-year period 2008–2012 (the first commitment period).

By imposing such constraint on CO₂ emission, UNCCC laid the basis for a price for the main greenhouse gases to be assigned, creating a new flexible market in Europe, the EU Emission Trading System (EU ETS).

A further step in climate change combat has been taken in December 2015, during the Paris Agreement, the so-called COP21, when the Parties belonging to United Nations Framework Convention on Climate Change (UNFCCC) officially decided to *“reaffirm the goal of limiting global temperature increase to well below 2 degrees Celsius, while pursuing efforts to limit the increase to 1.5 degrees.”* (Art. 2) [11]. In order to respect such target, the Paris Agreement requires that all members prepare, communicate and maintain further Nationally Determined Contributions (NDCs), consisting in the actions that each Party intends to implement to reduce national emissions and cope with the impacts of climate change.

“Parties shall communicate their NDCs every 5 years and provide information necessary for clarity and transparency. To set a firm foundation for higher ambition, each successive NDC will represent a progression beyond the previous one and reflect the highest possible ambition” (Art. 4) [11]

1.4 EU Emission Trading System and white certificates market

In order to find an instrument able to assist the EU in reaching emission reduction target, the EU ETS was introduced. In March 2000, the European Commission presented a green paper with an initial outline of the EU ETS Directive, adopted in 2003, while the system was launched in 2005.

The EU ETS is the world’s first and largest *‘cap-and trade’* system for cutting greenhouse gas emissions by *“promoting reductions of emissions in a cost-effective and economically efficient manner”*(Art.1) [12].

The emission cap is one of EU ETS main features and represents a ceiling for the maximum amount of GHG release in atmosphere. Its role is to guarantee that total emissions are kept under a pre-defined level. The total quantity of allowances in circulation in the System is set at European level according to the EU emission targets.

From 2010 the main target for EU growth have been included in a 10-year strategy, the Europe 2020. The purposes in the field of “Climate change and energy” are:

- greenhouse gas emissions 20% lower than 1990 levels;
- 20% of energy coming from renewables;
- 20% increase in energy efficiency.

The cap for 2017 is 1.931 billion units and, in the period 2013-2020, it is reduced annually by a linear factor equal to 1.74% of the total annual average quantity of allowances issued by the Member States in the period 2008-2012, and equal to over 38 million units.

In 2014 a new strategy was adopted by EU, by fixing new goals for 2030. In the official document published by the European Commission [13], the 2030 climate and energy framework is reported and its key targets with respect for climate change are:

- At least 40% cuts in greenhouse gas emissions (from 1990 levels);
- At least 27% share for renewable energy;
- At least 27% improvement in energy efficiency;

Depending on those changing targets the emission cap of EU ETS is continuously adapted.

Parallel to the imposition of this maximum ceiling, another fundamental aspect of EU ETS is the trading system of EU emission allowances (EUAs). Installations included in this system are required to submit an EUA for each ton of carbon dioxide equivalent they emit over a year. Allowances can be allocated upon payment or free. In the first case, they are sold through public auctions in which accredited entities take part, and buy mainly to offset their emissions. In the second case, free allocation take place for operators at risk of relocation of production to countries characterized by less stringent environmental standards compared to European ones.

Regardless of the allocation method, the total quantity of allowances available to operators, that is the cap, decreases over time, effectively imposing a reduction in greenhouse gas emissions in the ETS sectors: in particular, in 2030, the mechanism is expected guarantee a decrease of 43% compared to the levels of 2005.

EU ETS involves over 11,000 operators at European level, including aircraft operators, industrial thermoelectric plants, manufacturing and production, storage and transport facilities of different types. In Italy, more than 1,200 power plant are involved, covering about 40% of national greenhouse gas emissions.

Hospitals are excluded from the EU ETS, and so are “small emitters” i.e. plants with emissions of less than 25,000 tonnes of CO₂ equivalent and, in the case of combustion plants, with a nominal heat output of less than 35 MW, excluding emissions from biomass.

Since its beginning in 2005, the EU ETS system has gone through three different phases, the so-called three commitments, with several modifications and redefinitions of the emissions reduction targets.

1.4.1 Phase 1 (2005-2007)

It is a 3-year pilot before entering phase 2, when the EU ETS is expected to become effective. The main points of this first phase were:

- only CO₂ emissions from power generators and energy-intensive industries were considered;
- free allowances were assigned to businesses;
- Non-compliance penalty was 40€ per tonne;

The outcome of Phase 1 mainly consists in the fact that a price for carbon was fixed, the carbon free trade in emission allowances was established across the EU and an overall system for monitoring, reporting and verifying emissions from the businesses covered was created. Initially the ceilings were based on estimates, because reliable data on emissions were missing. Thus, the total amount of allowances exceeded the emissions. For this reason, in 2007 the allowances supply exceeded the demand and their price fell to zero.

1.4.2 Phase 2 (2008-2012)

During Phase 2, first commitment period of the Kyoto Protocol, actual emissions reduction targets were set for countries belonging to EU ETS. The main aspects of this second phase are:

- Number of assigned allowances was reduced (6.5% lower compared to 2005);
- free allocation amount was reduced to around 90%;
- auctions started to be held by several countries;
- non-compliance penalty was increased to €100 per tonne;

Because verified annual emissions data from the pilot phase were now available, the cap on allowances was reduced in phase 2, based on actual emissions. During this phase the economic crisis led to a greater emission reduction than expected and carbon price significantly lowered.

1.4.3 Phase 3 (2013-2020)

In this phase the main modifications with respect to previous phases are:

- instead of considering different national caps an EU-wide cap on emission has been set;
- allowances are allocated through auctions;
- More sectors and gases are included;

1.4.4 Phase 4 (2021-2030)

According to changes introduced by EU 2030 climate and energy policy framework, various modifications have been made on EU ETS Phase 4 [14] with respect to the past ones.

From 2021, in order to encourage investments aimed at emission reduction, the annual linear reduction factor in allowances has been set to 2.2%, resulting in a reduction of around 55 million allowances per year to meet the target of 40% to 2030.

Moreover, as a safeguard for the international competitiveness of industrial sectors at risk of carbon leakage, the free allocation of allowances has been maintained. Phase 4 will also focus on helping industry and power sector to meet the challenges of innovation and investment required by the low-carbon transition through funding mechanisms.

1.5 Energy efficiency and white certificates

Moving in the direction of Climate Change mitigation, since 2005 the European Union has also started to stress the importance of energy efficiency, with the “*Directive on energy end-use efficiency and energy services*” [15]. In fact, the improvement in energy end-use efficiency would contribute to reduction of primary energy consumption, thus mitigating GHG emissions.

In the mentioned Directive *white certificates* (also called TEE: “titoli di efficienza energetica”) are introduced and defined as: “*certificates issued by independent certifying bodies confirming the energy savings claims of market actors as a consequence of energy efficiency improvement measures.*” (Art. 3)

The white certificates system is an incentive mechanism based on a mandatory primary energy saving scheme for some obliged electricity and natural gas distributors. Mandatory saving targets are set every year and obliged parties can fulfil the obligation by implementing measures to improve energy efficiency that give entitlement to certificates or purchase them from third-party companies.

As a result of energy efficiency improvements energy savings are achieved and their measured values in Tonnes of Oil Equivalent (TEP) determine the number of white certificates. The saving of a TEP is rewarded with the assignment of a white certificate.

Until now, white certificates market has been characterized by a strong sensitivity to supply and demand. In fact, in the last few years, white certificates prices have been affected by their limited availability in the market, with consequent very high values.

However, the corrective ministerial decree of 10 May 2018 [16] fixed new directives aimed at regulating the white certificates market. The maximum recognition value for each White Certificate is set at € 250, representing the fee issued by the GSE to the obliged subjects for the withdrawal of the white certificates.

Therefore, for the next period it is assumed that the market price at which obliged parties will purchase the certificates stays around the mentioned value of 250 €/each.

1.6 CO₂ price

CO₂ market trend has been changing substantially over the past EU ETS phases, for certain adjustment in its initial period has been necessary and also because of the heavy consequences of economic crisis in the industrial sector. The following figure, showing the historical trend of CO₂ market, is taken from *Annual Report on 2017 auctions* [17] published by GSE (Gestore Servizi Energia), the Italian board that is responsible for allowances allocation.



Figure 6: Historical trend of volumes and prices of the first chained annual futures (Dec-AA) of EUA and CER on ICE. Period from April 2005 to September 2018.

In its initial phase from 2006 to 2008, the price of allowances fell to zero due to the non-transferability of the units to the second phase. As previously mentioned, the second period was strongly affected by economic crisis, leading the drop in goods production to the progressive accumulation of surplus allowances. Conversely, as a result of regulatory changes and reduction in auction volumes (backloading), the third phase was characterized by a speculative recovery, with a positive trend for CO₂ price.

Phase 4, because of the end of backloading measures, showed again a negative trend, that has remained unchanged in fifth phase despite the reform process. The price has started to rise from the middle of 2017, with the end of the negotiations on the ETS reform.



Figure 7: Performance of EUA prices on the primary market in the first three trimesters of 2018

The positive trend is confirmed by the *Report of third trimester 2018* [18] of GSE, that shows a certain stability in the increase.

The analysis that will follow in the next chapters is based on the consideration that the carbon market will have a greater and greater impact on the energy sector, with a positive trend in CO₂ allowances price. As well as the price of NG, of electricity from the grid and

of white certificates, CO₂ price is a major index for the evaluation of the economic feasibility of the various scenarios.

1.7 Italian energy framework

In the context of climate change mitigation, in 2009 the European Parliament issued the *Directive 2009/28/EC* [19], on the promotion of the use of energy from renewable sources. This Directive fixed for each EU Country a National overall target to 2020 for the share of energy from renewable sources in gross final consumption of energy. With respect to Italy the target assigned for 2020 was 17%. A National Action Plan (PAN) was then structured in order to reach this goal gradually. In the following graph (Figure 8: Total share of gross final consumption covered by RES), taken from National Monitoring of GSE on renewable energy sector [20], the curve of NAP is shown in red.

According to GSE, in 2016 the share of gross final consumption of energy covered by renewable sources is equal to 17.41%, well above the PAN reference value. The difference compared to the trajectory identified in the PAN for 2016 is more than 5 percentage points.

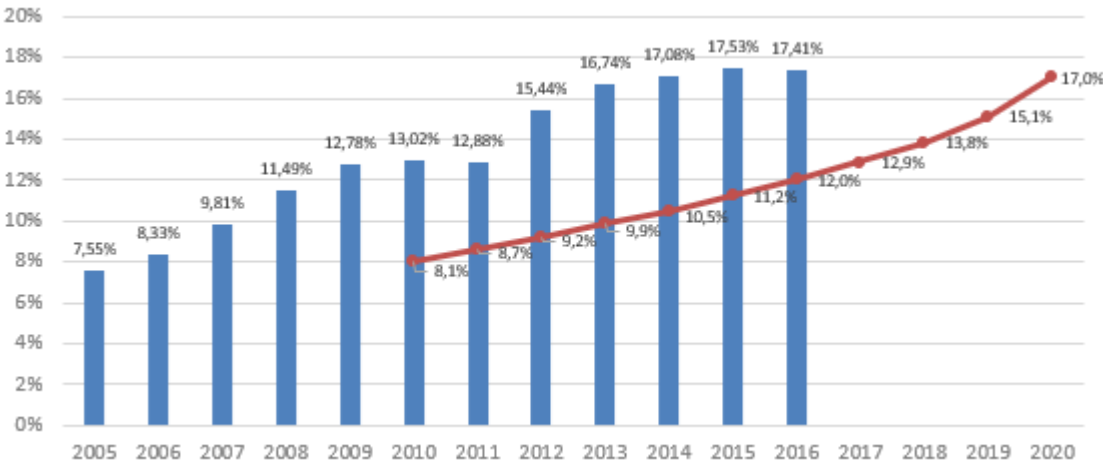


Figure 8: Total share of gross final consumption covered by RES

1.8 Industrial sector as main actor in fighting climate change

The Figure 9, taken from the *Technical Summary of AR5* [7], shows the distribution of GHG emissions per economic sector. As we can see the industrial sector has the main impact on the phenomenon, accounting for 21 % on direct emissions and for 11 % on indirect ones. Hence, strong efforts have to be done in the industrial field in order to reduce the quantity of equivalent CO₂ emitted.

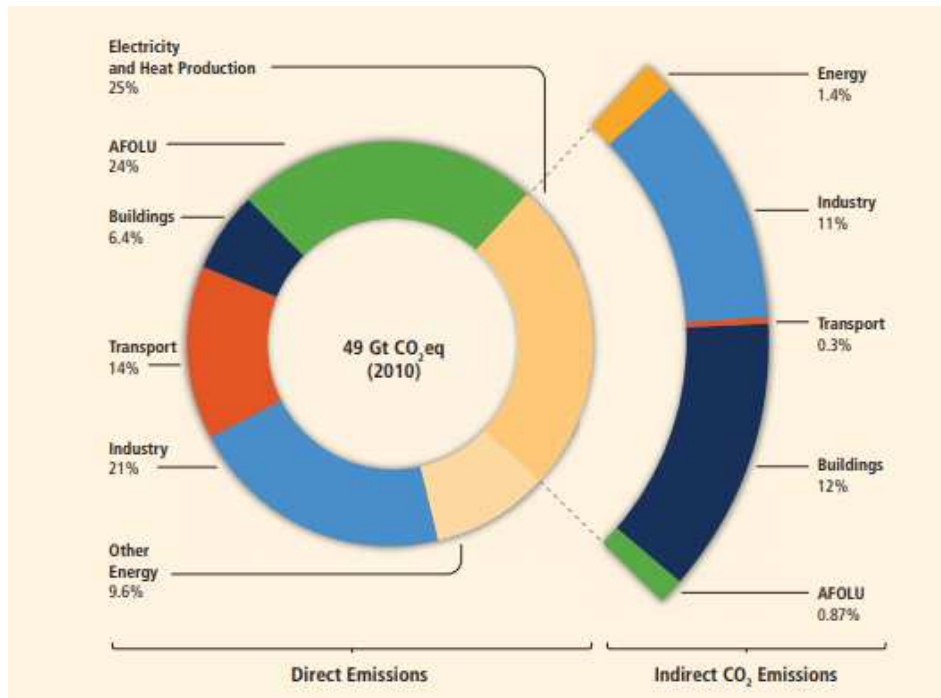


Figure 9: Greenhouse gas emissions by economic sectors [7]

In the last few years many companies have moved in the direction of climate change mitigation, by setting goals in the field of GHG emission reduction, renewable energy sources and energy consumption per ton of product.

With regard to companies working in the food sector, many of them fixed for 2020 GHG different reduction goals per ton of product. In some of their sustainability reports we read objectives in the field to emission reduction.

Moreover, GHG emissions have been classified into three “scopes”. Scope 1 emissions are direct emissions from owned or controlled sources. Scope 2 emissions are indirect emissions from the generation of purchased energy, while Scope 3 emissions are all indirect emissions that occur in the value chain of the reporting company, including both upstream and downstream emissions. Only a few companies accepted the challenge of expanding their goals also to Scope 3, fixing their deadline further.

In the field of renewable energy sources (RES) some courageous targets have been set by declaring for the next decades a certain share of energy from RES to be produced on-site. Other important goals consist in the reduction of energy consumption per ton of product.

While the latest mentioned objectives could be reached essentially by energy efficiency improvement, a strong drop in GHG emissions along with the increase of energy from RES require specific investments. Alternative solutions have been implemented by some companies to shift power production from fossil fuel to renewables, moving towards Carbon Neutrality. In this framework, with the aim of encouraging companies to accept the carbon neutrality challenge, RE100 [21] was founded. It is a collaborative global bringing together more than 100 influential businesses committed to 100% renewable electricity. Companies joining RE100 set a public goal to take 100% of their global electricity from renewable sources by a specified year. They publish their electricity data annually with RE100 reports on their progress.

Chapter II: Case study description

As mentioned in the first chapter, in parallel to the commitments taken by the countries belonging to EU ETS, since 2015 many companies have started to show some preoccupation to Climate change. The goals set for the following five or more years are declared in their sustainability reports and cover different areas. Under the item “social and environmental responsibilities”, the main topics are the reduction of water consumption, waste, energy absorption and GHG emission.

Focusing on GHG emission reduction in the industrial sector, until now several steps have been taken concentrating on process efficiency, thermal recovery from waste, energy loss cutting. However, in order to reach greater results in fighting climate change, a new approach to the problem is needed.

The present analysis moves forward trying to answer the need to find solutions that can be applied to industrial sector and help to reach the target of emission reduction.

The basic idea of this study is that the way energy vectors are produced is more important than the way they are simply made more efficient. When energy is produced from sources with extremely low carbon emissions, or virtually no emission, the answer to global warming is a radical one with a stronger impact on the environment.

Therefore, the present study attaches a crucial importance to the decarbonization process to be obtained through the conversion of thermal and electric power from fossil fuels to renewables.

Aiming at developing technologies that exploit renewable energy sources, several efforts have been done in the last period. Some solutions have come to the stage of actual applicability to real cases. The chosen technical solutions depend on the specific conditions and location of the plant and, accordingly, the availability of renewable sources on site.

In this study the decarbonization pathway is applied to a specific industrial plant located in the center of Italy. Considering its geographical position, its thermal and electrical needs and the productive processes taking place there, a selection of the technically feasible solutions is done.

2.1 Productive processes: pasta processing

The main product of the industrial plant considered in this study is pasta. All processing phases take place there, from durum wheat conditioning till packaging of the final product. The main steps of the production process are listed below:

1. Pre-cleaning and tidying up;
2. Conditioning;
3. Milling;
4. Mixing dough and rolling;
5. Drying;
6. Packaging;
7. Storage and distribution.

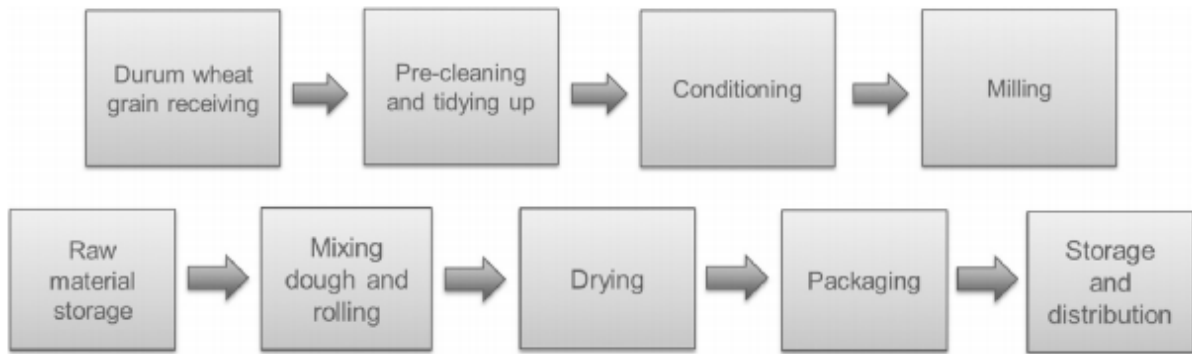


Figure 10: Main steps in pasta production [22]

1. Pre-cleaning and tidying up: the raw wheat is thoroughly cleaned, to remove undesired material, such as other cereals, stones, metal contaminants, feed, bran layers, seeds and powders.
2. Conditioning: the three main components of the grain are bran, germ and endosperm. Conditioning, that is the process of adding water to raise grain humidity from about 10% to 17%, causes the separation of bran from the endosperm due to hardening of the bran, and allows a more effective endosperm rupture in the following process phases.
3. Milling: it is a series of progressive grinding steps to crush the endosperm and stretch the external cortical particles. Flours are then classified according to the size of the granules through a series of vibrating sieves. A purifier separates grain with pure endosperm (heavier) from grains with adherent particles of bran (lighter). At the end of the process, most endosperm has been transformed into semolina, with starting moisture content of 10 to 14 %.
4. Raw material storage: durum wheat semolina is stored in silos and sent to the production area.
5. Mixing dough and rolling: semolina and water are mixed to make dough. In the mixing operation, 22 to 30 kg of water is added per 100 kg semolina [23]. The moisture content during mixing varies between 30 and 35 %, depending on the quality and the type of semolina, and the shape of the pasta being produced. At this stage it is important for the semolina to be well hydrated and in a uniform way, to maintain an equal consistency in the dough. From the mixers a worm screw conveys it into bells where it is pressed in dies: wet pasta is sent to the drying process. The pasta comes out of the die with a moisture content of about 30 %.
6. Drying: in hot air dryer ovens with controlled humidity, pasta stays from 6 to 12 h depending on the shapes and lines. The final moisture content should not exceed 12.5 %, to achieve the required specific consistency and enable a long shelf-life.

7. Packaging: pasta is weighed, placed into individual or primary packaging, then placed into secondary packaging (cartons/ exhibitors) and lastly into tertiary packaging (pallets wrapped with stretch film).
8. Storage and distribution: every wrapped pallet is moved to the finished product storehouse and then sent to distribution.

2.2 Industrial Plant Energy requirements

The thermal and electric yearly energy consumption is reported in Table 2: Plant energy needs

Table 2: Plant energy needs

Plant Energy consumption		
Thermal Energy for superheated water	119.817	MWh _{th} /y
Thermal Energy for hot water	25.831	MWh _{th} /y
Electric Energy	107.044	MWh _e /y

2.2.1 Thermal needs

The main thermal and electrical needs of the industrial plant are for the production processes.

With respect to thermal energy, two levels of temperature at which heat is requested can be found, on the basis on final utilization. Around 82% of the thermal energy need is associated with superheated water at the thermodynamic conditions of

$$T_{\text{water}} = 160^{\circ}\text{C}$$

$$P_{\text{water}} = 10 \text{ bar}$$

This thermal vector is used to a greater extent for the drying process. In fact, upstream of the pasta dryer there is a heat exchanger in which superheated water has the function of increasing inlet air temperature entering the hot-air based process.

Superheated water also comes to a vapor generator for the production of steam to be sent to fresh pasta production processes.

The rest of thermal energy is used to produce hot water at a temperature of around

$$T_{\text{water}} = 80^{\circ}\text{C}$$

for production processes, space heating, DHW. In Figure 11: Plant thermal needs the share of thermal energy in the various plant processes and final uses is shown, giving evidence to the temperature level at which heat is requested.

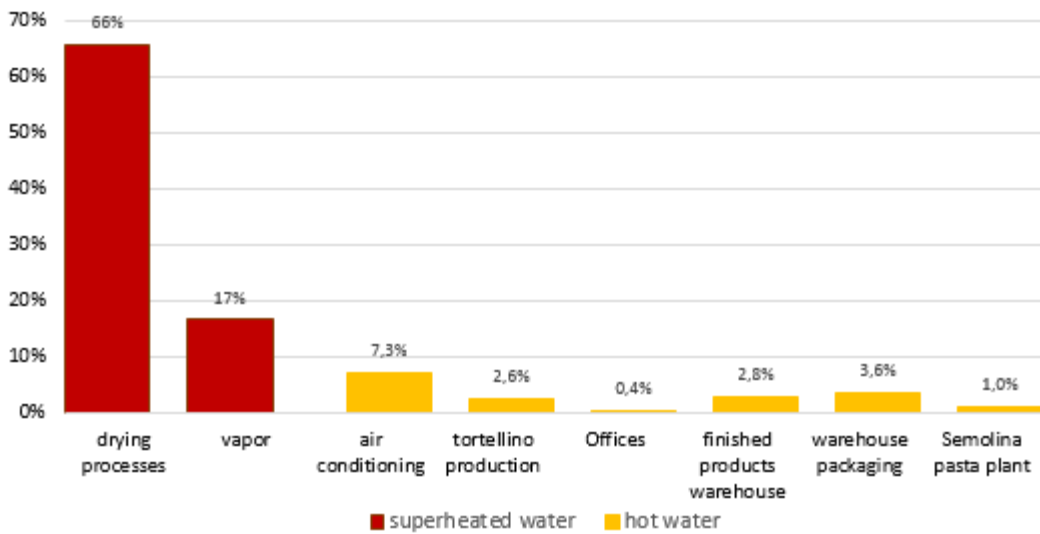


Figure 11: Plant thermal needs

Concerning superheated water request, it must be notice that its trend during the whole year appears to be quite constant, as shown in Figure 12: yearly profile of thermal power for high temperature final uses. This is due to the fact that high temperature level heat is mainly exploited in production processes, on which seasonality has a small impact.

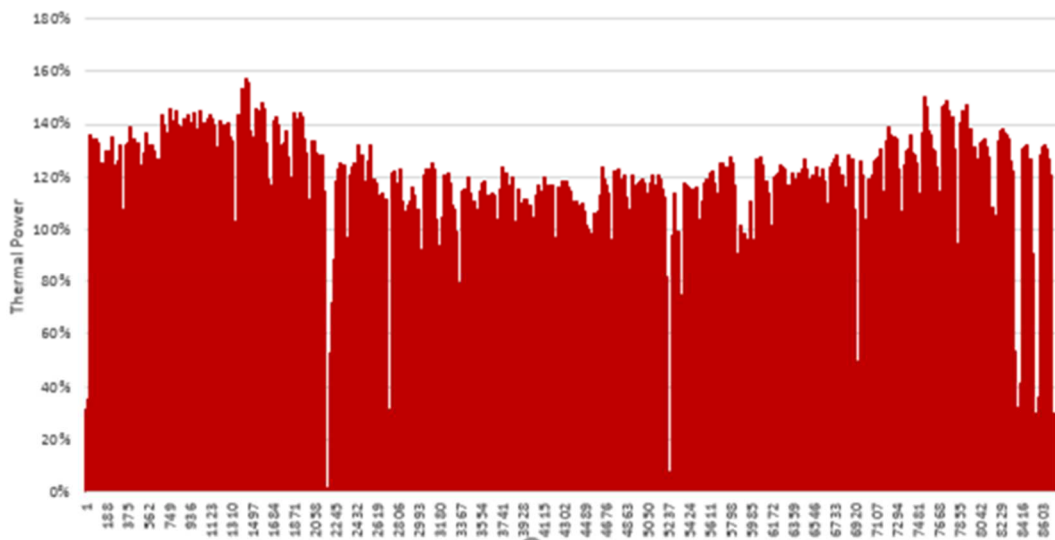


Figure 12: yearly profile of thermal power for high temperature final uses

On the opposite, the thermal requirement associated with the consumption of hot water strongly changes during the year (Figure 13: yearly profile of thermal power for 80° C final uses). The reason of its changing trend is that hot water is exploited for space heating, with much higher thermal power need in winter compared to spring and summer one,. Thus, a strong sensitivity to outdoor temperature follows.

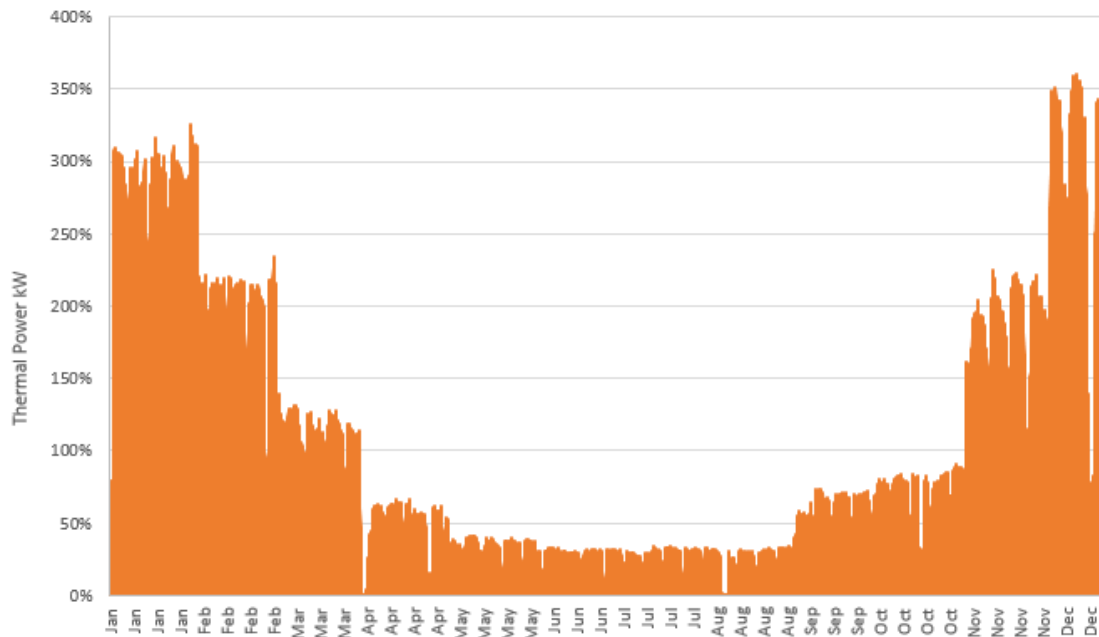


Figure 13: yearly profile of thermal power for 80° C final uses

2.2.2 Electric Energy needs

With regard to annual electric consumption, it results to be spread in the various production lines, as in Figure 14: Plant electrical needs

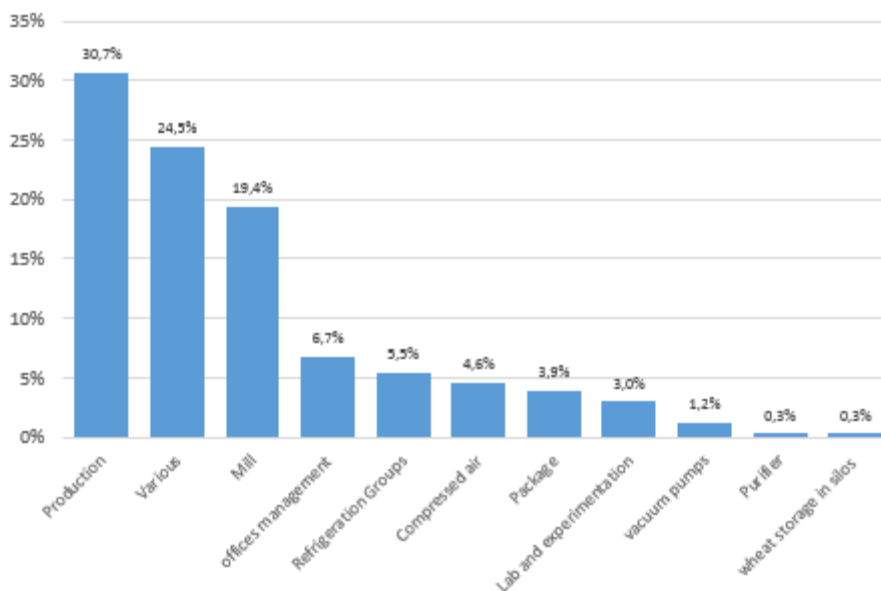


Figure 14: Plant electrical needs

The previous graph shows that the largest amount of electricity is used in production and in the milling process. These needs do not change with seasons, thus electrical consumption would have a quite constant trend during the year (Figure 15).

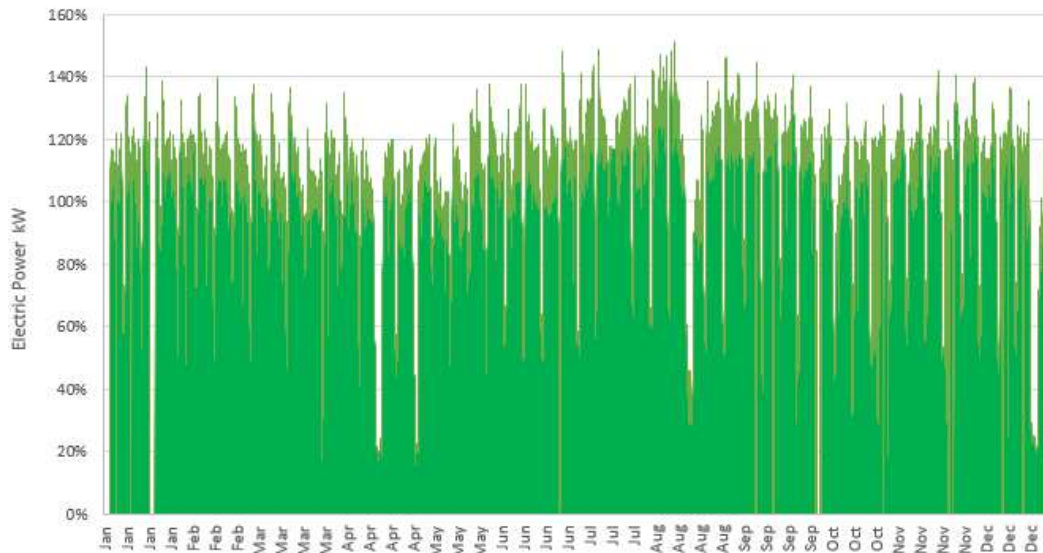


Figure 15: electric power profile

2.3 Today plant emissions

Considering the thermal and electric energy yearly absorbed in the studied industrial plant, an estimation of the CO₂ emissions to date is carried out.

It has been assumed that the total amount of thermal energy comes from Natural Gas-fed boilers installed in the industrial plant. Considering a thermal efficiency of the boiler of around 90% and a CO₂ production from NG of 1,956 ton_{CO2}/kSmc, the emissions for heat production are found.

$$ton_{CO_2,thermal} = 33.252 \text{ ton/year}$$

For the EU ETS emission counting method, only this quantity is considered. Thus, in the following analysis the economic benefit associated to industrial plant emission reduction are calculated only from the mentioned quantity.

Nevertheless, also electric energy from the grid comes from combustion processes in a certain share, given by electricity National mix. Therefore, even if this quantity is not included in economic saving for the following study, the emissions associated to electric energy from the grid in the starting case are calculated.

According to Italian emission factors for electricity production in 2017, reported by ISPRA database [24], the emission factor per unit of electric energy from the grid is

$$emission\ factor_{electric} = 325,5 \text{ g}_{CO_2}/kWh$$

Estimation of to date industrial plant emissions for electric energy are so obtained by multiplying the electric energy need by the mentioned emission factor. The result follows:

$$ton_{CO_2,electric} = 34.746 \text{ ton/year}$$

In conclusion, the starting plant emissions considered in the performed analysis are given by the sum of these two quantities.

Table 3: Plant emissions to date

TODAY PLANT EMISSIONS		
NG consumption	17.000.000	Smc/y
Electric Energy from the grid	107.044.358	kWh/y
Electric associated emissions	34.810	ton _{CO2} /y
Thermal associated emissions	33.252	ton _{CO2} /y
TOT	68.062	ton _{CO2} /y

Chapter III: Technological scouting

The decarbonisation pathway has been studied with reference to the previously described industrial plant and several technical solutions have been considered with the aim to reduce CO₂ emissions.

The identified pathways move in the following main directions:

1. Thermal Energy from RES;
2. Electric Energy from RES;
3. Waste to Energy;
4. Power and Waste to Fuel;
5. Shifting Thermal towards Electric;
6. Carbon Capture and Utilisation;

Each of those actions includes alternative technologies. The objective of this study is to identify the best solutions and build an optimal configuration by combining them.

3.1 Thermal Energy from RES

According to the report “*Heating without global warming*” [25], published by IEA in 2014, heating processes account for more than 50% of global energy consumption today, as in Figure 16: Heat Consumption per sector [TJ] from IEA[26].

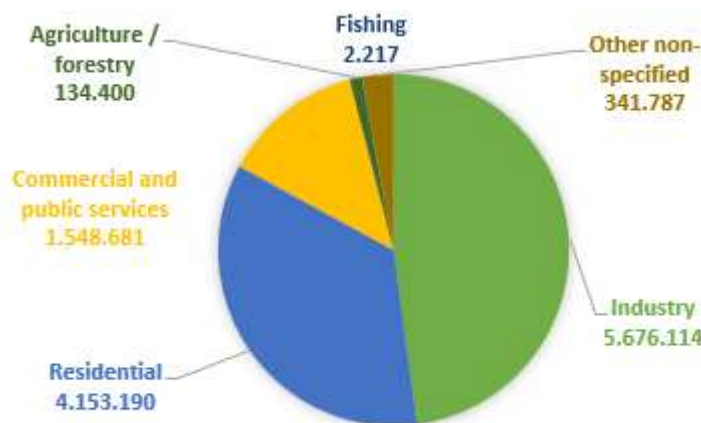


Figure 16: Heat Consumption per sector [TJ] from IEA[26]

The mentioned publication also reported that in the industry sector renewable energy for heat accounts only for 10% of the total, of which 99% is bioenergy-based. Similarly, in all the sectors the contribution given by RES is very small as far as heat production is concerned, due to the complexity and diversity of heating production and utilisation.

However, many renewable heating technologies are already mature and can provide heat at costs competitive with fossil fuel-based technologies.

From a technical point of view, thermal power needed for a certain use is most of the time associated with a specific temperature range at which it has to be provided so that different temperature levels may be distinguished: low (<100°C), medium (between 100°C and 400°C) and high (>400°C). It is important to fix the temperature level of a specific thermal need, in order to define the suitability of the available supply technologies to meet that specific heat requirement.

Since heating processes in industry often use vapor or superheated water as a thermal vector, to supply them fossil fuels-fed boilers are extensively used. This leads to great CO₂ emissions that contribute to a large extent to the global GHG emissions. Figure 17: Heat requirements by temperature range in different industry sectors, based on the report *The European Heat Market* [27], shows the share of thermal demand in various industrial sectors depending on temperature levels.

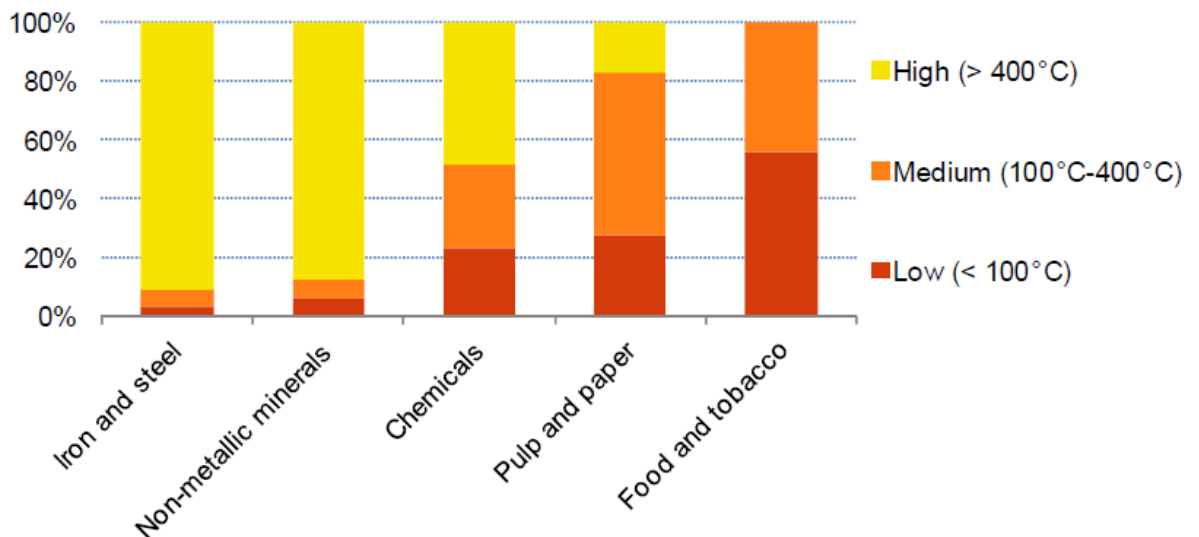


Figure 17: Heat requirements by temperature range in different industry sectors

As it can be seen, thermal needs in the food sector are mainly below 400°. According to IEA report, two-thirds of the medium-temperature heat required in industry processes is below 200°C, thus several technically feasible alternatives using RES can be considered. In this study the solution analysed to produce heat from RES is solar thermal technology. Figure 18: Solar collectors and working temperatures for different applications [25] shows different types of devices able to exploit the energy coming from the Sun generating useful heat at a specific temperature level depending on the specific technology.

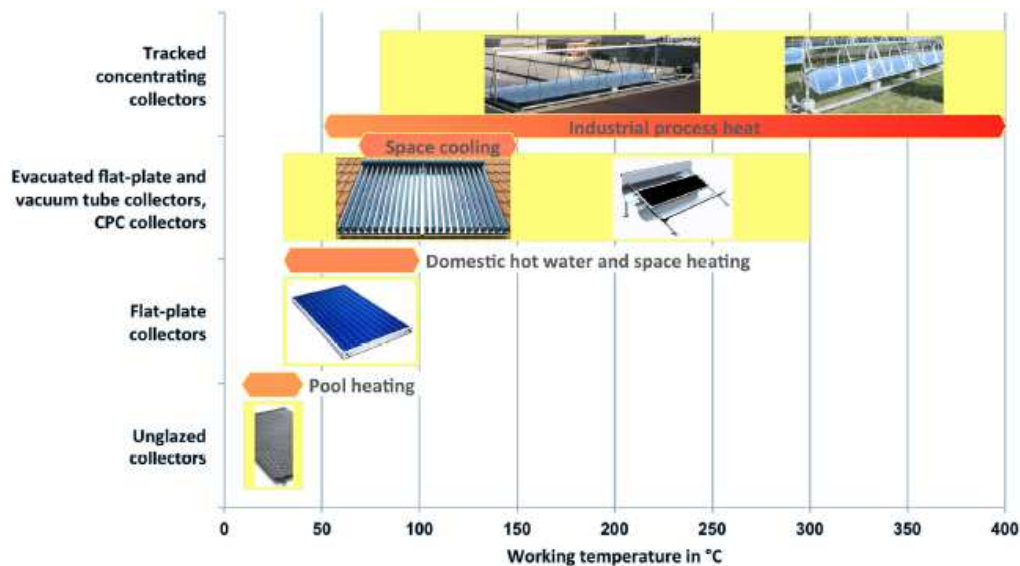


Figure 18: Solar collectors and working temperatures for different applications [25]

As previously described, in the analysed industrial plant heat requirements are in the form of 160°C superheated water and 80°C hot water. Therefore, as an alternative to the boilers in use now, two different kinds of technologies have been considered to produce such thermal energy, both recovering energy from the Sun: Solar Collectors and Concentrated Solar Power technology.

3.1.1 Solar Collectors

The solar collector is a component able to generate thermal energy from Sun radiation, by intercepting, capturing and transferring it to a heating fluid.

To evaluate the thermal energy that could be produced during a whole year, a specific model of Flat Plate Collector (FPC) has been considered.

Generally speaking, FPCs have been designed for operating in the low (ambient to 60°C) to medium temperature range (ambient to 100°C). They absorb radiation from all wavelengths (integral absorber) and directions (beam, diffuse and reflected radiation), and can be installed on the top of a building or other structure, so that a fundamental parameter for the calculation of the maximum thermal power is the available area.

An FPC solar collector usually consists on the following components:

- Cover → A glazing for the passage of sun beams. It must be as transparent as possible;
- Absorber plate → It collects the incoming near-infrared and visible solar radiation. A selective absorber reduces the release of infrared radiation, retaining as much heat as possible;
- Flow tubes → for transferring the heat to the fluid flowing from the inlet to the outlet;
- Inlet and Outlet connection → to admit, distribute and discharge the fluid, reducing pressure losses as much as possible;

- Insulation → to minimize heat loss from the back and sides of the collector;
- Collector Housing → encloses the various-components and protects them from dust, moisture, etc.

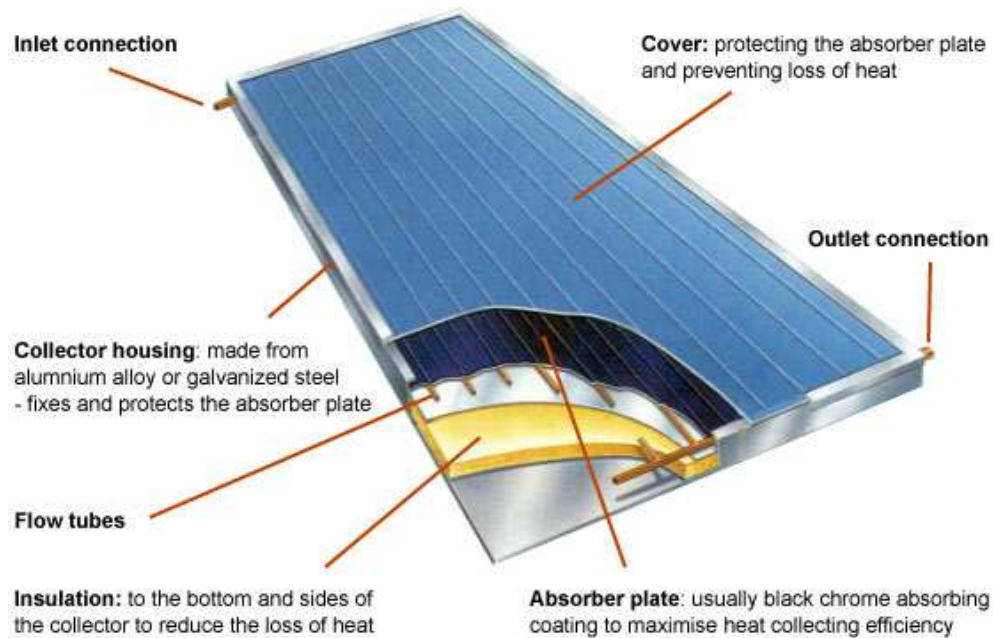


Figure 19: Flat Plate Solar collector structure

The main parameters needed for the estimation of the useful power produced by the collector are the incident solar radiation and the collector efficiency.

$$P_{th} = \eta \cdot G$$

Where

- η : collector efficiency;
- G : Incident Solar radiation expressed in [W] and given by the product between the radiation per square meter [W/m^2] and the whole area occupied by the collectors;

Incident solar radiation data are to be found on meteorological databases such as Photovoltaic Geographical Information System (PVGIS). Collector efficiency depends in turn on radiation values and on the working fluid temperatures through the factor x :

$$x = \frac{T_m - T_a}{G}$$

where:

- T_m represents the average temperature of the collector resulting from the average of water temperatures of delivery to the user and of return;
- T_a represents the ambient temperature;

The efficiency formula is based on standard EU collector efficiency formulation

$$\eta = \eta_0 - a_1 \cdot x - a_2 \cdot G \cdot x^2$$

Where

- η_0 : conversion factor, linked to optical efficiency;
- a_1 and a_2 are the first and second order heat loss coefficients;

Once the collector type and model has been fixed these parameters can be find in the datasheet of the product [28]:

- $\eta_0=0.805$;
- $a_1=0.699 \text{ W/m}^2\text{K}$;
- $a_2=0.0087 \text{ W/m}^2\text{K}$;

The efficiency curve, traced for three different values of the solar irradiance, follows

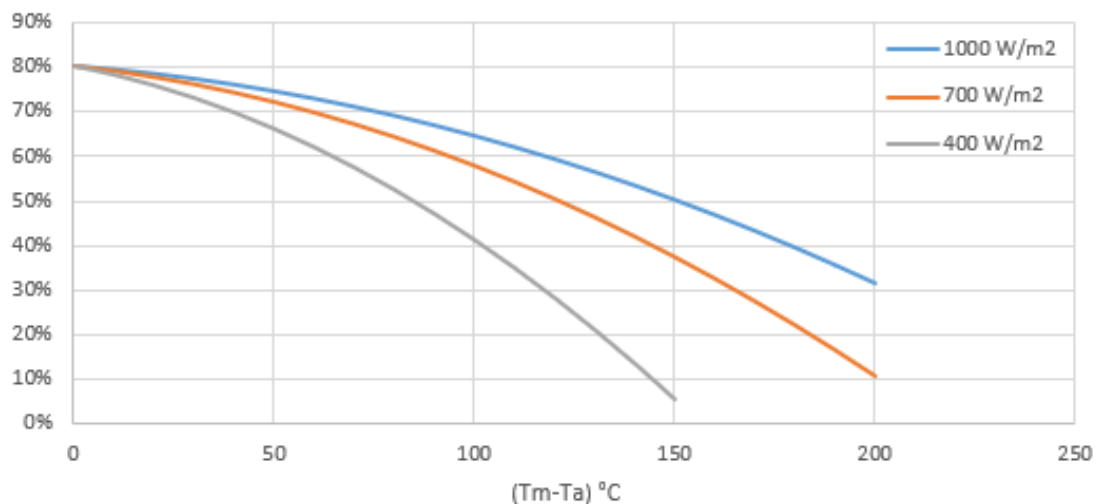


Figure 20: Collector efficiency

The decreasing trend of the efficiency curve is justified by the increase in thermal losses when temperature difference between the panel and external ambient reaches too high values. As a consequence, when considering panels able to reach temperature above 150°C consistent efficiency losses have to be expected.

Together with the area available, other determining factors for the maximum thermal power are: tilt angle, the angle between the horizontal plane and the solar panel, and orientation. Simulations show that, given the geographical position of the considered industrial plant, the optimal way to install the collectors would be

- tilt angle $\theta=30^\circ$;
- orientation towards South;

3.1.2 Solar Thermal concentrator

Concentrating Solar Power (CSP) technologies are able to focus sunlight from a large aperture area onto a smaller one by means of mirrors. They range from simple solar ovens to high-tech, large-scale collectors for high temperature heat and/or power generation.

The solar energy used by CSP is measured as Direct Normal Irradiance (DNI), which represents the energy received directly from the sun on a surface perpendicular to sunbeams. Thus, these technologies require clear skies and sufficient DNI to reach high levels of performance, strongly limiting the favourable areas for their deployment. Good locations could be arid and semi-arid areas with reliably clear skies, which typically lay at latitudes from 15° to 40° North or South.

The main parameter characterizing CSP technology is the concentration ratio (C), representing from a physical point of view the factor by which the incident energy flux (I₀) is optically enhanced on the receiving surface (I_r). This enhancing effect is obtained by confining the available energy coming through a chosen aperture to a smaller area on the receiver. Thus, a geometric concentration ratio is defined

$$C_{geo} = \frac{\text{Area of the aperture}}{\text{Area of the receiver}}$$

When the concentrated light is converted to heat, very high temperatures are reached: the higher the concentration ratio the higher the maximum temperature. Therefore, in regions with sufficient levels of DNI CSP technologies could provide heat for industrial processes between 150°C to 450°C, in the medium-temperature range.

At present, there are four main CSP technology families, which can be categorised by the way they focus the Sun’s rays and the technology they use to receive the solar energy. In Figure 21, from *Technology Roadmap on Solar Heating and Cooling* [29] such families are listed.

		Focus type	
		Line focus	Point focus
Receiver type	Fixed	Collectors track the sun along a single axis and focus irradiance on a linear receiver. This makes tracking the sun simpler.	Collectors track the sun along two axes and focus irradiance at a single point receiver. This allows for higher temperatures.
	Mobile	Fixed receivers are stationary devices that remain independent of the plant’s focusing device. This eases the transport of collected heat to the power block.	Mobile receivers move together with the focusing device. In both line focus and point focus designs, mobile receivers collect more energy.
		Linear Fresnel Reflectors	Towers (CRS)
		Parabolic Troughs	Parabolic Dishes

Figure 21: CSP technology families

With regard to the industrial plant in exam a Linear Fresnel Reflector (LFR) technology has been considered with the aim to produce superheated water. The sun rays hit rows of Fresnel flat mirrors and are reflected to a receiver tube in which flows a fluid (molten salt,

synthetic oil or water). The fluid reaches a high temperature and generates the useful effect in a heat exchanger, releasing heat to the fluid of the plant primary circuit.

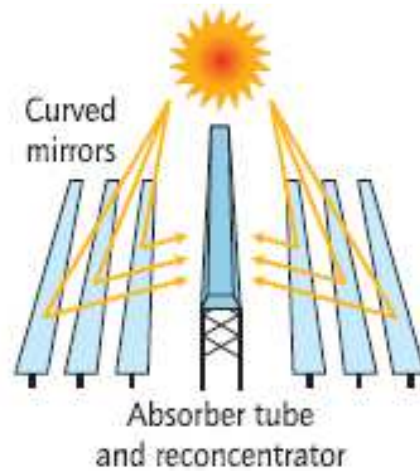


Figure 22: Linear Fresnel Reflector

The main advantage of LFR system is that its simple design based on bent mirrors and fixed receivers requires lower investment costs. LFR plants are, however, less efficient than parabolic troughs in converting solar energy to thermal power, due to a lower concentration ratio.

If a LFR field is installed on a flat ground near the plant, to estimate the peak power associated to the CSP installation the available area would be needed. Once the peak power per square meter is known, the system thermal power could be evaluated.

3.2 Electric Energy from RES

The composition of the national mix for the production of electricity introduced into the Italian electricity system in 2017 is reported in Figure 23, built on GSE data [30]

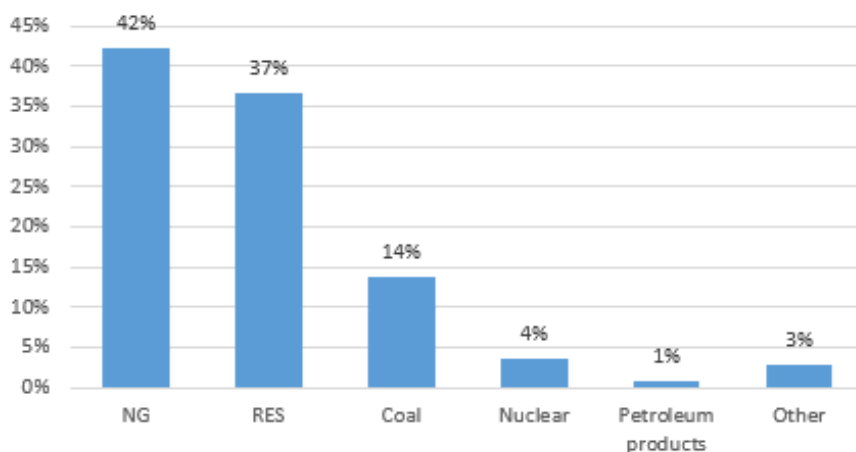


Figure 23: 2017 National mix for the production of electricity in Italy

As a result of this energy mix a certain amount of emission expressed in ton CO₂ is associated to each MWh of electric energy absorbed from the national electric grid.

Italian emission factors for electricity production in 2017 is reported by ISPRA database [24]. With respect to gross electric production the emission factor per unit of electric energy from the grid is

$$g_{CO_2}/kWh = 325,2$$

This factor takes into account the overall electricity production efficiency, starting from the conversion from thermal to electric power and including also the transport. Thus, the electricity production process being equal, the primary energy associated to a single MWh of electric energy from the grid could be higher than the MWh produced on site, if higher efficiency energy production processes are considered. As a consequence, also the emission factor would be higher.

Moreover, if a renewable source is exploited for the electricity production on site a double advantage is obtained: on one hand, the target of reducing GHG emission would be met, by producing electricity CO₂ free; on the other hand, depending on the specific technical solution adopted, an economic benefit is gained if the cost of MWh produced is lower than the price from the grid.

The best available and mature technology to produce electricity from RES is the PV technology, able to directly transform solar energy into DC electricity.

In the last 5 years the PV industry has experienced huge change, with a considerable increase in manufacturing capacities, and a shift of module manufacturing from European countries and the United States to Asia. As a consequence, market prices have been drastically reduced by factor of five for modules, and almost three for the whole system.

Referring to the last ten years, cumulative installed capacity has grown at an average rate of 49% per year, as shown in Figure 24 taken from *Technology Roadmap on Solar Photovoltaic Energy* [31].

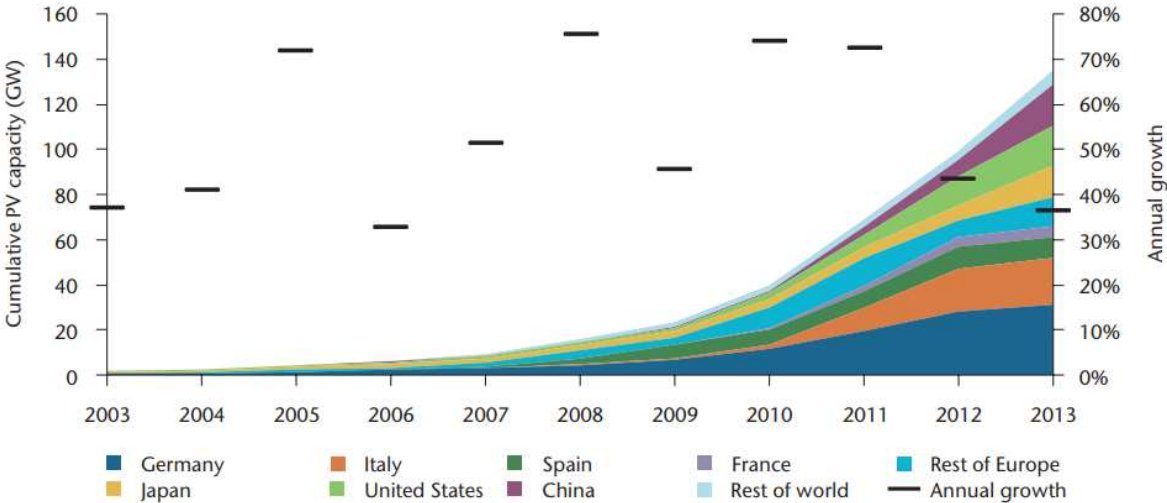


Figure 24: Global cumulative growth of PV capacity

3.2.1 PV technology

PV cells are semiconductor devices that generate direct current (DC) electricity.

The most important part of a photovoltaic module is the set of photovoltaic cells that are responsible for the transformation of solar radiation into electrical energy. The rest of the elements that are part of a solar panel have the function of protecting and lending firmness and functionality to the system.

A PV panel has the following structure, as in Figure 25:

- Front cover → its protective function from atmospheric agents is obtained by tempered glass with low iron content, since it presents a good protection against impacts and is a very good transmitter of solar radiation;
- Encapsulated layers → responsible for protecting the solar cells and their contacts. The materials used (ethyl-vinyl-acetylene or EVA) acts as a thermal and transparent insulator to let the solar rays pass through to the photovoltaic cells;
- Support framework → is the part that gives mechanical robustness to the system and allows it to be inserted in structures that make up modules;
- Subsequent protection → it gives a posterior protection against atmospheric agents, preventing moisture from penetrating;
- Electrical connection box → Two wires come out of the electrical connection box, one positive and the other negative, being connected to the electric circuit;
- Photovoltaic cells → the core of the photovoltaic panel. These are semiconductor devices capable of generating electricity from solar radiation.
- Front cover → The frame is usually made of aluminium;

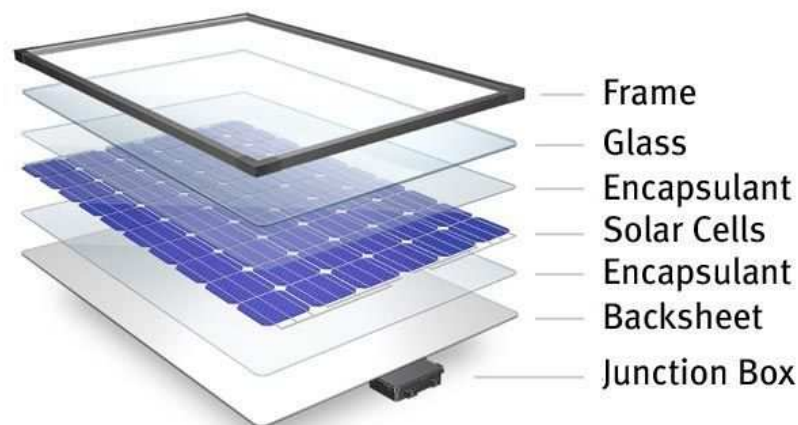


Figure 25: Structure of a PV panel

The modules are then combined to form strings, arrays and systems. The balance of system includes inverters, transformers, wiring and monitoring equipment, as well as structural components for installing modules, whether on building rooftops or facades, above parking lots, or on the ground.

The fundamental parameter of a PV module is the related Nominal Maximum Power, that represents the power generated under so-called Standard Test Conditions (STC): module temperature of 25°C, vertical irradiance of 1.000 W/m², air mass of 1.5 (distance travelled through the atmosphere 50% greater than when the sun is exactly overhead) and a specific irradiance spectrum. Nominal efficiency of the panel is evaluated in these specific conditions and is the ratio between the Max Power and the STC Irradiance.

With respect to the output, in terms of Watt produced in different conditions, it depends on solar irradiance, orientation of the modules and *performance ratio* (PR) of the system, which takes into account all efficiency losses resulting from actual module temperature, module mismatch, varying irradiance conditions, dirt, line resistance and conversion losses in the inverter.

For the estimation of the electric energy that can be produced over a year, an orientation and tilt angle for the system have to be fixed first. Considerations based on industrial plant latitude and geographical position lead to decide for an optimal configuration characterized by

- tilt angle $\theta=30^\circ$;
- orientation towards South;

The peak power for the system is given by the product of the peak power per single panel and the total available area. This area does not correspond to the total surface of the field or roof in which the system is designed to be installed, because shaping effects must be taken into account and a minimum distance between the panels is so necessary.

$$W_{p,field} = W_{p,module} \cdot n_{modules}$$

Where

- $W_{p,module}$ is expressed in [W] and is defined once the PV panel type has been chosen;
- $n_{modules}$ is given by the ratio between the available area and the area of a single module;
- $W_{p,field}$ is expressed in[W];

As the peak power refers to the previously mentioned specific condition of 1 kW/m² of irradiance, its value must be multiplied by the annual irradiation expressed in kWh/m² to obtain real PV production potential. In this way the latitude and meteorological data for the analysed plant are taken into account, and the electric useful energy produced by the whole system is evaluated.

Moreover, an overall PV panel efficiency of 75% is considered, in which panel inefficiency losses are included (Figure 26: PV system losses).

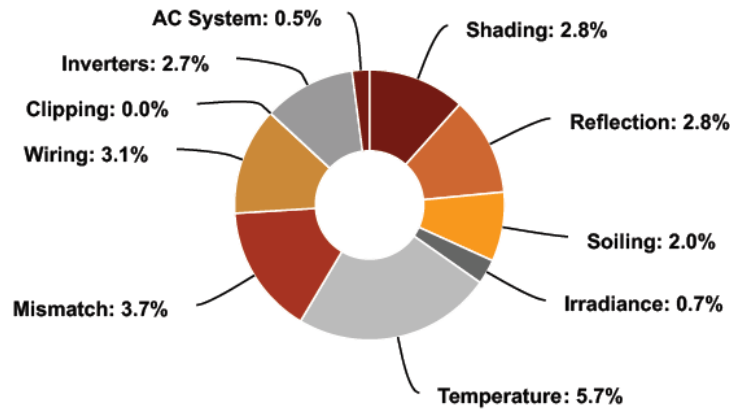


Figure 26: PV system losses

The formula for estimating the energy produced by the system is given below:

$$E_{PV,field} = G \cdot W_{p,field} \cdot \eta_{PV}$$

Where

- G is the irradiation in [kWh/m²], whose values can be taken from the database PVGIS, based on Meteorological data averaged on 10 years for the selected position.
- η_{PV} is the PV efficiency equal to 75%;
- E_{PV} is measured in [kWh]: this is due to the fact that the peak power is referred to STC, thus considering an irradiance value of 1kW/m². When moving to actual condition, this irradiance should be included in the previous formula, dividing the various member for this quantity;

A final passage is needed, in which degradation rate is considered. This factor includes the fact that year by year the PV performance decreases due to material degradation. Thus, a 2.5 % reduction in useful electric energy produced must be taken into account.

$$E_{user} = E_{PV,field} \cdot (1 - 2,5\%)$$

Once the useful energy for the first year has been obtained, to get the overall energy production year by year for the successive 10 years, degradation increase must be considered. Thus, in the previous formula an additive factor of 0,7 % for degradation losses must be included for each of the past years.

For the nth year:

$$E_{user,n} = E_{PV,field} \cdot (1 - 2,5\% - 0,7\% \cdot n)$$

3.3 Waste to Energy

When dealing with Waste-to-energy (WtE) we are referring to the process of generating electric and/or thermal energy from the primary treatment of waste, or from the processing of waste into a fuel source. Thus, WtE represents a form of energy recovery and includes a number of processes such as incineration, gasification, pyrolysis, anaerobic digestion, and landfill gas recovery.

- Incineration represents a waste treatment process that involves the combustion of organic substances contained in waste materials at ultra-high temperatures allowing for energy recovery;
- Fast pyrolysis can thermo-chemically convert waste products into clean liquid fuels;
- landfill gas recovery refers to the process of capturing the gases emitted from municipal landfills and transform it into energy;
- anaerobic digestion (AD), that biologically converts organic material into compost as well as biogas for energy.

In this decarbonization study, among the mentioned WtE technologies, the focus will be on biogas production from anaerobic digestion, exploiting the plant production waste streams.

Biogas production from waste streams is included in the previously mentioned Renewable Energy directive of 23 April 2009 [19], being considered a renewable fuel with a great potential in replacing fossil fuels and therefore reducing GHG emissions:

“The use of agricultural material such as manure, slurry and other animal and organic waste for biogas production has, in view of the high greenhouse gas emission saving potential, significant environmental advantages in terms of heat and power production and its use as biofuel.” (Art. 12)

From a chemical point of view, biogas is a mixture of methane and carbon dioxide with a small amount of other compounds. It is produced by anaerobic digestion (AD) of waste streams containing organic matter, such as wastewater, animal waste, food waste, or landfills.

Anaerobic digestion is a biological process consisting in a sequence of steps (Figure 27)(hydrolysis, acidogenesis, acetogenesis, methanogenesis) in which microorganisms break down biodegradable material in the absence of oxygen.

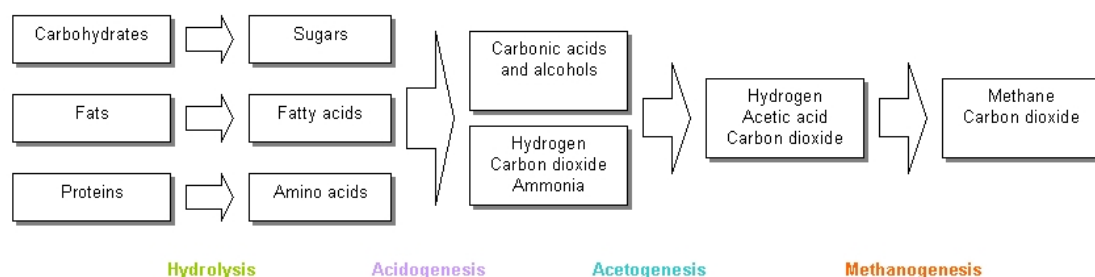


Figure 27: process of organic matter degradation during anaerobic digestion

The outputs of digestion process are biogas and digestate. Mainly composed by methane and carbon dioxide, biogas can be used as energy carrier.

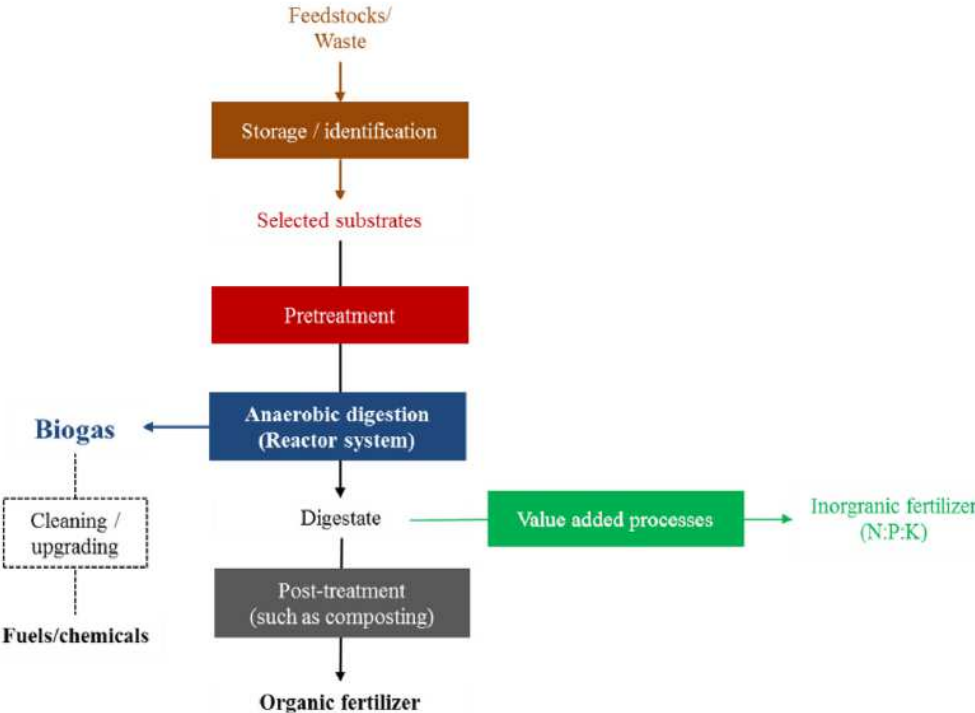


Figure 28: Theoretical analysis of AD technology

As opposed to fossil fuels, AD technology can reduce GHG emissions, exploiting locally available sources. Biogas composition strongly depends on feedstock properties. Biogas coming from wastewater, animal waste, or food waste typically consists in 50-70% CH₄, 30-50% CO₂, and 0-6% H₂O. The commonly encountered contaminants are hydrogen sulphide, H₂S (0-10,000 ppm) and silicon compounds (200-10,000 ppb).

Biogas production has seen a significant growth in the last years in Europe, mainly brought about by the favourable support schemes in operation in several EU countries. According to Eurostat Statistics [32] in 2015 the total biogas production in the European Union reached 654 PJ of primary energy, more than 18 billion m³ natural gas equivalent. As shown in Figure 29, the contribution of landfill gas recovery to biogas production has been almost constant over the last decade, while the major contribution has come from AD plants and to lower extent from sewage gas exiting wastewater treatment. This great increase in AD system installation has led to a sufficient maturity of the technology.

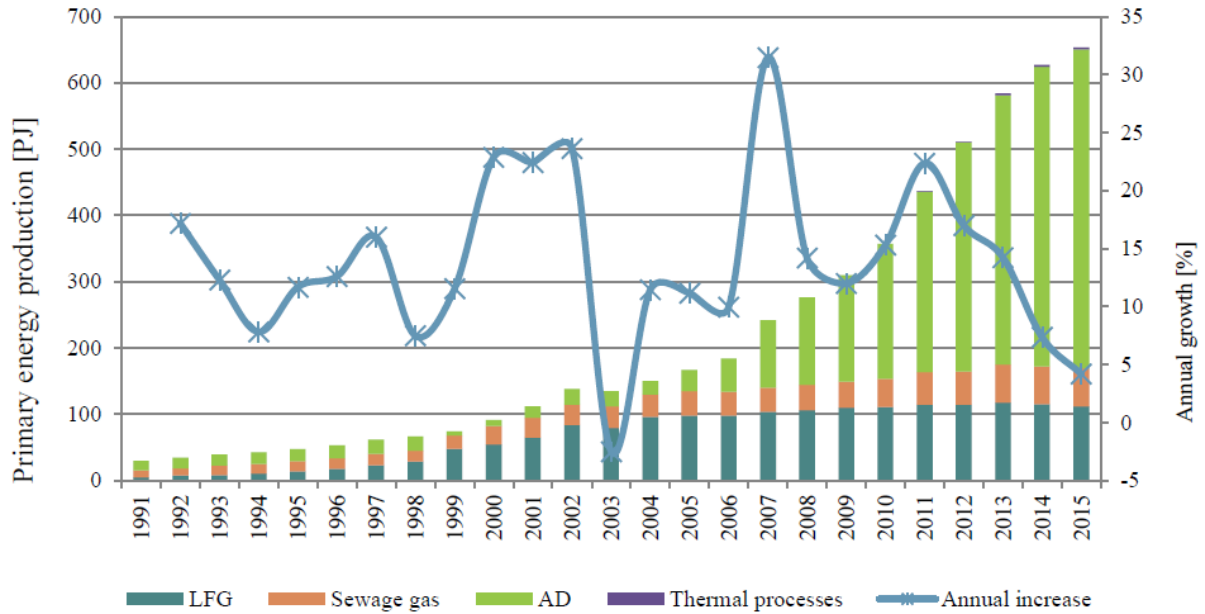


Figure 29: Evolution of primary energy biogas production in the EU[33]

In the case of the industrial plant that is being discussed, the greater amount of waste streams comes from the milling process. The main products of this process are: flour for 73-80 %, middlings for 2-3 %, bran for 16-21 %.

Middling and bran represent the most significant waste streams of the plant, and their daily flowrates and mass compositions are given in Table 4: flowrate and mass composition of waste streams.

Table 4: flowrate and mass composition of waste streams

	BRAN	MIDLINGS
Daily flowrate (ton/day)	130	90
Moisture %	12,95	13,78
Proteins % s.s.	17,71	15,97
Lipids % s.s.	4,9	4,83
Raw fiber % s.s.	7,57	11,92
Ashes % s.s	4,51	5,09
Starch % s.s.	30,76	21,92

In order to evaluate the technical and economic feasibility of the installation of AD for biogas production, initial assessment has been made based on given waste chemical

composition. The results obtained confirm the possible advantages resulting from this solution.

Flowrate of biogas exiting the anaerobic digester estimated from Engie internal expertise:

$$\dot{m}_{biogas} \sim 88.000 \text{ Nm}^3/\text{day}$$

Since the two main compounds of the biogas mixture are methane and carbon dioxide, it is also useful to estimate their equivalent flowrates. Biogas produced from each macromolecule (es. lipids, proteins, etc) has its own volumetric composition, with a certain percentage of CH₄ and CO₂. By combining flowrate of the various macromolecules, flowrate of equivalent is:

$$\dot{m}_{CH_4} \sim 45.000 \text{ Nm}^3/\text{day}$$

The produced biogas could have several applications. We distinguish the following cases:

- biogas in boiler;
- biogas in CHP with Internal Combustion Engine (ICE);
- biogas in CHP with Solid Oxide Fuel Cell (SOFC);
- biogas upgrading in biomethane;

All these technical solutions will be now explained in detail.

In Figure 30: biogas utilization pathways the different biogas utilization pathways are schematically represented

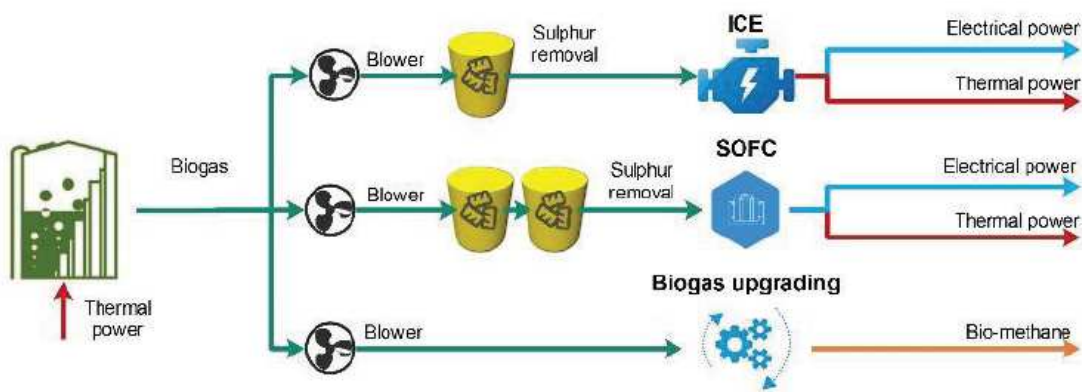


Figure 30: biogas utilization pathways

It is important to notice that, before being exploited in a CHP or upgrading system, biogas must be purified through pre-treatments, to prevent corrosion and mechanical wear of the equipment in which the biogas is introduced. In fact, in addition to methane and carbon dioxide, biogas may also contain water, hydrogen sulphide, nitrogen, oxygen, ammonia, siloxanes and particles. The concentrations of these impurities vary according to the composition of the substrate from which the gas was produced.

3.3.1 Biogas in boiler

This is considered the base case, in which the biogas is directly used to feed the installed boilers to produce thermal power. No investment in new boilers is needed, except for the installation of a burner to be specific for biogas.

For the evaluation of yearly produced thermal energy, the hourly flowrate is multiplied by the number of working hours of the industrial plant, by the boiler thermal efficiency and by the methane Higher Heating Value (HHV). In fact, rather than considering the biogas HHV, only the flowrate of equivalent methane is considered.

$$E_{th} = \dot{m}_{CH_4} \cdot HHV \cdot h \cdot \eta$$

Where

- E_{th} is expressed in [kWh/y];
- $HHV_{methane} = 9.596$ [kWh/Smc];
- $h = 8000$ hours;
- $\eta = 90\%$;

3.3.2 Biogas in ICE CHP

The produced biogas can be exploited to generate thermal and electric power at the same time, in a Combined Heat and Power (CHP) system. Cogeneration is one of the most efficient ways to produce energy, as it allows to use excess heat in electric power generation, that would otherwise be lost.

Compared to conventional power plants, the exploitation of heat produced allows for an overall efficiency for the cogeneration plant around 90 % of the energy value of the fuel burned, while traditional power plants reach 15-40 % efficiency. The simultaneous production of electric and thermal energy has a twofold effect: on one hand, emission reduction takes place, due to the lower fuel consumption; on the other hand, the cost of energy production decreases due to more efficient use of sources.

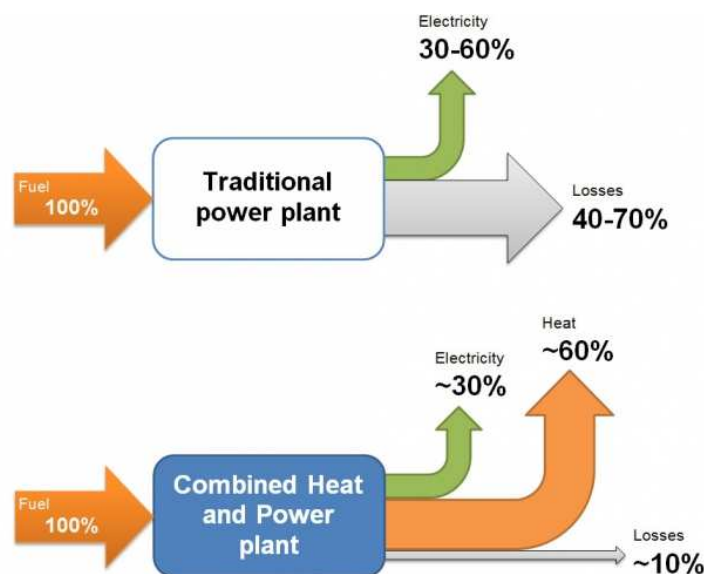


Figure 31: comparison between traditional power plant and CHP system

The core of standard CHP system can be either an Internal Combustion Engine or a gas turbine. When considering a small size, the most efficient system is ICE CHP (Figure 32), with electric efficiency less than 45%. Thermal recovery takes place through the cooling jacket of the motor and in a recovery boiler in which flue gases are cooled down, with an overall thermal efficiency around 40%. The overall efficiency of the system is given by the sum of these two quantities.



Figure 32: CHP internal combustion engine

In this framework, the exploitation of a renewable fuel such as biogas makes CO₂ emissions equal to zero, and fuel cost only depends on biogas production process and the cost of feedstock. In this specific case a biogas fed ICE cogenerator has been selected. Details on electric and thermal efficiency are reported on CHP datasheet (Figure 33).

			100%	75%	50%
Potenza introdotta	[2]	kW	7.324	5.617	3.910
Quantità di gas	*)	Nm ³ /h	771	591	412
Potenza meccanica	[1]	kW	3.431	2.573	1.715
Potenza elettrica	[4]	kW el.	3.360	2.518	1.671
Potenze termiche recuperabili					
~ Primo stadio intercooler	[9]	kW	943	534	204
~ Olio		kW	353	311	270
~ Acqua di raffreddamento motore		kW	533	459	378
~ Gas di scarico raffreddati a 346 °C		kW	~	~	~
Potenza termica complessiva	[5]	kW	1.829	1.304	852
Potenza erogata complessiva		kW totale	5.189	3.821	2.523
Potenza termica da dissipare					
~ Secondo stadio intercooler		kW	202	142	93
~ Olio		kW	~	~	~
~ Calore insuperficie	ca. [7]	kW	232	~	~
Consumo elettrico specifico del motore					
Consumo elettrico specifico del motore	[2]	kWh/kWel.h	2,18	2,23	2,34
Consumo specifico del motore	[2]	kWh/kWh	2,14	2,18	2,28
Consumo olio motore	ca. [3]	kg/h	0,69	~	~
Rendimento elettrico			45,9%	44,8%	42,7%
Rendimento termico			25,0%	23,2%	21,8%
Rendimento complessivo	[6]		70,8%	68,0%	64,5%
Circuito acqua calda:					
Temperatura di mandata		°C	87,3	83,8	80,7
Temperatura di ritorno		°C	75,0	75,0	75,0
Portata nominale		m ³ /h	127,7	127,7	127,7
Potere calorifico inferiore del gas (PCI)		kWh/Nm ³	9,5		

Figure 33: datasheet for the model JMS612_J612, General Electric [34]

Once the model of CHP to be installed is decided, the thermal and electric power are known. Different values of the various parameters are reported depending on the loading condition. To simplify we will assume that the engine always works at full load. Flowrate of biogas supply is evaluated as

$$\dot{m}_{biogas} = \frac{P_{el}}{\eta_{el} \cdot HHV}$$

Where

- m_{biogas} is expressed in [Nm³/h];
- HHV of methane has been used;

The thermal and electric energies yearly produced are evaluated as follows

$$E_{el} = \dot{m}_{biogas} \cdot \eta_{el} \cdot HHV \cdot h$$

$$E_{th} = \dot{m}_{biogas} \cdot \eta_{th} \cdot HHV \cdot h$$

Where

- E_{el} and E_{th} are expressed in [kWh/y];

3.3.3 Biogas in SOFC CHP

An alternative to internal combustion engine CHP is represented by fuel cell technology. Fuel cells are direct energy conversion devices which transform the chemical energy of fuel into electrical one. They are characterized by high electrical efficiency, with low pollutant emissions. Exothermic reactions take place inside the cell, so that an additional benefit is the possibility to exploit the heat generated.

Various kinds of fuel cells exist, with different thermodynamic working conditions, types of fuel, chemical reactions driving the process. Among them, Solid oxide fuel cell (SOFC) is the most promising technology, with characteristics such as fuel flexibility and higher values of efficiency with respect to other models. These cells operate at high temperatures, between 600° C and 1000 °C, leading to the following advantages: fast electrochemical reaction kinetics, fast species transport and high energy conversion efficiency. Moreover, the high working temperature makes the direct internal reforming process possible, and waste gas released from the SOFC can be used for thermal recovery.

The mentioned fuel SOFC flexibility is one of the most prominent aspects of this technology, because any of the hydrocarbons (C_xH_y) or any of the alcohols/ ethers (C_xH_yO_z) can be used.

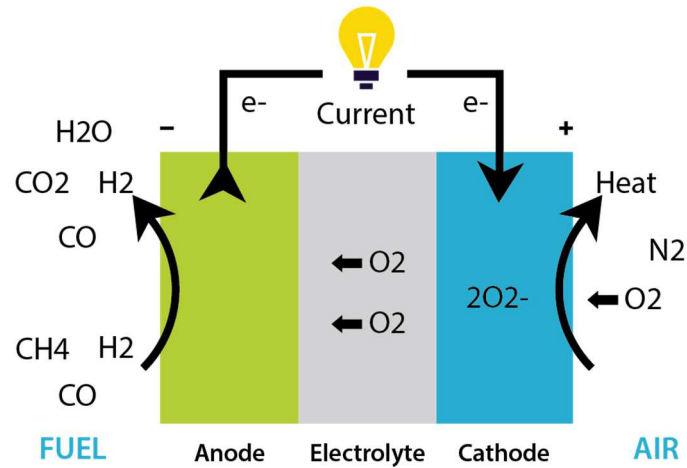


Figure 34: CH₄ SOFC schematic functioning

With regard to a CH₄ fed SOFC, the main reaction taking place in the electrolyte layer is shown in Figure 34: CH₄ SOFC schematic functioning and expressed as follows:



Some SOFC prototypes are also able to work using biogas as fuel. A gas clean-up is needed for those models, to feed the electrochemical cell with free pollutant gas. Before entering the stack, biogas and air are preheated. Once reactions in the electrolyte happen, the anode exhaust still has a few molecules of H₂, CO and CH₄, whose chemical energy is then recovered in an afterburner. Temperature of system exhaust is around 900°C, and exiting flow is sent to heat exchangers for fuel preheating, thus decreasing its temperature at ~250°C. This mass stream can be finally exploited to achieve thermal recovery. A scheme of SOFC based CHP is reported in Figure 35, underlying the electricity and heat provided.

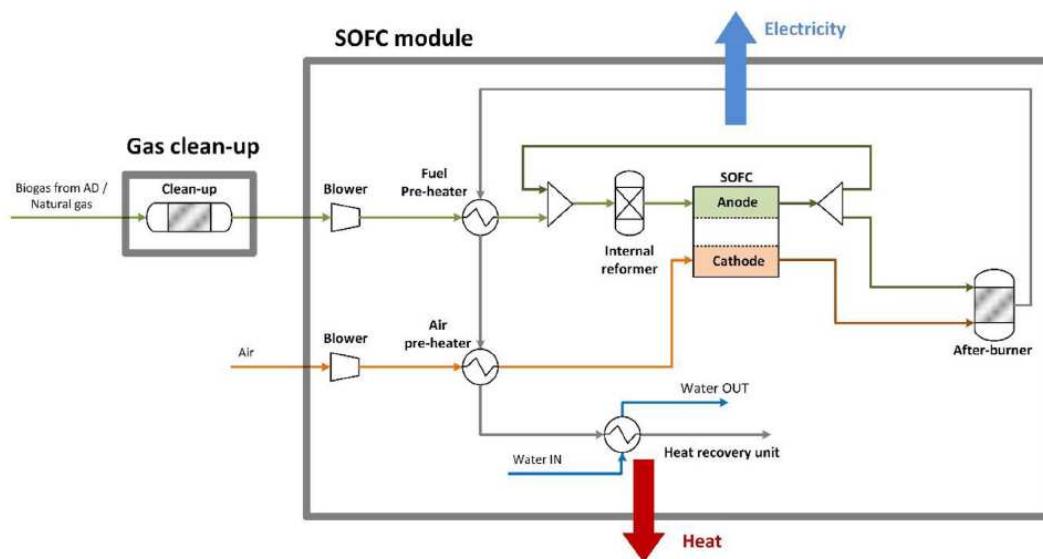


Figure 35: SOFC based CHP

Electric and thermal efficiency is written in SOFC module datasheet. An example is given in Figure 36:

Convion C60

Electric output	60	kW net-AC
Electrical efficiency	60	% (LHV)
Thermal output	27	kW (exhaust cooled to 40°C)
Total efficiency	84	% (LHV) (exhaust cooled to 40°C)
Range of electric output	65 - 33 kW (normal modulation range 100-50%, temporary modulation down to 30%)	

Figure 36: SOFC example datasheet [35]

In order to reach higher values of electric power several modules can be combined, the fuel cell technology being scalable. To determine the electrical and thermal energy the same formula of the ICE based CHP can be used.

3.3.4 Biogas Upgrading

An alternative to the direct use of biogas in boiler or CHP for thermal and/or electrical power is the purification of biogas from CO₂ through upgrading processes, finally obtaining biomethane.

In the last few years an increasing number of projects in upgrading biogas to biomethane have been developed, thanks to the advancement of upgrading technology combined with poor economics of electricity biogas plants and new opportunities of using biomethane for transport. In line with the development of biomethane plants, biomethane production has greatly increased since 2011. According to the European Biogas Association (EBA) *Statistical Report 2017* [36], biomethane production rose from 752 GWh in 2011 to 17,264 GWh in 2016 (+16,512 GWh). In 2016, biomethane production in Europe increased by 4,971 GWh (+40%).

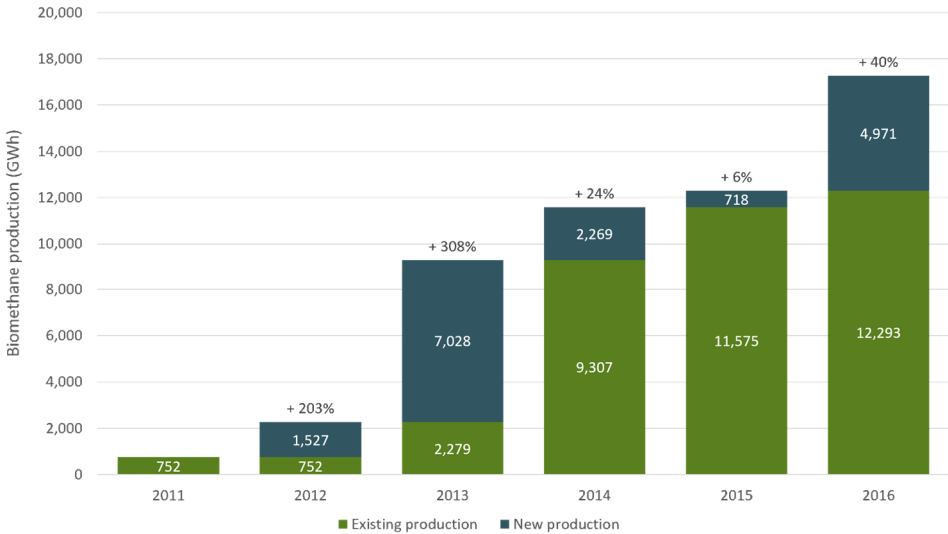


Figure 37: biomethane production [36]

Biomethane, being similar to Natural Gas in methane quantity and the content of trace gases, could be a substitute for fossil fuels and be injected in natural gas grid or used to supply traditional end-users (power plants, industries and households). Grid injection offers the most feasible possibility for storing renewable energy and applying it to RES based electricity generation at times of need.

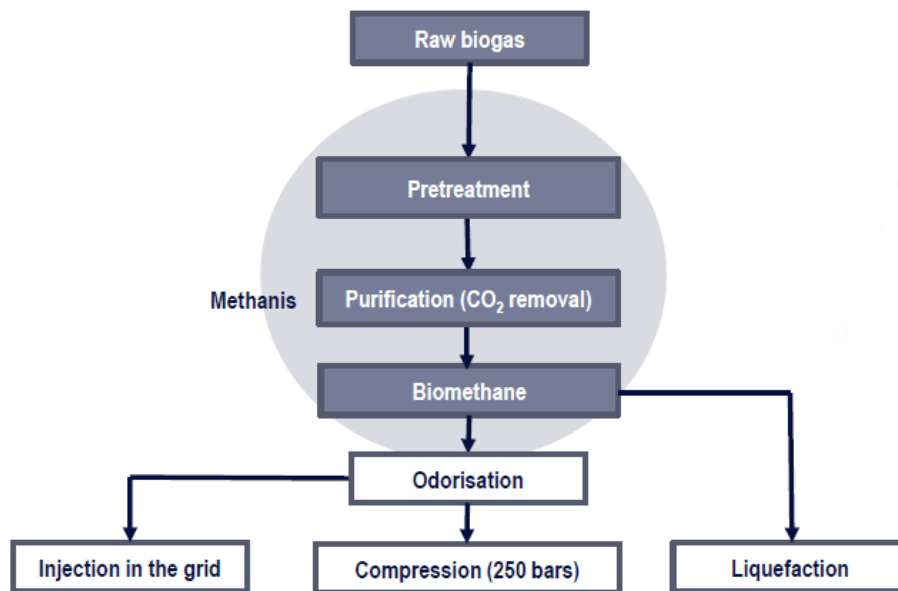


Figure 38: biogas upgrading process and possible utilization pathways

Biogas upgrading consists in a process in which CO₂ is removed from the gas, leading to an increased energy density since the concentration of methane is enhanced. Several technologies have been developed: Pressure Swing Adsorption, Water scrubbing, Amines scrubbing, Membranes, Cryogenics.

Pressure Swing Adsorption (PSA)

The separation of CO₂ is realized by adsorption on a surface under elevated pressure. The adsorbing material, usually activated carbon or zeolites, is regenerated by a sequential decrease in pressure before the column is reloaded again.

Absorption

The raw biogas meets a counter flow of liquid in a column where the contact area between the gas and the liquid phase is enhanced as much as possible. Since CO₂ is more soluble than methane, the liquid leaving the column will thus contain increased concentration of carbon dioxide, while the gas exiting the column will be rich in methane. There are three absorption technologies using different types of absorbents: water scrubbing, organic physical scrubbing and chemical scrubbing.

- **Water scrubbing:** In the scrubber column CO₂ is dissolved in water, making CH₄ content in the gas increase. Water leaving the absorption column is transferred to a flash tank where the dissolved gas, rich in CO₂, is released and transferred back to the raw gas inlet. To recycle water, it is transferred to a desorption column where CO₂ is released when it meets a counter flow of air. The water is cooled down

to achieve the large difference in solubility between methane and carbon dioxide before it is recycled back to the absorption column.

- Organic physical scrubbing: Similar to water scrubbing, with the important difference that the CO₂ is absorbed in an organic solvent such as polyethylene glycol. CO₂ is more soluble in polyethylene glycol than in water, thus lower liquid flow is needed which make smaller plants possible. The polyethylene glycol solution is regenerated by heating and/or depressurizing.
- Chemical scrubbers: They use an amine solution, mainly mono ethanol amine (MEA). In this case CO₂ is not only absorbed in the liquid, but it also reacts chemically with the amine in the liquid. Since the chemical reaction is strongly selective, the methane loss might be as low as <0.1%. The liquid in which carbon dioxide is chemically bound is regenerated by heating.

Membranes

Dry membranes for biogas upgrading are made of CO₂ permeable materials, water and ammonia and are usually built in hollow fibres bundled together. Hydrogen sulphide, and oxygen permeate through the membrane to some extent while only a very small amount of nitrogen and methane pass. Before the gas enters the hollow fibres, it passes through a filter that retains water, oil droplets and aerosols, which would otherwise negatively affect the membrane performance. By cooling the methane rich gas after the membranes, nitrogen can be separated from methane, due to the difference in their boiling points.

Cryogenic upgrading

This technology is based on the distinct boiling/ sublimation points of the different gases. The raw biogas is cooled down to the temperatures where the CO₂ in the gas condenses or sublimates and can be separated as a liquid or a solid fraction, while methane accumulates in the gas phase. Water and siloxanes are also removed during the cooling of the gas. The sublimation point of pure carbon dioxide is 194.65 K. However, the content of methane in the biogas affects the characteristics of the gas, i.e. higher pressures and/or lower temperatures are needed to condense or sublimate carbon dioxide when it is in a mixture with methane.

Among the described CO₂ removal technologies, the most widely used for biogas upgrading are PSA, water scrubbing, organic physical scrubbing and chemical scrubbing with MEA. The upgrading cost of these techniques, depending on the specific technology, is also strongly influenced by the size of the plant.

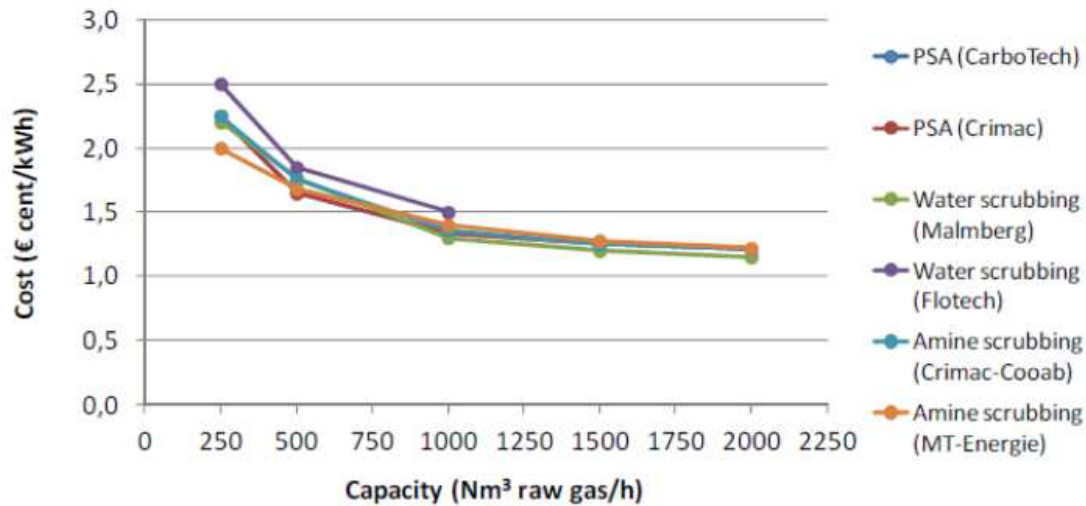


Figure 39: Cost for biogas upgrading for methane [37]

As shown in Figure 39, the higher the upgrading process size the lower the CO₂ removal cost. However, as explained above, biogas upgrading is developing rapidly and thus the cost is also expected to considerably decrease. In this framework the solution to produce bio-methane from industrial plant waste streams becomes very interesting. As for raw biogas, when referring to biomethane various uses can be considered.

In this study when dealing with biogas upgrading, in order to obtain economic and technical results associated to this intervention, the case in which biomethane is exploited in a GN-fed ICE CHP is considered.

3.4 Power and Waste to Fuel

As mentioned in chapter I, in order to keep the average global temperature rise below 2°C, the role played by renewable energy sources must become more significant. However, the intermittent nature of RES makes it difficult to match supply and demand. Because the supply of RES can hardly be scheduled, the greater the share of RES, the more difficult the match becomes. This will result in discrepancies between power produced by RES-based energy systems and requested power from the load. Therefore, there will be periods of over-production of energy from RES and periods of energy shortage. For this reason, the need for long term, large scale energy storage solutions is becoming increasingly important.

In this study we focus on how to turn the excess of power produced by RES into fuel that can be stored and reused when needed, i.e. the so-called Power-to-Fuel.

Power-to-Fuel is the process of converting surplus renewable energy, and it allows the storage of significant amounts of energy in the form of CO₂ neutral fuels. In this specific case we consider to produce methane starting from hydrogen produced in electrolysis, driven by renewable electricity, and combining it with CO₂.

H₂ coming from RES-driven electrolyser is thus combined with CO₂ coming from the treatment of the industrial plant waste. Hence, the described process can be also defined Waste-to-Fuel, referring to the exploitation of CO₂ from waste valorisation. A twofold effect is then obtained: on one hand, energy from renewables is stored, mitigating their intermittent nature; on the other hand, CO₂ is valorised.

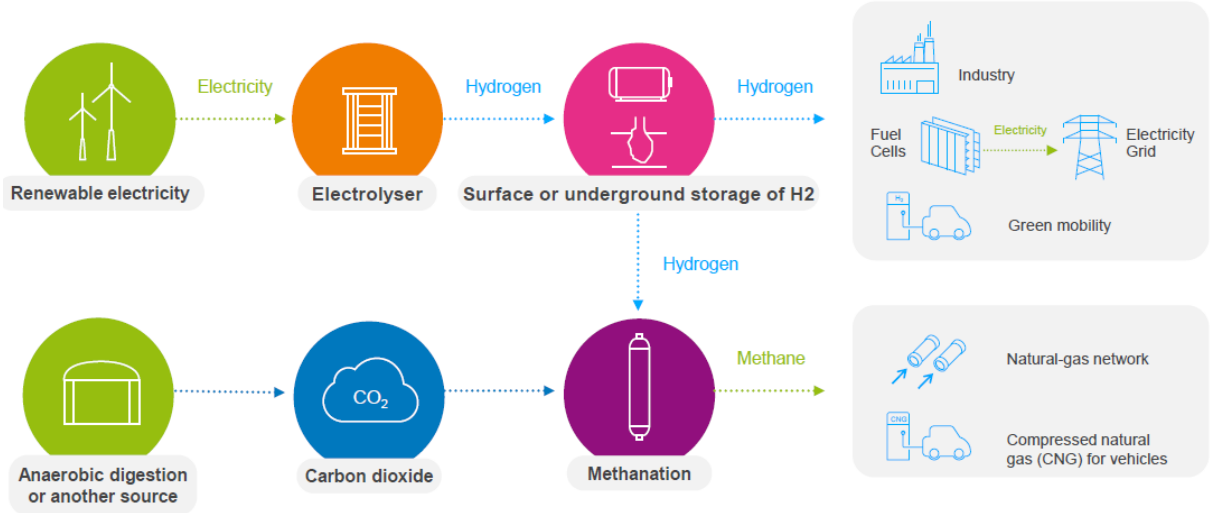


Figure 40: Power and Waste to Fuel scheme[38]

The main advantages of producing Synthetic Natural Gas (SNG) are:

- A carbon cycle close to zero;
- To avoid extracting fossil hydrocarbons and releasing the stored carbon into the atmosphere;
- The possibility of re-using the existing gas infrastructures (transmission and distribution network, underground storages).

However, the valorisation of CO₂ requires a considerable amount of high-quality energy, e.g. electricity for green hydrogen production. Thermodynamically, it is never efficient to convert high quality energy vectors into lower quality ones such as methane and other fuels, unless the amount of available renewable or low carbon energy is abundant.

Waste to energy is carried out through the following steps:

1. CO₂ is captured from biogas exiting an AD system;
2. Water electrolysis to produce pure hydrogen;
3. Hydrogen and carbon dioxide combination into synthetic Natural Gas (SNG);
4. Energy is then stored for short or long period of time, transported, distributed.

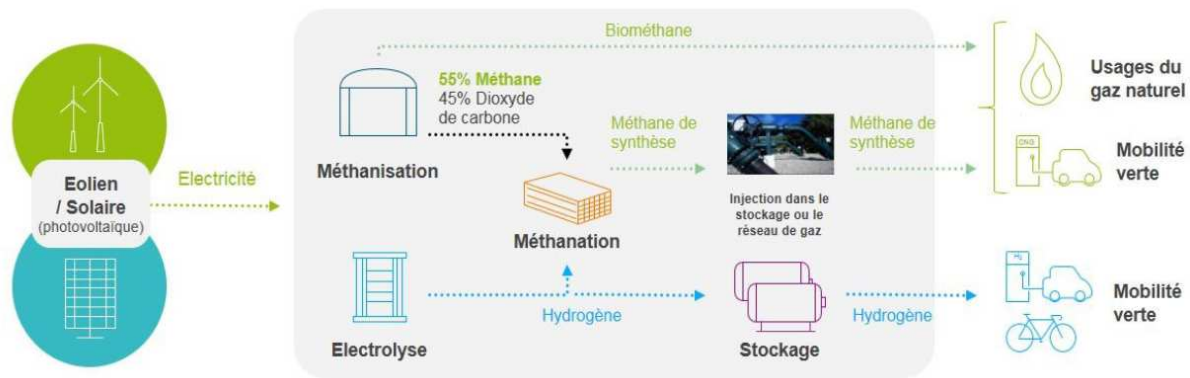


Figure 41: Power and Waste to Fuel main steps

CO₂ separation technologies have been discussed in biogas upgrading description. As for hydrogen production, electrolysis can be realized in a number of different devices:

- Alkaline electrolysis: proven concept for base production of hydrogen,
- PEM electrolysis: less developed but promising in terms of flexibility,
- SOEC/SOFC: still in the R and D phase.

Since excess power is intermittent, electrolysis and methanation have to be flexible and reactive. Thus, further developments are needed.

Another key point of methanation is inlet gas quality, as to reach the quality target energy expenses have to be considered, thus leading to downgrade the overall performance. Quality of in-gas required for methanation may vary: depending on the source of CO₂ and depending on the purification system.

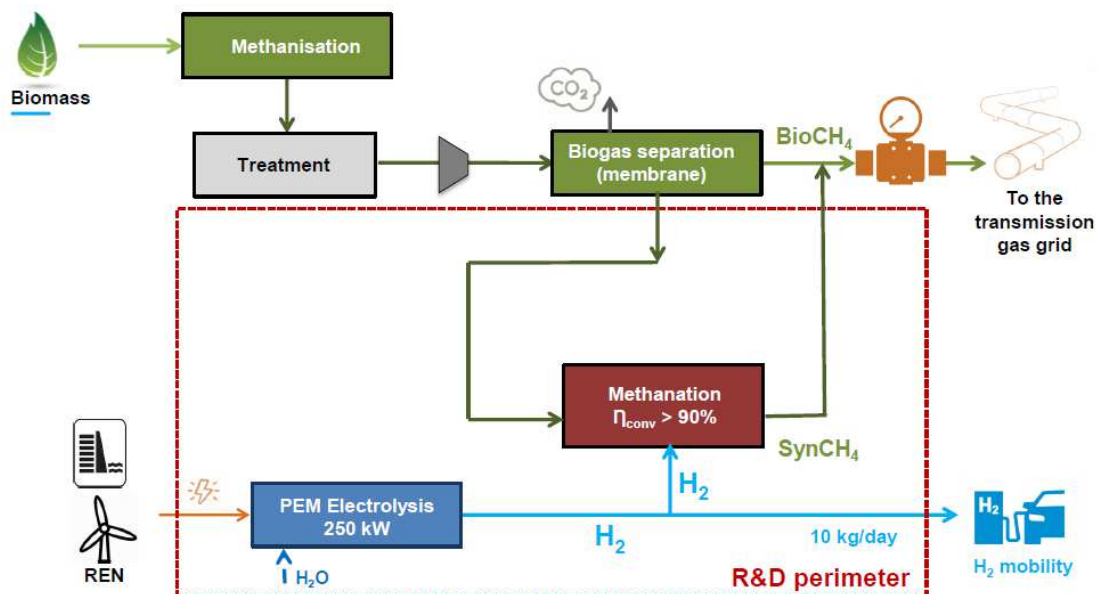
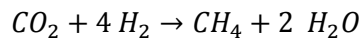


Figure 42: schematic demonstration of Methanation system based on a real project[38]

Once the electrolyser technology is selected, H₂ production potential can be estimated from system efficiency value, given in [kWh/Nm³], and the electric energy generated by the PV field.

The chemical reaction taking place in the methanation unit, and representing the core of the process is:



Four moles of H₂ and one of CO₂ are required to produce one mole of CH₄. Therefore, since the amount of CO₂ coming from the anaerobic digester is much greater than that needed to form CH₄, only a part of the carbon dioxide is used.

3.5 Shifting Thermal towards Electric

As previously discussed, thermal energy produced by industry covers a large part of the total amount of GHG emitted. Hence, solutions aimed at reducing CO₂ released in combustion processes in the boiler have to be introduced. As an alternative to thermal power production from RES and in order to avoid combustion, the possibility to generate heat from an electric vector has been then developed. This could be an advantage for decarbonisation of heat supply once primary electricity production relies more and more on renewable sources.

It must be noticed that, considering the target of GHG reduction of this study, the idea of shifting thermal consumption to electricity represents no advantage unless electricity derives from RES. In the opposite case, if we do not supply electricity from grid from a zero-emission source, we must resort to traditional combined cycle generators, powered by fossil fuels and thus emitting GHG in atmosphere. If such electricity is then used as an energy vector to be transformed back into thermal energy, this process of transformation is also associated to energy losses. The final result would be that, to produce the same amount of thermal energy, much more CO₂ is released in atmosphere than it would be using traditional boilers.

For industry or services, a large variety of electric technologies may respond to the demand for heat. Some will simultaneously use another source of heat, often waste heat from an industrial process nearby, such as industrial heat pumps and mechanical vapor recompression devices. Moreover, in some cases the use of electricity can be more efficient than the direct use of heat, offering the possibility to reduce the carbon intensity of industrial processes if renewable electricity is used.

Starting from the hypothesis of consuming electricity on-site produced from renewables, the possible technologies able to supply thermal energy at 160° are:

- Heat pump;
- Microwave or technologies based on non-conductive/non-convective processes;

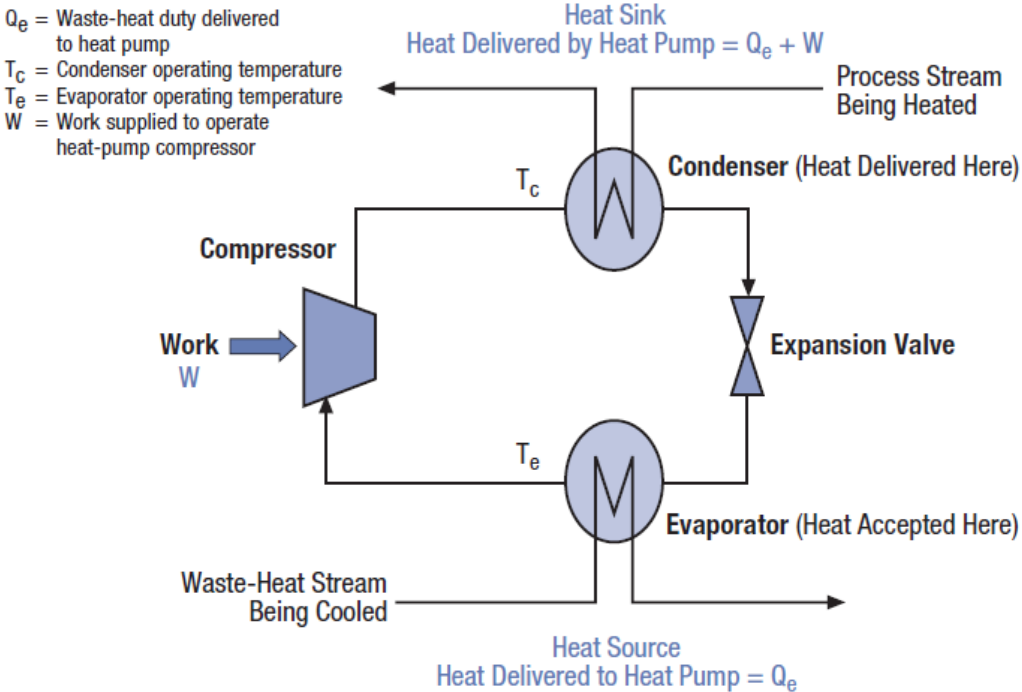
3.4.1 Heat Pumps for thermal recovery

A heat pump is a device where temperature of a low enthalpy stream is increased to a temperature where the waste heat becomes useful, by supplying it with external mechanical or thermal energy.

The installation of this machine to cover the industrial plant thermal needs would be advantageous: first it would permit thermal recovery of waste energy streams otherwise lost; second, when considering an innovative and performant prototype of heat pump, this intervention would allow the valorisation of low temperature streams, whose enthalpy is enhanced by providing it with external work; third, if electric power is used to drive the process, no fossil fuel combustion in boilers is needed for heat generation. Therefore, when electricity comes from RES the thermal output of the system does not cause GHG emissions.

Although there are several types of heat pumps, they all perform the same three basic functions: collect heat from the waste-heat source, increase its temperature, deliver useful heat at higher temperature.

In Figure 43 the scheme of the most common heat pump type, the mechanical one, is given.



1. Waste-heat stream evaporates heat-pump working fluid at low temperature and pressure
2. Compressor increases pressure of heat-pump working fluid
3. Heat-pump working fluid condenses at high temperature and pressure in the condenser, providing useful heat to a process stream
4. Condensed working fluid is expanded back to the evaporator

Figure 43: Simple Schematic of Mechanically Driven Heat Pump [39]

The most common types of heat pumps are listed below:

- Closed-Cycle Mechanical HP: they use mechanical compression of a working fluid to achieve temperature lift. The working fluid is commonly a refrigerant (e.g. R134);

- Open-Cycle Mechanical Vapor Compression (MVC) HP: a mechanical compressor increases the pressure of waste vapor. The typically used working fluid is water vapor. MVC heat pumps are considered to be open cycle because the working fluid is a process stream;
- Open-Cycle Thermocompression HP: it uses energy in high-pressure motive steam to increase the pressure of waste vapor using a jet-ejector device. It is common in evaporators, with steam as working fluid;
- Closed-Cycle Absorption HP: it uses a two-component working fluid and the principles of boiling-point elevation and heat of absorption to achieve temperature lift and to deliver heat at higher temperatures.

Regarding the industrial food sector, because of the great share of heating processes in the medium temperature required, in the last decade high temperature heat pumps have been strongly implemented.

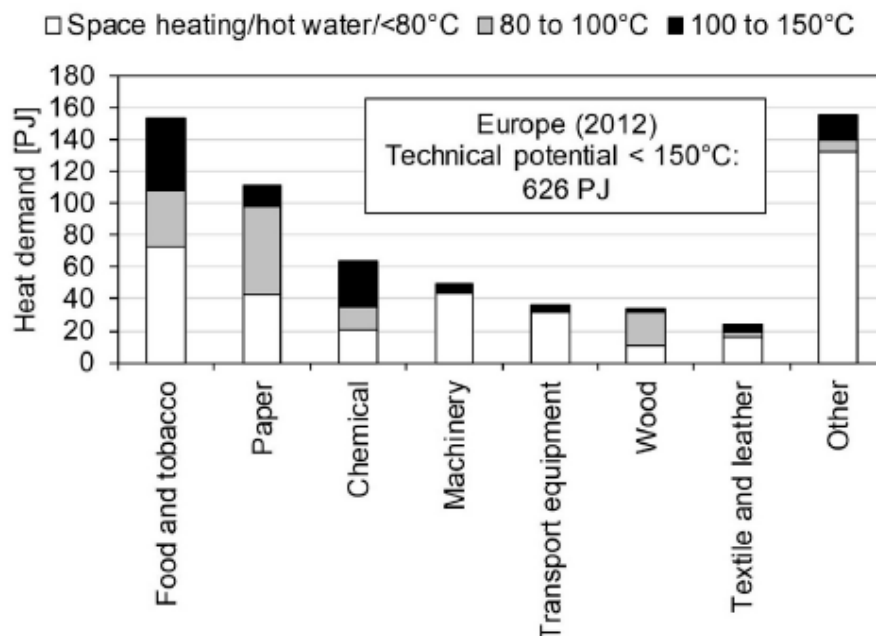


Figure 44: Technical market potential of process heat in Europe accessible with industrial heat pumps distributed by temperature and industrial sector [31]

However, until now only a few heat pumps are able to reach temperature in the range of 120-160 °C. Some commercially available prototypes of closed cycle mechanical devices are shown in Figure 45: Commercially available industrial HTHPs sorted by maximum heat sink temperature [40].

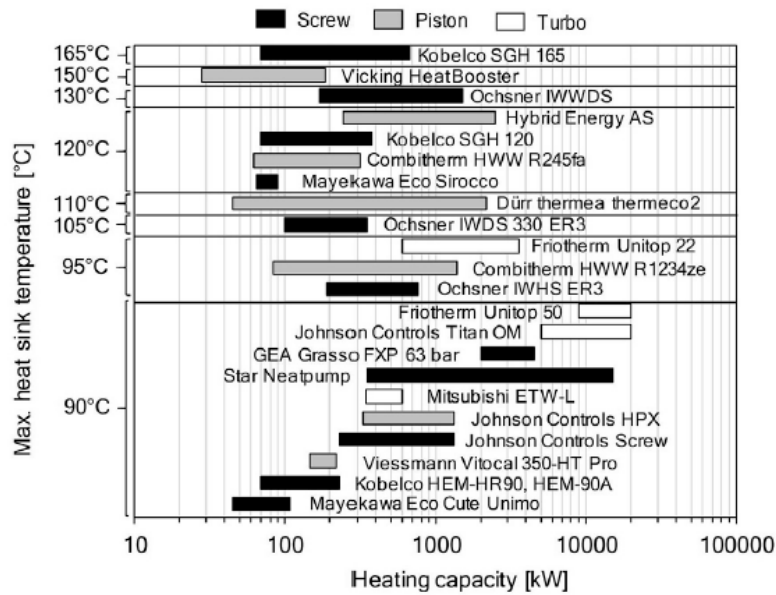


Figure 45: Commercially available industrial HTHPs sorted by maximum heat sink temperature [40]

Among the different models, Kobelco SGH 165 and Viking Heat Booster have been considered in detail, as they can reach the temperature level needed in the studied industrial plant.

Designed by the Japanese company Kobe Steel, the SGH165 model generates steam at 165°C from process waste heat at 35° to 70 °C and obtains 120 °C steam, then recompressed to 165 °C (6 bar). The semi-hermetic twin-screw compressor has been specially developed for high pressure ratio and temperature. Steam at 165 °C is generated with a heating COP of 2.5 when using waste heat of 70 °C.

The SGH120 is composed of a heat pump unit and a flash tank. The heat pump unit lifts the heat from the heat source water and sends the heat to the pressurized circulating water. In the flash tank, the pressurized water is decompressed and evaporated. Consequently, the flash steam (up to 120°C, 0.1MPaG) is supplied to each process, and the remaining saturated water goes back to the heat pump unit.

Furthermore, a steam compressor is added to the above system to compresses the saturated steam generated in the flash tank. For preventing the superheat of the discharge steam, water is injected to the compressor. The discharge steam (up to 175°C, 0.8 MPaG) is separated from the mist at the drain separator and supplied to each process.

The refrigerant is a mixture of R134a and R245fa to achieve a good performance.

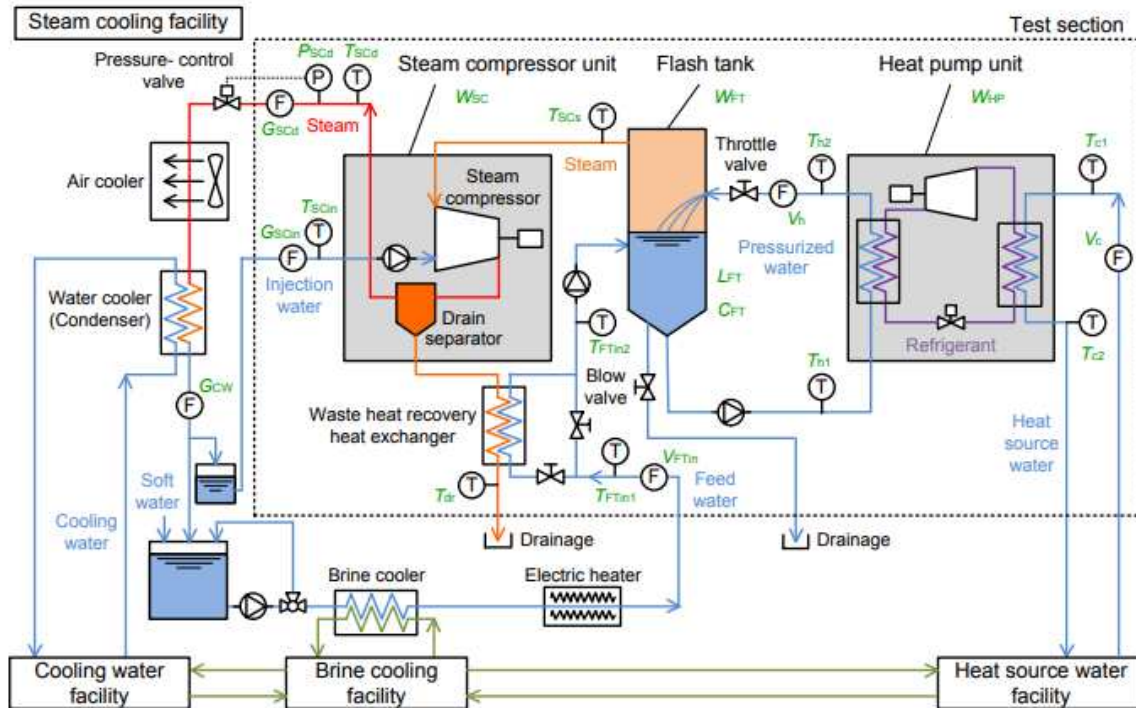


Figure 46: Schematic diagram of an Open Cycle Mechanical HP

This technology, still under development, seems to be very promising. However significant steps are needed for it to become competitive in the heat pump market.

Therefore, in this analysis simulations have been carried out with *Viking Heat Booster* piston compressor heat pump [41]. The share of electric power absorbed by its mechanical compressor strongly depends on temperature conditions at recovery and delivery sides. The Coefficient Of Performance (COP) of the machine is then responsive to the mentioned temperature levels and, as a consequence, useful thermal power is related to thermodynamic conditions of source and sink. The relationship between COP and useful heat is given by the following formula:

$$P_{th,user} = P_{el} \cdot COP$$

Where

- P_{el} and $P_{th,user}$ are respectively the electrical power to the compressor and the useful power to the user, in [kW];
- COP can be found with the formula that follows;

Starting from a certain value of electric power absorbed, higher COP values lead to a greater useful effect.

For the chosen heat pump prototype the COP curve is built in Figure 47, based on experimental data. The COP dotted trend line together with its polynomial formulation is reported, being traced as a function of temperature lift. The temperature lift is a parameter used to represent the temperature drop between the exiting temperature of heat transfer fluid source side and the exiting temperature of heat transfer fluid sink side.

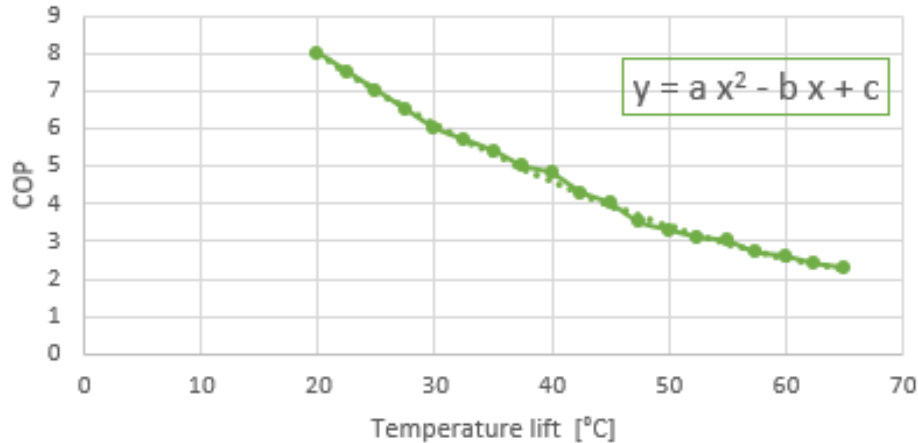


Figure 47: COP curve

In comparison with standard heat pump technology, the considered prototype is able to work with higher temperature lift, thus permitting the generation of thermal power at high temperature starting from much lower temperature at recovery side. However, the COP curve decreases monotonically, as a consequence of the fact that machine performance degrades as the temperature difference between source and sink increases.

3.4.2 Electro-heat technologies

As previously said, in the studied case, the greatest share of thermal energy is required by the drying processes. The same happens in general in the food sector industry, where one of the most energy consuming unit operations is thermal processing including pasteurization, sterilization, dehydration, drying, chilling, and freezing.

The present study focuses on the drying processes mentioned above, to find technical solutions able to save energy and consequently reduce emissions. These processes are conventionally driven by heat transfer to the food material through convection, conduction, and radiation. Nevertheless, novel technologies, still commercially available, are based on other effective methods of heat transfer. Hence, the application of these food processing techniques could bring to energy savings and emission reduction.

Emerging technologies are divided into two main categories:

- thermal (e.g., ohmic heating (OH))
- nonthermal processing (e.g., high-pressure processing, electro-technologies, and irradiation).

These methods are based on different mechanisms such as electromagnetic, electric field, and pressurization, resulting in better heat transfer than conventional methods. Moreover, in addition to generating energy saving, most of them also lead to water saving, reliability increment, emissions lowering, better product quality, and productivity enhancement.

With respect to pasta drying, this process reduces the water availability (water activity) and makes the growth of microorganisms during storage difficult. The conventional method of drying food products is hot air, used in the studied plant as well. In this

technique, convection is the way the heat is transferred from gas to the treated product. Drying consumes a significant amount of energy and the rate of convective heat transfer could be written as

$$Q = h_c \cdot S \cdot (T_s - T_\infty)$$

Where

- Q is the thermal energy needed to realize the drying process, expressed in [W];
- h_c [W/m² K] is the convective heat transfer coefficient;
- S [m²] is the boundary surface area;
- T_s and T_∞ are the temperatures at the surface and at the bulk fluids, respectively.

An average of 6 MJ is required to remove 1 kg of water from a product [42].

A synthetic description of the mentioned electro-heat technology is provided in the table below, based on the publication “*SUSTAINABLE FOOD SYSTEMS FROM AGRICULTURE TO INDUSTRY Improving Production and Processing*” [34].

Table 5: Electro-Heat technologies

TECHNOLOGY	How it works	Advantages	Limitations
Pulsed Electric Fields (PEF)	electrical treatment of short time (from μ s to ms) with electric field strength from 100–300 V/cm to 20–80 kV/cm	Destruction of vegetative cells with preservation colors, flavors, and nutrients; relatively short treatment time; no environmental hazard;	no effect on spores and enzymes; high initial cost; possible adverse effects due to products of electrolysis;
High-voltage electrical discharges	When the food matrix contains enough water and electrolytes to allow the passage of electric current, rapid and uniform heating of the sample, which leads to consistent and rapid heat generation; heating occurs in the form of internal energy transformation (from electric to thermal) within the material;	preservation of colors, odors, and nutrients with no temperature increment during treatment by arc discharge; inactivation of microorganisms and enzymes;	possibility of contaminations with chemical products of electrolysis and disintegration of food particles by shock waves;
Ohmic heating (OH)	Dielectric breakdown as the result of ionization of the liquid upon applying a high voltage (30–40 kV) and intensity (\sim 10 kA) pulse of short duration (μ s-ms) between two electrodes;	faster achievement of temperature required for processes; quicker heating rate with uniform heating of liquid sample; lower overheating problems; less maintenance costs; negligible heat losses; no	high costs of commercial systems; foods with fat globules, nonconductive, suffers the fact that any pathogenic bacteria in these globules may receive lower heat treatment;

		residual heat transfer after the current is shut off;	by increment of the temperature system, higher electrical conductivity is observed because of the faster movement of electrons, leading to higher possibility of “runaway” heating
High-pressure processing (HPP)	food products are exposed to very high pressure (ranged from 100 to 800 MPa)	minimized thermal degradation of food compounds → high retention of flavor, color, nutritional value and depression of freezing point of water; uniform and instantaneous pressure through the food sample independently of its mass, shape, and composition	High installation cost; essential need of presence of water in food samples being a compression-based process; higher attention requirement for structurally fragile foods;
Microwaves (MW)	electromagnetic energy with frequencies in the range of 0.3–300 GHz	Cooking throughout the whole volume of food internally → significant reduction in the processing time and energy; preservation of nutrients, flavor, and color as a result of quick heat transfer; removal of the hot heat transfer surfaces leads to minimum fouling depositions, since the piping applied is microwave transparent and remains relatively cooler than the product; suitable for heat-sensitive, high-viscous, and multiphase fluids; high heating efficiency	lack of ability to control, predict, and measure the exact temperature at different part of the sample; depending on several factors (e.g., nature of the food products, food geometry, dielectric properties, and oven designs), degradation kinetics of either quality, sensory, or nutrients may occur;
Ultrasounds	A sonotrode generates an intense sound wave (20 kHz–1 MHz), which passes through a liquid, and creates compression and rarefaction regions, so bubbles are formed. After a certain number of compressions and	more effective mixing and micromixing; faster energy and mass transfer; thermal and concentration gradients decrement, temperature reduction, selective extraction, equipment size lowering, quicker	depth of penetration affected by solids and air in product, needs to be used in combination, potential problems with scaling-up plant with another process (e.g., heating)

	rarefactions, the bubble reaches an instable size and may collapse violently. High local pressure and temperature are accompanied with implosion, which could reach 50 MPa and 5000°C	response to process extraction control, faster start-up, production increment, and removal of process steps	
Infrared processing	Electromagnetic waves in three different regions: the near-infrared (NIR; 0.78–1.4 μm), middle-infrared (MIR; 1.4–3 μm) and farinfrared (FIR; 3–1000 μm); no need of air for IR energy transmission. Generally, as air and gases can absorb very little IR energy, the IR heating process provides efficient heat transfer without contact between the heat source and the material being heated;	high thermal efficiency, alternate source of energy, quick rate of heating, shorter response time, uniform drying temperature, high control degree of process, cleaner working environment, and possibility of selective heating;	low power of penetration and fracturing possibility of biological materials as a result of prolonged exposure
Ultraviolet and pulsed light processing	using short-time pulses of an intense broadspectrum, rich in UV-C light; PL system consists of constituents including power supply, lamp, and configuration device. High energy is received in the lamp leading to an intense pulse, which typically lasts a few hundred microseconds	-UV: no chemical application, a nonheat-related process with less changes in color and flavor, no residual in the fluid stream - PL treatment: quality and nutrient components are relatively retained; PL is more environment friendly with respect to UV;	-UV: harmful for human eyes and longer exposure may lead to burns and skin cancer in humans; restricted range of commercially available equipment for disinfecting solids; - PL: presence of crevices or folds in food samples may result in microbial survival due to lower exposure in these parts; mostly applicable for liquid sample and surface of solid foods and thus limiting its usage; needed of controlling food heating, as undesirable color changes of the sample before microbial inactivation was completed due to thermal effect.

3.6 Carbon Capture and Utilization

Carbon capture technology falls among the various solutions proposed by IEA in its report *Energy Technology Perspectives 2017* [8]. As explained in first chapter, IEA built an ideal scenario, the Blue-Map scenario, in which through the combination of various technical solutions, the average global temperature rise would be kept below 2 °C with respect to preindustrial levels.

Compared to other solutions, carbon capture represents a fundamental instrument to stabilize GHG emission while still relying on fossil fuels technologies in the transition towards carbon free ones.

Two pathways are possible: Carbon capture and Storage (CCS) and Carbon capture and Utilization (CCU). Here, the option chosen is the latter, as CO₂ is considered to be an exploitable energy vector.

Carbon capture is implemented through three systems associated with different combustion processes:

- POST-COMBUSTION CC (suitable for existing infrastructure)
- PRE-COMBUSTION CC (suitable for new infrastructure)
- OXY-FUEL COMBUSTION

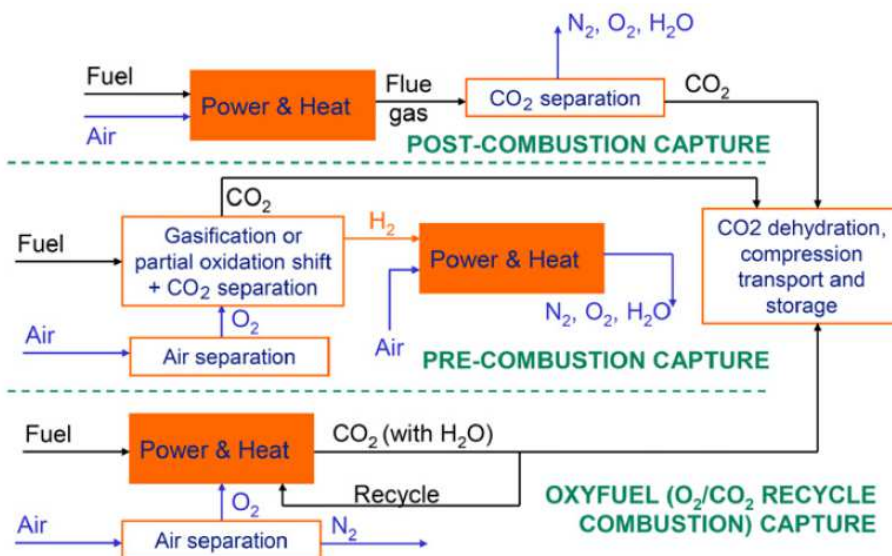


Figure 48: Carbon Capture different pathways

3.6.1 POST COMBUSTION

It consists in properly treating exhaust of a combustion process in order to remove CO₂. During the process chemical absorption takes place in an absorption column, where a counter flow of the gas to be solved with the solvent is realized.

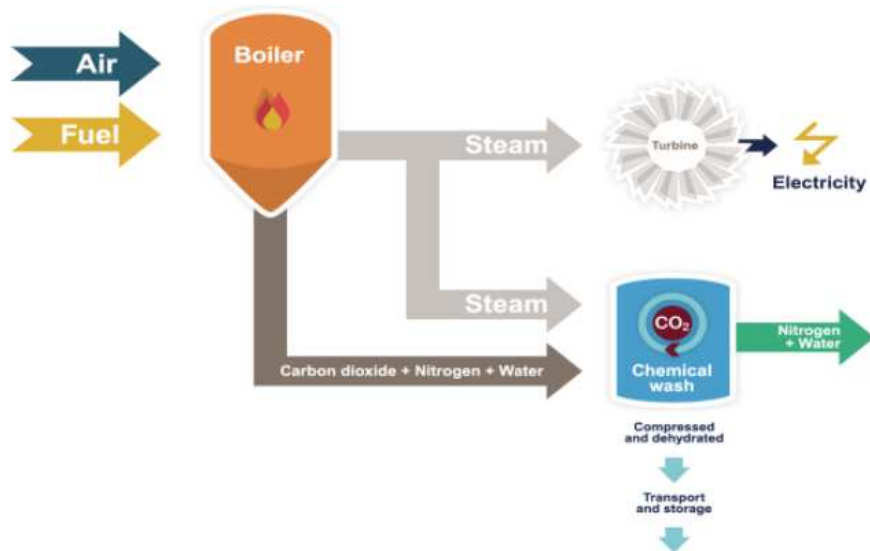


Figure 49: schematic representation of post- combustion CC [43]

The most commercially advanced methods use wet scrubbing with aqueous amine solutions, often a mixture of 30 % amine (most commonly used is Mono-Ethanol Ammine MEA) diluted in water.

The absorption of CO₂ in water would occur more easily at high pressure and low temperature. Nevertheless, flue gas is usually available at ambient temperature and it would be useless and very costly to re-pressurize it. To account for this problem MEA is used, as it enhances the process, permitting to work at approximately ambient thermodynamic conditions.

Typical capture units are made of two columns: the absorber and the desorber. In the absorber, a scrubber column where chemical wash is performed, the CO₂ in the flue gas reacts with the solvent. This CO₂ rich solvent is then sent to the desorber, a stripper column where, under the action of heat, the CO₂ is recovered, and the solvent regenerated and sent back to the absorber. The external expenditure is the heat to drive the reboiler, needed to improve solvent purity after the regeneration.

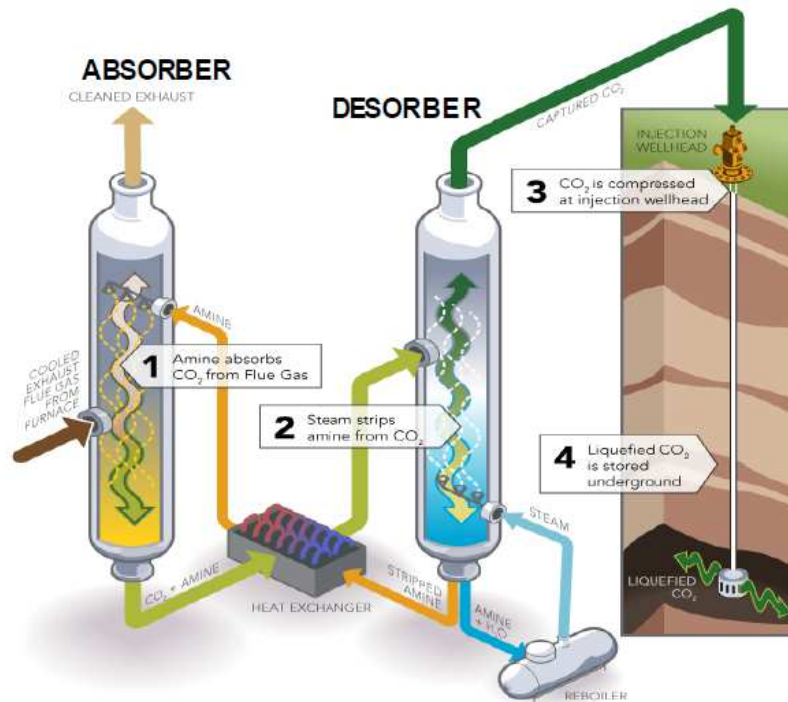


Figure 50: absorption process [43]

CO₂ is removed from the waste gas by the amine solvent at relatively low temperatures. The solvent is then regenerated for re-use by heating, before being cooled and recycled continuously. Thus, operating conditions are:

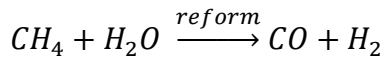
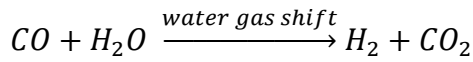
- At the Scrubber → T=40°C and P=1 bar;
- At the Stripper → T=140°C and P=2,1 bar;

Post-combustion technologies are the preferred options for retrofitting existing power plants. Since the CO₂ level in combustion flue gas is normally quite low (i.e. 7–14% for coal-fired and as low as 4% for gas-fired), the energy penalty and associated costs for the capture unit to reach the concentration of CO₂ (above 95.5%) needed for transport and storage are too high. [44]

3.6.2 PRE-COMBUSTION CC

Mainly applied to Integrated Gasification Combined Cycle (IGCC), a combined cycle power plant which burns a syngas produced by gasification of coal, pre-combustion carbon capture is a technology where syngas produced by the gasification of coal is shifted to pure hydrogen and CO₂.

Rather than being directly exploited to produce energy, the gaseous fuel is first pre-treated with steam in a Water Gas Shift (WGS) reactor, in order to shift all the carbons in CO₂ molecules, which are then separated from the other compounds. When considering a natural gas-fed plant, reforming of the methane is done before the CO and H₂ mixture enters the water gas shift unit. The two main chemical reactions on which pre-combustion is based are written below:



The hydrogen can then be burned in a gas turbine to generate power with an exhaust that is CO₂ free, or sold for other uses.

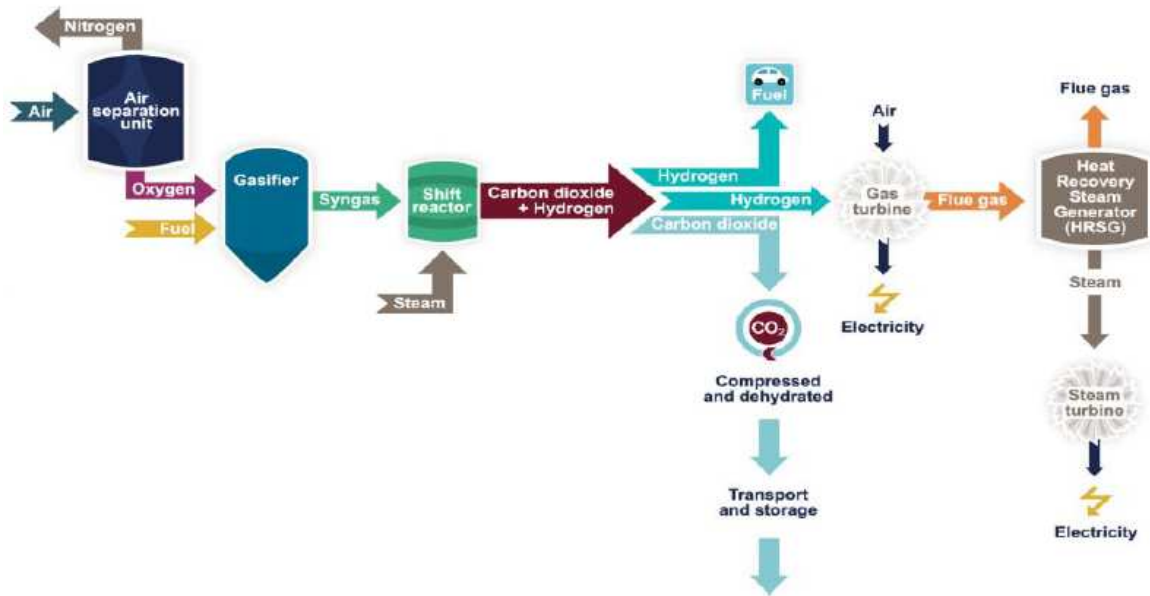


Figure 51: schematic representation of pre-combustion CC [43]

The separation process, driven by high P and low T, typically uses chilled methanol at -20/-40 °C as physical solvent in an Acid Gas Removal Unit.

Being dissolved at higher pressure, CO₂ is then released as the pressure is reduced. In comparison with post-combustion capture, pre-combustion systems do not require heat but pay an efficiency penalty for the shift reaction. In addition, the efficiency of hydrogen-burning gas turbines is lower than conventional ones since turbine inlet temperatures must be reduced in order to avoid too high metal temperature. The external expenditure is the energy required to cool methanol down to -20°C.

Only a few coal gasification units for power plant exist and a retrofit is complicated if not foreseen in the design.

3.6.3 OXY-FUEL COMBUSTION CC

This technology is based on stoichiometric oxidation of the fuel with pure oxygen in an oxygen enriched environment and in the absence of nitrogen, leading to flue gases containing mainly CO₂ and water vapor, then removed by condensation. The oxygen is diluted in flue gas, which is cooled, recirculated, and injected into the combustion chamber to control the temperature.

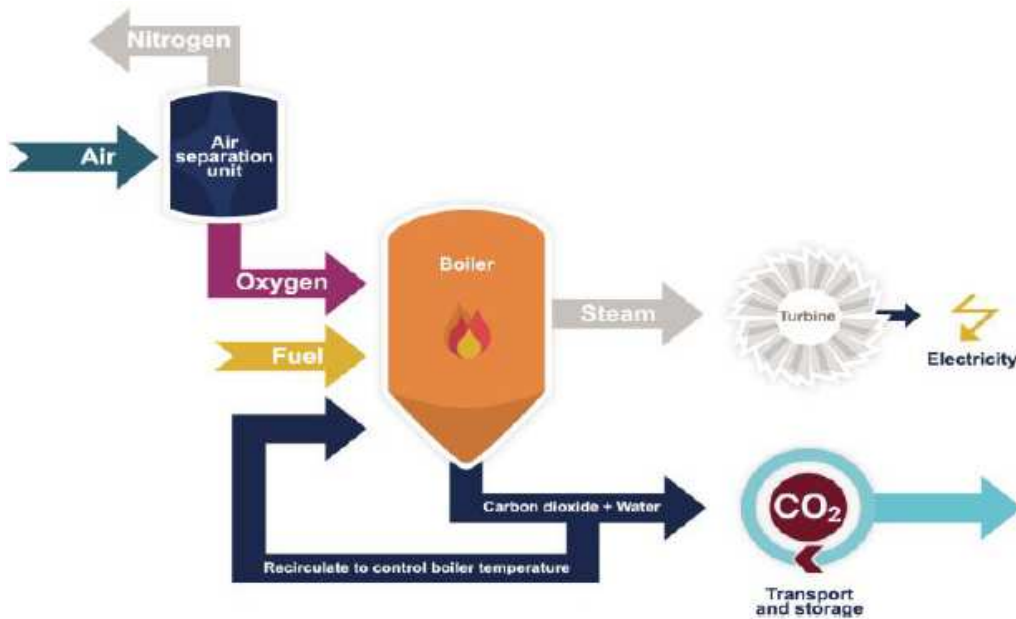


Figure 52: schematic representation of oxy-combustion CC [35]

A critical step in oxyfuel technology is the oxygen production, most of the time obtained in air separation unit ('Air Separation Unit'- 'ASU'). This results in high cost and the energy penalty may reach over 7% compared to a plant without CCS [45].

With oxyfuel technology, virtually zero emission power plants can be achieved with almost 100% CO₂ capture. The external expenditure in this case is the energy required to produce pure oxygen.

Oxyfuel technologies are used in some industrial processes such as glass manufacturing but is still in the demonstration phase in power generation.

3.6.4 Separation technologies

Many separation technologies can be applied to isolate the CO₂ from the flue/fuel gas stream, based on chemical, physical or hybrid absorption, adsorption, membranes separation or cryogenic separation. A more detailed description follows, with a final comparison in Table 6, in which advantages and disadvantages are listed, based on information taken by [44].

- Absorption

A liquid sorbent is used to separate the CO₂ from the flue gas. The sorbent is regenerated in a stripping or regenerative process by heating and/or depressurization. Most commonly used is mono-ethanolamine (MEA) with absorption efficiency over 90% [46]. This process is the most mature method for CO₂ separation.

- Adsorption

In this technology a solid sorbent is used to bind the CO₂ on its surfaces. Specific surface area, selectivity and regeneration properties must be as high as possible and impact the choice of sorbent material. Typical sorbents include molecular sieves, activated carbon,

zeolites, calcium oxides, hydrotalcites and lithium zirconate. The adsorbed CO₂ can be recovered by swinging the pressure (PSA) or temperature (TSA) of the system containing the CO₂-saturated sorbent.

- Chemical looping combustion

During this process a metal oxide, used as an oxygen carrier, reduces to metal while fuel oxidizes to CO₂ and H₂O. Furthermore, the metal is then oxidized in a subsequent stage and recycled back. Water is removed by condensation, while pure CO₂ can be obtained without consumption of energy for separation. There are a wide variety of metal oxides that are low-cost and suitable for this process, including Fe₂O₃, NiO, CuO and Mn₂O₃.

- Membrane separation

CO₂ permeable membranes are used, while excluding the passage to other components of the flue gas. The selective layer is made of a composite polymer, bonded to a thicker, non-selective and low-cost layer that provides mechanical support to the membrane. Highly efficient membranes can achieve a separation efficiency from 82% to 88%. However, the performance of a membrane system is strongly affected by the flue gas conditions such as low CO₂ concentration and pressure.

- Hydrate-based separation

This mechanism is based on the differences of phase equilibrium of CO₂ with other gases, where CO₂ can form hydrates easier than other gases such as N₂. In fact, hydrates are formed when exhaust gas containing CO₂ enters in contact with high pressure water. The CO₂ is so selectively engaged in the cages of hydrate and is separated from other gases. This technology is current in the R&D phase.

- Cryogenic distillation

Cryogenic distillation is a gas separation process using distillation at very low temperature and high pressure. Flue gas containing CO₂ is cooled to de-sublimation temperature (−100 to −135 °C) and then solidified CO₂ is separated from other light gases and compressed to a high pressure of 100–200 atmospheric pressure. The amount of CO₂ recovered can reach 90–95% of the flue gas. Since the distillation is conducted at extremely low temperature and high pressure, it is an energy intensive process.

Table 6: Comparison of different separation technologies

Technology	Advantage	Disadvantage
Absorption	<p>High absorption efficiency (>90%).</p> <p>Sorbents can be regenerated by heating and/or depressurization.</p> <p>Most mature process for CO₂ separation.</p>	<p>Absorption efficiency depends on CO₂ concentration.</p> <p>Significant amounts of heat for absorbent regeneration are required.</p> <p>Environmental impacts related to sorbent degradation have to be understood.</p>

Adsorption	Process is reversible and the absorbent can be recycled. High adsorption efficiency achievable (>85%).	Require high temperature adsorbent. High energy required for CO ₂ desorption.
Chemical looping combustion	CO ₂ is the main combustion product, which remains unmixed with N ₂ , thus avoiding energy intensive air separation.	Process is still under development and there is no large-scale operation experience.
Membrane separation	Process has been adopted for separation of other gases. High separation efficiency achievable (>80%).	Operational problems include low fluxes and fouling.
Hydrate-based separation	Small energy penalty.	New technology and more research and development is required.
Cryogenic distillation	Mature technology. Adopted for many years in industry for CO ₂ recovery.	Only viable for very high CO ₂ concentration >90% v/v; Should be conducted at very low temperature; Process is very energy intensive.

3.6.5 Comparison of different combustion technologies for CO₂ capture

In Table 6 the carbon capture technologies described above are compared, underlying application areas, advantages and disadvantages of each one of them.

Table 7: Advantages and disadvantages of the different CO₂ capture technologies

Capture process	Application area	Advantages	Disadvantages
Post-combustion	Coal-fired and gas-fired plants	more mature technology; can easily retrofit into existing plants;	Low CO ₂ concentration affects the capture efficiency;
Pre-combustion	Coal-gasification plants	High CO ₂ concentration enhance sorption efficiency; fully developed technology, commercially deployed at the required scale in some industrial sectors; opportunity for retrofit to existing plant;	Temperature associated heat transfer problem and efficiency decay issues associated due to the use of H ₂ -rich gas turbine fuel; high parasitic power requirement for sorbent regeneration; inadequate experience due to few gasification plants currently operated in the market; high capital and operating costs for current sorption systems;
Oxyfuel combustion	Coal-fired and gas-fired plants	Very high CO ₂ concentration that enhances absorption efficiency; mature air separation technologies available; reduced volume of gas to be treated, hence required smaller boiler and other equipment;	High efficiency drop and energy penalty; cryogenic O ₂ production is costly; corrosion problem may arise;

Pre-combustion is mainly applied to coal-gasification plants, while post-combustion and oxyfuel combustion can be applied to both coal and gas fired plants. Post-combustion technology is currently the most mature process for CO₂ capture [47].

Table 8 instead refers to cost of the different technologies and is based on a IEA study [48]. For Coal-fired plants the pre-combustion technology presented the lowest cost per tonne of CO₂ avoided, while the post-combustion and oxyfuel technologies are of similar costs. However, for gas-fired plants, the cost per tonne of CO₂ avoided for the post-combustion capture was almost 50% lower than the other two capture technologies. Moreover, the post-combustion CO₂ capture is normally the least efficient option, with an energy penalty of about 8% and 6% for the coal-fired and gas-fired plants, respectively.

Fuel type	Parameter	Capture technology			
		No capture	Post-combustion	Pre-combustion	Oxy-fuel
Coal-fired	Thermal efficiency (% LHV)	44.0	34.8	31.5	35.4
	Capital cost (\$/kW)	1410	1980	1820	2210
	Electricity cost (c/kWh)	5.4	7.5	6.9	7.8
	Cost of CO ₂ avoided (\$/t CO ₂)	–	34	23	36
Gas-fired	Thermal efficiency (% LHV)	55.6	47.4	41.5	44.7
	Capital cost (\$/kW)	500	870	1180	1530
	Electricity cost (c/kWh)	6.2	8.0	9.7	10.0
	Cost of CO ₂ avoided (\$/t CO ₂)	–	58	112	102

Table 8: Cost comparison for different capture processes. Costs include CO₂ compression to 110 bar but excluding storage and transportation costs

On the basis of the mentioned values from literature, post-combustion technology with MEA has been chosen for the case under exam. The estimation of CAPEX, OPEX and energy penalty to drive the process, requires more detailed research on the state of art.

3.6.6 CO₂ utilization

Another fundamental topic when considering carbon capture technology is its final utilization. Many solutions are possible (Figure 53: Carbon capture and Utilisation).

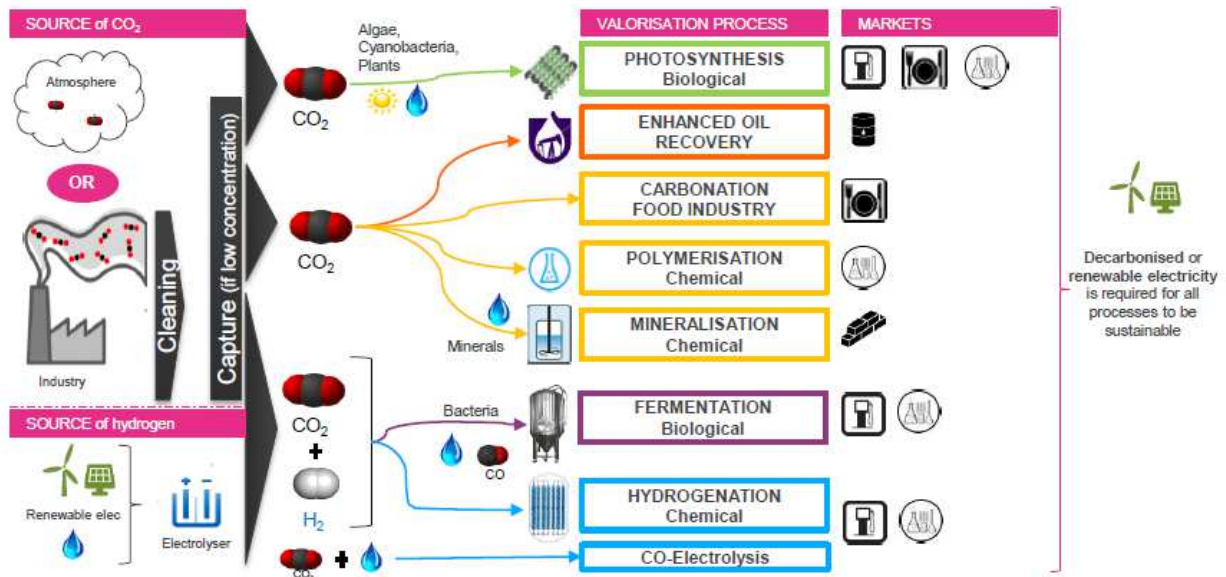


Figure 53: Carbon capture and Utilisation

After capture, the high CO₂ content stream can be transported for geological storage or be assigned to other purposes such as recovery and reuse in industry, agriculture or energy production.

CO₂ can be exploited in industrial areas such as chemicals, food and beverages, refrigerants and fire extinguishing gases. Many valorisation processes require high quality CO₂. This means a significant amount of energy is required to concentrate and purify the CO₂ before it can be used in most valorisation processes.

As previously mentioned, in this study the chosen pathway to exploit captured CO₂ is the valorisation through hydrogenation, explained more in detail in “Power and Waste to Fuel” paragraph.

Chapter IV: Economics and technical results

4.1 Price assumptions

In the following paragraphs results of all the previously described technology are summarized, with a focus on economics and technical details. In the framework in which evaluations are carried out, the main price indices are fixed at the values shown below:

- CO₂ price= 21,49 €/ton_{CO2};^[18]
- White certificate price =250 €/TEE;

For the estimation of economic savings associated to natural gas and electric energy, the following reference prices are considered:

- NG price= 0,315 €/Smc;
- EE price= 125 €/MWh;

4.2 Discriminating Indexes

In order to select the more suitable interventions some indexes have been introduced:

- Levelized Cost of Carbon dioxide (LCOC);
- Unit price per ton of CO₂;
- Payback time (PB);

4.2.1 LCOC

The levelized cost of carbon dioxide (LCOC) represents the price of CO₂ in EU ETS that would be required to null the Net Present Value (NPV) ten years after the investment with an Internal Rate of Return (IRR) of 10%.

The NPV is defined as: the value of all future cash flows (positive and negative) over the entire life of an investment discounted to the present. To evaluate this quantity, it is necessary to know the initial capital expenditure (CAPEX), the annual operating expenditures (OPEX) and the savings.

$$NPV = FC \cdot \frac{(i + 1)^n - 1}{(i + 1)^n \cdot i} - I_0$$

Where:

- *FC* is the cash flow, calculated as the difference between earnings and costs;
- *i* is the interest rate, in this case the IRR=10% mentioned before;
- *n* is the year at which we are evaluating the NPV, chosen as 10 in our analysis;
- *I₀* is the initial investment;

The LCOC is so found by changing the price per ton of CO₂ until reaching the objective of NPV=0.

4.2.2 Unit price per ton of CO₂

This index is used to understand which solution is advantageous from an economic point of view. In fact, among the interventions considered to lessen the CO₂ emission of the industrial plant, there are some that also lead to economic savings associated to the produced energy.

To evaluate this quantity, expressed in €/ton_{CO2}, the cost of production of the energy obtained through the proposed technology is compared to the cost at which it would be bought in the base case. In parallel, at the denominator we place the difference between the amount of emitted carbon dioxide in the base case and the one emitted with the new technology (equal to zero in most cases).

$$\text{€/ton}_{CO_2} = \frac{\text{€/MWh}_A - \text{€/MWh}_B}{\text{ton}_{CO_2}/\text{MWh}_A - \text{ton}_{CO_2}/\text{MWh}_B}$$

Where:

- A represents the base case, “as is”. We would consider as base case the configuration “from the grid”, in which the electric energy comes from the grid and the thermal energy from the boiler.
- B is the scenario where decarbonized technologies are one by one installed, providing thermal or electric energy depending on the solution under analysis.

The parameter expressed in €/MWh for each solution is found in a different way depending on whether we are dealing with the generation of electrical, thermal energy or both of them. The formula used for the evaluation of the price associated to a MWh is

$$\frac{\text{€}}{\text{MWh}} = \frac{\text{annual costs} - \text{saving}}{\text{yearly energy production}}$$

Where:

- The annual costs include the yearly operational expenses and the depreciation of the initial investment;
- The saving calculation differs from case to case.

Considering electric energy production, the evaluation of the energy vector cost is just the yearly cost divided by the energy generated. This quantity is compared with the price of electricity from the grid, equal to 125 €/MWh. The quantity at the denominator is generally null, with respect to emission given by the proposed solution, while for the base case it is equal to the emission factor taken by ISPRA database, 325,2 g_{CO2}/kWh [24].

Referring to thermal power produced, saving to be insert in the previous formula is given by the sum of the economic share associated to white certificates and emission reduction. The obtained quantity in €/MWh is then compared with the €/MWh of the “as is” case. This last-mentioned value is found considering the price of Natural Gas, its HHV and thermal efficiency of boilers. Thus, the reference cost from a unit quantity of thermal energy obtained in the boiler is

$$Unit\ cost_{thermal\ energy} = 0,3154 \frac{\text{€}}{\text{Smc}} \cdot \frac{1000}{9,59 \cdot 0,9} \frac{\text{Smc}}{\text{MWh}} = 36,54 \frac{\text{€}}{\text{MWh}_{as\ is}}$$

The difference between this value and the price of energy for the single treated case is then divided by its linked emission factor, often equal to zero, and the emissions obtained in combustion processes taking place in the boiler. Considering the chemical composition of Natural Gas and the combustion reaction, the CO₂ emitted when burning a Smc of NG is 1,956 ton/Smc. Therefore, for the production of a MWh of thermal power the emission factor to be included in the formula of €/ton_{CO2} is

$$Emission\ factor_{thermal\ energy} = \frac{1000}{9,59 \cdot 0,9} \frac{\text{Smc}}{\text{MWh}} \cdot 0,001956 \frac{\text{ton}}{\text{Smc}} = 0,227 \frac{\text{ton}_{CO_2}}{\text{MWh}_{as\ is}}$$

The same considerations have been carried out in the case of simultaneous production of electric and thermal energy in cogeneration systems. The energy vector to be compared in the determination of the ton_{CO2}/MWh index is the electric one. However, in this specific case the saving is given by the sum of NG avoided too, considering also the associated emission quantity.

By doing the described evaluations for all the proposed solutions, a comparison among them can be done. The most advantageous solutions are those that result in negative values of this index, which means that they have doubly beneficial effects in permitting to reduce the amount of CO₂ emitted and at the same time lowering energy prices.

Therefore, the best interventions are those with the most negative values of this index.

4.2.3 Payback time

The payback period is the length of time required to recover the cost of an investment, considering both annual costs and earnings. This quantity, expressed in years, has been evaluated through a simplified formula:

$$PB = \frac{I_0}{FC}$$

Where:

- FC is the cash flow [€/year];
- I_0 is the initial investment [€];

A synthetic formula of Cash Flow (FC) is provided below:

$$FC = S - A - O$$

Where:

- FC is the cash flow expressed in €/year;
- S is the sum of various savings;
- A is the depreciation of initial investment, obtained by dividing the CAPEX for the technology lifetime;
- O are the OPEX, given by the sum of yearly operation and maintenance costs.

4.3 Results for the individual solutions

4.3.1 Thermal Energy from RES

SOLAR THERMAL TECHNOLOGY

As explained in detail in chapter 3, one of the main parameters to estimate the thermal energy production potential is the area available for the solar plant. Considering the localization of suitable areas and final uses, it has been chosen to place the installation above the roofs of the factories where thermal power is requested, in order to minimize the distance between thermal power production and utilization.

Two buildings have been selected, amounting to a total available area of around 34.000 m². As roofs are now partially occupied, only 70% of the total area has been considered. In addition, also the orientation of the buildings affects the final number of solar panels to be installed. As they are South-West oriented, while the optimal orientation is South, panels have to be placed obliquely, with much space lost.

As a result, the available area for the calculation is 23.800 m².

The solar panel module selected for the simulation is from TVP Solar, whose specific model is MT Power, described in the datasheet as Thermal Vacuum Power Charged: high-end, high-vacuum flat solar thermal panel designed as an ideal thermal energy source in the medium temperature range (100°C – 180°C) [28].

Technical data from the datasheet are listed below.

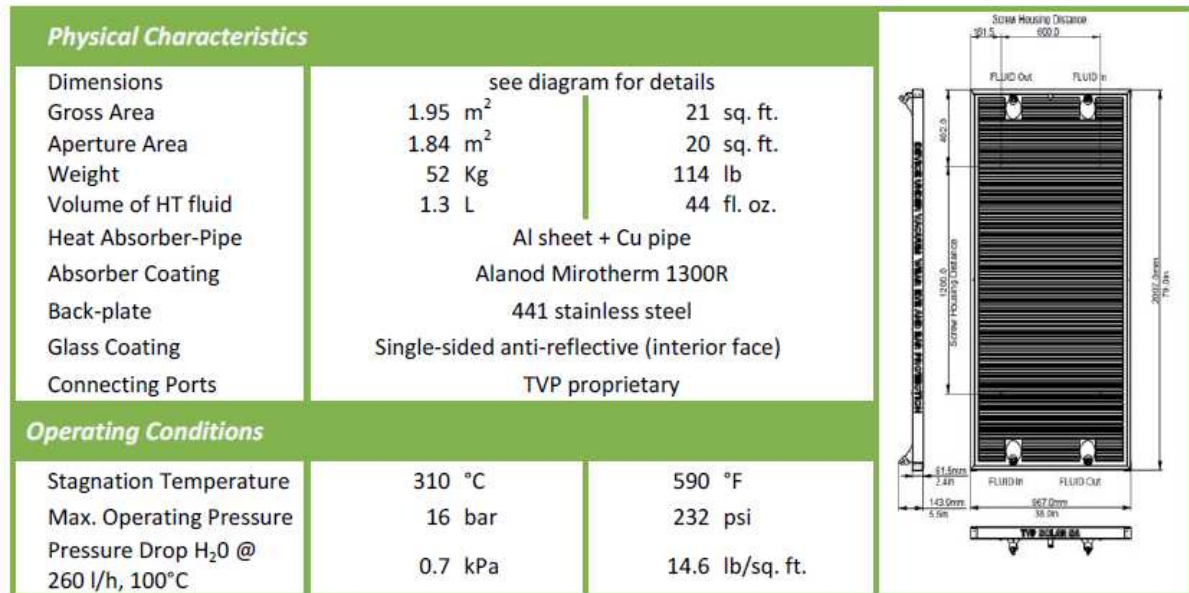


Figure 54: TVP Solar MT-Power Specifications

Once the gross area is known from the product supplier (1.95 m² for this specific model), an estimation of the number of solar panels can be done, taking also into account the shading effect. In fact, depending on the tilt angle and on latitude of the installation, an optimal distance between the panel rows can be fixed, in order to avoid the shading of one panel on the other and the reduction of useful thermal power produced. Considering all the factors mentioned a footprint factor of 1,8 for each panel is taken.

Thus, the number of panels to be installed is 6.611.

As mentioned in the description of the solar thermal technology, thermal power produced is found as the product of solar irradiance for panel efficiency.

The terms η_0 , a_1 , a_2 , appearing in the efficiency formula, are given once the panel model is chosen. For the MT power, considered values are:

- $\eta_0=0.805$;
- $a_1=0.699 \text{ W/m}^2\text{K}$;
- $a_2=0.0087 \text{ W/m}^2\text{K}$;

Two different simulations have been carried out, considering the two levels of temperature related to thermal power needs:

- $T_{\text{delivery}}=165^\circ\text{C}$;
 $T_{\text{return}}=135^\circ\text{C}$;
 $T_m=150^\circ\text{C}$;
- $T_{\text{delivery}}=90^\circ\text{C}$;
 $T_{\text{return}}=70^\circ\text{C}$;
 $T_m=80^\circ\text{C}$;

For both cases, efficiency is calculated separately for each hour of the day, by adapting the changing parameters of external temperature and irradiance (included in the x-factor in the formula), taken from the online available database PVGIS.

The maximum thermal power is gained in summer, as irradiance reaches its maximum value in the year, and higher ambient temperature leads to fewer thermal losses.

Simulation outputs are consistently different. Considering the 165°C case, the production of water at much higher temperature compared to ambient temperature causes a strong efficiency drop. Therefore, in cold months the efficiency falls to zero and solar panels do not work. Global solar field efficiency has been calculated as the ratio between the thermal energy yearly produced and the solar irradiance yearly absorbed (with an optical efficiency of 80%). For the 165°C case, the efficiency is around 37%.

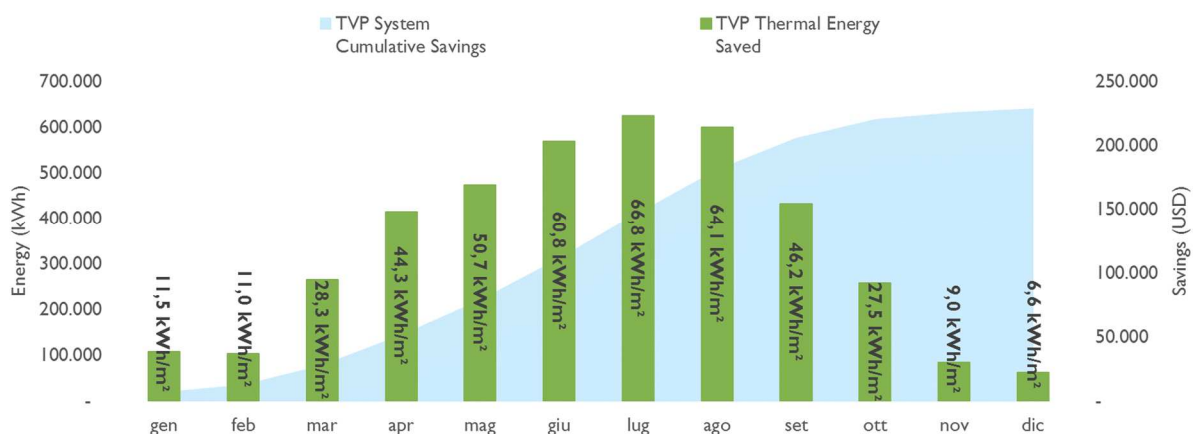


Figure 55: Thermal Energy produced

To increase the solar field productivity the alternative solution with exiting water at 90°C has been introduced. In this case, thermal losses are consistently reduced, reaching an efficiency of around 87%, making this solution the optimal one. Thermal energy production in the 165° case is reported monthly in the following graph.

The total amount of thermal energy produced yearly by the panel is given by the sum of power hour by hour.

Economics

For the estimation of capital costs, the gross area of the whole field is multiplied by the unit price fixed by the supplier. Opex are given as a percentage of total investment.

Table 9: economic data for solar collectors

Unit price	280 €/m ²
N° of panels	6.611
Gross area	12.222 m ²
CAPEX	3.700.000 €
OPEX	2 % CAPEX

The unit price includes the cost of each panel, the installation and piping. OPEX include operation, maintenance and electricity needs for water pumps.

CONCENTRATED SOLAR COLLECTOR

In comparison with solar thermal technology, CSP is much less widespread. Therefore, for a preliminary assessment of the concentrated solar plant, a reference plant has been considered.

Table 10: CSP example

Peak Power	10	MWth
Reflecting area	15.000	m ²
Total area	25.000	m ²

A scale effect has then been applied.

The considered area to carry out the simulation of thermal energy produced is 55.000 m², the size of a plot of land near the industrial plant. The same occupation factor has been used, calculated as the ratio between the reflecting and total area and equal to 60%. Thus, the reflecting area applied to the field in our specific case is 30.000 m². Peak power is estimated to be around 22 MW of thermal power, obtained by the formula

$$W_{p,field} = W_{p,0} \cdot \left(\frac{S_{field}}{S_0} \right)$$

The next step is the evaluation of solar irradiance. Unlike solar thermal technology, in this case the irradiance that has been collected from PVGIS refers to an horizontal plane. Monthly data are given in Table 11: Solar Energy on a horizontal plane.

Table 11: Solar Energy on a horizontal plane

	irradiation on horizontal plane Wh/m ² /day	monthly irradiation on horiz plane kWh/m ²	Thermal energy kWh/month
Jan	1.210	37,5	705.563
Feb	2.310	64,7	1.216.631
Mar	3.780,00	117,2	2.204.156
Apr	4.760,00	142,8	2.686.068
May	6.180,00	191,6	3.603.620
Jun	6.780,00	203,4	3.825.954
Jul	7.130,00	221,0	4.157.574
Ago	6.020,00	186,6	3.510.322
Set	4.450,00	133,5	2.511.135
Ott	2.660,00	82,5	1.551.073
Nov	1.480,00	44,4	835.164
Dec	1.140,00	35,3	664.745
TOT [MWh/y]			27.472

Thermal energy produced is found by multiplying the annual irradiance by the field peak power.

Economics

Based on data referring to the existing plant, unit prices have been obtained, differentiating the price of the solar panel alone and the price inclusive of piping, civil works and others.

Table 12: economics of CSP

Unit price for panels	200	€/m ²
Unit price all inclusive	400	€/m ²
CAPEX	13.200.000	€
OPEX	100.000	€/year

SAVING

For both technologies dealt with in “Thermal Energy from RES”, heat production takes place exploiting solar energy instead of burning natural gas in boilers. Thus, these technological solutions would lead to consistent carbon dioxide emission reduction, otherwise produced in combustion process.

Natural gas saving is estimated dividing the thermal energy supplied by the panel for the methane HHV and the boiler efficiency:

$$m_{NG} = \frac{E_{th}}{\eta \cdot HHV}$$

Where:

- E_{th} is expressed in [MWh/year];
- $HHV= 9,596$ [kWh/Smc];
- $\eta= 90$ %;

CO₂ emission produced in natural gas combustion is equal to 1,956 ton_{CO2}/kSmc [49]. Thus, to find tonnes of CO₂ yearly avoided this factor is multiplied for the previously found NG yearly saved. As explained in the first chapter, an additional economic contribution for the RES diffusion are the white certificates, whose economic value is imposed by its specific market. Only some interventions are included in white certificates system, and actions aimed at producing thermal energy from renewables are among them. Solar Thermal panels and concentrated solar collector plants can so lead to gain a certain value of white certificates, depending on the tonnes of oil equivalent (tep).

Tep are given by the primary energy that would be needed to produce an equivalent value of useful energy, through NG combustion in boilers in this specific case

$$E_{fuel} = \frac{E_{th}}{\eta}$$

$$tep = E_{fuel} \cdot k$$

Where:

- E_{fuel} is given in [MWh/year];
- $\eta= 90$ %;
- k is the emission factor. From Italian official document [50] tep associated to 1000 Smc are 0,82 tep/Smc. When including natural gas PCI, the emission factor associated to thermal energy expressed in tep/MWh is 0.086.

No electric energy savings are linked to these two interventions. Results are reported in Table 13, where TEE stands for white certificates.

Table 13: costs and savings for Thermal Energy from RES Technology

	Useful effect		CAPEX	OPEX	Saving EE		Saving NG		Saving CO ₂		TEE	
	MW _{el} /y	MWh _{th} /y	K€	K€/y	MWh/y	K€/y	kSmc/y	K€/y	ton/y	K€/y	TEE/y	K€/y
Solar thermal 90°C	-	13.055	3.702	56	-	-	1.513	477	2.960	64	1.254	312
Solar thermal 165°C	-	5.643	3.702	56	-	-	654	206	1.279	27	539	135
CSP	-	27.500	13.200	100	-	-	3.180	1.000	6.225	135	2.625	656

The estimation of the determining indexes described in the first part of this chapter has been done based on data that have just been found.

Table 14: Thermal energy from RES indexes

	PB	LCOC IRR=10%	€/MWh	€/tonCO ₂
Solar Thermal 90°C	4,7	-44	-10	-207
Solar Thermal 165 °C	11,8	248	14	-100
CSP	7,8	94	7	-131

4.3.2 Electric energy from RES

PV PANELS

As for solar thermal technologies, in order to evaluate the feasibility of a PV field installation the suitable area has to be verified. Two main available areas have been identified: a field of 55.000 m² next to the industrial plant and the roof of the finished products warehouse of around 37.500 m².

The number of panels is given considering panel dimensions, tilt angle and distance between two PV modules rows. In fact, in order to avoid shading effect, a certain distance must be kept, strongly dependent on the plant latitude and the inclination of panels. In this case 1,30 m is needed.

Thus, a second fundamental step is the choice of the panel model. For this evaluation a CS6K from Canadian Solar has been selected. Technological data are provided in Figure 56: Technical data of CS6K Canadian panel [51], taken by the product datasheet

ELECTRICAL DATA | STC*

CS6K	270P	275P	280P
Nominal Max. Power (Pmax)	270 W	275 W	280 W
Opt. Operating Voltage (Vmp)	30.8 V	31.0 V	31.3 V
Opt. Operating Current (Imp)	8.75 A	8.88 A	8.95 A
Open Circuit Voltage (Voc)	37.9 V	38.0 V	38.2 V
Short Circuit Current (Isc)	9.32 A	9.45 A	9.52 A
Module Efficiency	16.50%	16.80%	17.11%
Operating Temperature	-40°C ~ +85°C		
Max. System Voltage	1000 V (IEC) or 1000 V (UL)		
Module Fire Performance	TYPE 1 (UL 1703) or CLASS C (IEC 61730)		
Max. Series Fuse Rating	15 A		
Application Classification	Class A		
Power Tolerance	0 ~ + 5 W		

MECHANICAL DATA

Specification	Data
Cell Type	Poly-crystalline, 6 inch
Cell Arrangement	60 (6×10)
Dimensions	1650×992×40 mm (65.0×39.1×1.57 in)
Weight	18.2 kg (40.1 lbs)
Front Cover	3.2 mm tempered glass
Frame Material	Anodized aluminium alloy
J-Box	IP68, 3 diodes
Cable	4.0 mm ² (IEC), 12 AWG (UL), 1000 mm (39.4 in)
Connector	T4 series
Per Pallet	27 pieces, 538 kg (1186.1 lbs)
Per Container (40' HQ)	756 pieces

* Under Standard Test Conditions (STC) of irradiance of 1000 W/m², spectrum AM 1.5 and cell temperature of 25°C.

Figure 56: Technical data of CS6K Canadian panel [51]

Considering the panel area obtained from the previous data, the number of panels is around 33.000.

The most important datum for the simulation of electric energy yearly produced is the peak power, associated to Standard Test Conditions. To find the field peak power, the data provided in the datasheet and referred to one single panel have to be multiplied by the total amount of panels of the PV plant. The final outcome for peak power is

$$W_{p,field} = 7.740 [kWp]$$

By multiplying this quantity by the yearly solar irradiance, collected from weather database, we get the thermal energy. Here PVGIS has been used, and the Solar radiation database considered is PVGIS-classic. Once the orientation towards South and a tilt angle of 30° have been selected, the Average Daily Solar Irradiance on the fixed plane is found month by month. The global irradiance expressed in [W/m²] is then summed hour by hour, obtaining the solar energy G mentioned in the theoretical description of PV technology at Chapter 3 and expressed in [kWh/m²].

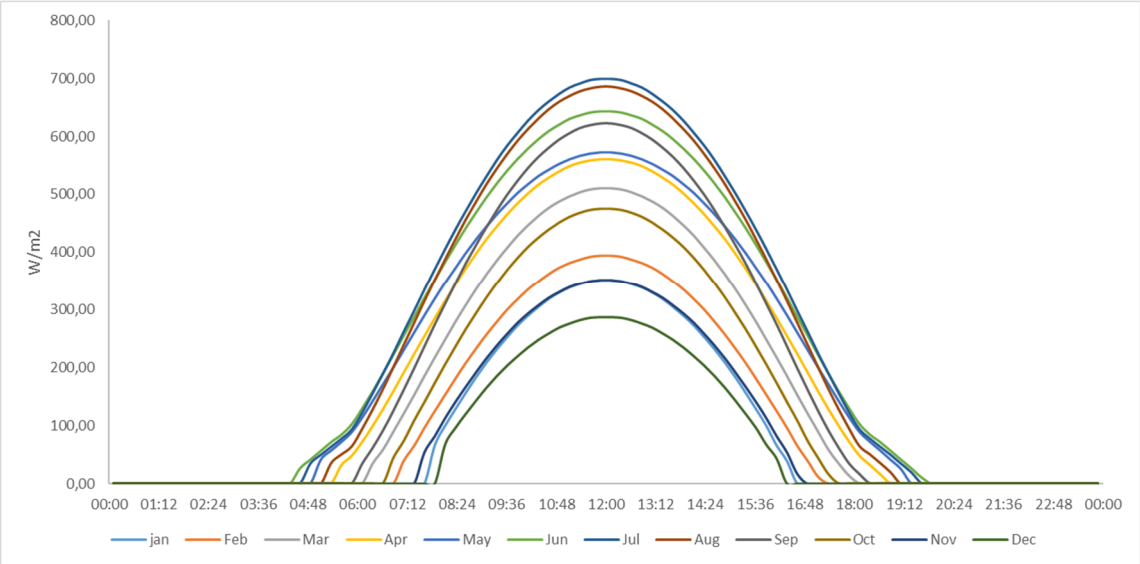


Figure 57: Average daily solar Irradiance

The monthly solar energy is reported in Table 15.

Table 15: Monthly Solar Energy

Jan	65.913	Wh/m ²
Feb	73.262	Wh/m ²
Mar	116.459	Wh/m ²
Apr	135.885	Wh/m ²
May	152.775	Wh/m ²
Jun	166.237	Wh/m ²
Jul	182.132	Wh/m ²
Ago	173.321	Wh/m ²
Set	139.950	Wh/m ²
Ott	101.897	Wh/m ²
Nov	65.707	Wh/m ²
Dec	51.979	Wh/m ²
TOT	1.425	kWh/m ²

Economics

The capital cost of the PV plant is found starting from the price per unit, taken by an offer made by the Panel supplier, and expressed in €/Wp. In the price, panel cost, installation, civil works are included. The same happens for operation and maintenance cost, given in €/kWp.

Table 16: economics of a PV plant

Unit price	0,64	€/kWp
N° of panels	32.954	
CAPEX	5.184.000	€
OPEX	8	€/kWp/y

Simulation results are given in Table 17.

Table 17: costs and savings for Electric Energy from RES Technology

	Useful effect		CAPEX	OPEX	Saving EE		Saving NG		Saving CO ₂		TEE	
	MW _{el} /y	MWh _t /y	K€	K€/y	MWh/y	K€/y	kSmc/y	K€/y	ton/y	K€/y	TEE/y	K€/y
PV	8.750	-	5.184	40	8.750	1.095	-	-	2.845	-	-	-

The determining indexes for the PV technology, in the table below, show the economic convenience of their installation. In fact, compared to electricity price from the grid, the cost of energy produced on-site by the PV fields is much lower.

However, the emission reduction obtained in this case is not valorised since the EU ETS emission counting method does not include emissions for electricity from the grid. As a consequence, the LCOC cannot be found.

Table 18: Electric energy from RES indexes

	PB	LCOC IRR=10%	€/MWh	€/tonCO ₂
PV	4.9	-	34	-279

4.3.3 Waste to Energy

As explained before, all the scenarios included in Waste to Energy pathway derive from the alternative uses of biogas, obtained from the industrial plant waste streams through the process of anaerobic digestion. Biogas flowrate has been calculated from milling waste chemical composition and daily amount, expressed in tons per day. Its daily production is:

$$\dot{m}_{biogas} \sim 88.000 \text{ Nm}^3/\text{day}$$

The investment cost for the AD system must be included in each case that is dealt with below. The capex is made up by the equipment, civil works, sewage treatment plant and other components belonging to Balance of Plant [52]. A block diagram of analogy is shown in Figure 58.

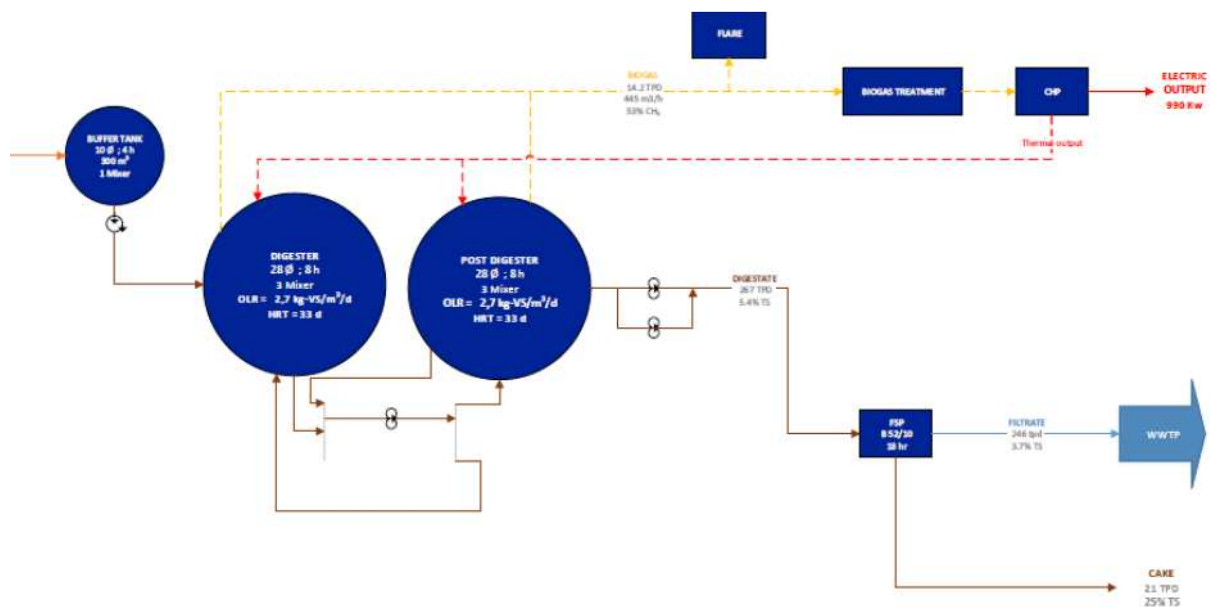


Figure 58: schematic representation of an AD system example

Based on Engie internal offers referring to the size of the AD system to be installed, equal to 4 digesters of 15.000 m³ each, the capex finally obtained are given in Table 19: Anaerobic Digestion system investment costs.

Table 19: Anaerobic Digestion system investment costs

CAPEX [M€]	
equipment	2,5
Civil works	1,5
Treatment plant and others	1,5
Total	5,5

Additional costs to be considered in the economic feasibility analysis are included in the OPEX, made up of operational and maintenance yearly costs. The AD system component that brings about the greatest energy expense is the digester itself, as it requires specific working thermodynamic conditions. In fact, in order to allow for chemical reactions to take place in AD processes (hydrolysis, acidogenesis, acetogenesis, methanation), predefined thermodynamic conditions must be maintained inside the system. The optimal temperature must be kept, based on the specific waste streams composition which requires thermal energy. Therefore, this energy penalty has an impact on the final amount of energy associated to each biogas exploitation alternative.

The thermal duty is evaluated considering that, to treat waste biomass, assumed to be at an ambient temperature of around 20 °C, it must be heated up to at least 35-37° C. It is then necessary to maintain that temperature inside the digesters.

The thermal need is estimated to be around 1.200 kW in winter and around 800 kW in summer.

Moreover, for the considered industrial plant, a cost is also associated to waste streams entering the digester. This is due to the fact that a large amount of that production waste is now sold in zoo-technique markets, to be exploited in animal feed sectors.

Table 20: biogas cost

bran cost	122	€/ton
biogas production rate from waste	207,87	Nm ³ /ton
biogas cost	0,59	€/ Nm ³

Biogas cost is therefore evaluated by multiplying that cost expressed in [€/Smc] by the yearly biogas consumption, in [Smc/year], considered in each of the following systems.

Energy production potential and economics of the alternative scenarios of biogas utilization are described more in detail below.

BIOGAS IN BOILER

As mentioned in chapter 3, the base-case for biogas utilization is the scenario in which biogas is fuelled in the installed boilers. The investment for replacing the burner has been included. Thermal energy yearly produced is evaluated considering that the total amount of biogas exiting the AD is exploited.

The hourly flowrate of methane produced is calculated from daily production, to be divided by the number of working hours of the digester. Anaerobic digestion being a continuous process, 24 hours each day are accounted for. The yearly biogas used for thermal power in the boiler is obtained by multiplying the found flowrate by the total amount of hours when heat is required by the plant, equal to 8000 hours a year.

$$M_{CH_4} = \frac{45.000 \text{ Nm}^3/\text{day}}{24 \text{ h/day}} \cdot 8000 \frac{\text{day}}{\text{year}} = 15.000 \text{ Nm}^3/\text{year}$$

The energy associated with the biogas is thus obtained by making the product of the just evaluated methane consumption by the HHV of methane.

Economics

With respect to the capex, the additional cost of a biogas burner is added to the investment needed for the AD system. Based on Engie internal sources, the investment cost for the burner has been assumed equal to 120 k€.

The opex associated to this solution are for the most part due to waste material for biogas production, valorised as explained before.

The savings from this intervention would consist in avoiding the expense for natural gas, replaced by biogas, as well as CO₂ emissions, to be neglected in case of renewable fuels.

Table 21: costs and savings for Biogas in Boiler case

	Useful effect		CAPEX	OPEX	Saving EE		Saving NG		Saving CO ₂		TEE	
	MW _{el} /y	MWh _{th} /y	K€	K€/y	MWh/y	K€/y	kSmc/y	K€/y	ton/y	K€/y	TEE/y	K€/y
Biogas in Boiler	-	123.570	5.620	8.945	-	-	14.317	4.515	28.000	600	-	-

BIOGAS IN ICE CHP

The configuration in which biogas is exploited in an Internal Combustion Engine based Cogenerator has been considered. In this case, the size of the CHP to be installed is decided depending on the available biogas from AD. Various alternatives have been checked, finally selecting three biogas fed engines supplied by Jenbacher and characterized by the following details:

Table 22: J620 data [53]

Model J620		
P_{el}	3.044	kW
η_{el}	44%	
P_{th}	2.782	kW
η_{th}	40%	
η_{tot}	84	

Table 23: J612 data [34]

Model J612		
P_{el}	1.820	kW
η_{el}	44%	
P_{th}	1.668	kW
η_{th}	40%	
η_{tot}	84%	

Two models of J20 and a J612 are considered to be installed, to reach a total electric power equal to 7.900 kW and a thermal potential of 4.450 kW. A certain share of thermal energy is absorbed within the digestion process, as previously explained. With the hypothesis of 4000 working hours in winter and 4000 working hours in summer, the yearly thermal duty is estimated to be 8.000 MWh. Thus, only the rest of the heat produced is delivered to the final uses.

The calculation of the yearly energy production derives from the total amount of available biogas exploited in CHP.

Economics

The CAPEX for the installation of the three CHP systems have been estimated considering offers from the supplier for similar engine type and size.

Table 24: CAPEX for biogas in ICE CHP

CAPEX		
AD system	5.500	k€
J620	2.800 (x2)	k€
J612	1.800	k€
TOT	12.900	k€

Regarding the OPEX, maintenance costs for the cogenerator have been added to the fuel price, considering a fix yearly cost of 50 k€ and a variable one linked to working hours (25€/h for J620 model and 12 €/h for J612 model).

Savings obtained by the installation of the described system are connected to electric energy, natural gas, carbon dioxide emissions and white certificates. In fact, if we consider that we are simultaneously producing heat and electricity in the biogas-fed CHP, a twofold effect is obtained: on one hand, the equivalent amount of electric energy produced in the system is not supplied by the grid, thus leading to an economic saving calculated by multiplying the energy by cost of electricity from the grid; on the other hand, the amount of heat exiting the CHP requires no burning of natural gas in boilers, with the consequence to reduce NG yearly consumption.

In addition to economic savings due to NG reduction, calculated by multiplying the amount of NG avoided by its price, the benefit not to emit carbon dioxide in combustion processes is also obtained. Moreover, if we consider the emission rate associated with the electricity from the grid, equal to 325,2 g_{co2}/kWh, a further reduction in CO₂ emission is reached. Nevertheless, the emission reduction due to on-site electric energy production is not economically valorised by the EU ETS system, as only the CO₂ emitted in combustion process is counted.

Cogeneration systems are also included in solutions that benefit from incentives such as white certificates because they work with high efficiency. An economic saving is furthermore added to those previously listed, calculated as the product of the number of white certificates, equal to 8.000 for the written power values, by their price fixed by the market.

Table 25: costs and savings for Biogas in ICE CHP case

	Useful effect		CAPEX	OPEX	Saving EE		Saving NG		Saving CO ₂		TEE	
	MW _{el} /y	MWh _{th} /y	k€	k€/y	MWh/y	k€/y	kSmc/y	k€/y	ton/y	k€/y	TEE/y	k€/y
Biogas in ICE CHP	63.264	49.855	12.900	9.790	63.264	7.908	5.777	1.822	31.872	243	8.000	2.000

BIOGAS IN SOFC CHP

In analogy to the case just described, this technical solution is characterized by the simultaneous production of thermal and electric energy. However, because of chemical reactions taking place in the SOFC stack instead of burning fuel, this system has the benefit of a higher efficiency. Thus, the amount of electric energy obtained is greater compared with traditional CHP systems.

For this reason, the SOFC is considered to be a very promising technology. Nevertheless, many improvements are needed to ensure that it stands out in the energy-technology market. In fact, the presence of very rare and costly material in the electrolyte layer as well as in the whole stack makes it far more expensive than traditional CHP.

To find out more about the technical and economic feasibility of the SOFC CHP case, a fuel cell model characterized by high fuel flexibility has been chosen. The model selected is C60, working with biogas, produced by the Swedish company Convion. Its technical data from datasheet [35] are in Table 26.

Table 26: C60 Datasheet

Convion C60		
electric output	60	kW net_AC
electrical eff	60%	(LHV)
Thermal output	27	kW net_AC (exhaust cooled to 40°)
Range of electric output	65 - 33	kW (normal modulation range 100-50%, temporary modulation down to 30%)
Electric efficiency at 50% output	60%	(LHV)
Exhaust gas flow 200°C	575	kg/h, dew point 37°C
Fuel supply pressure	4	bar-g (+/- 0.2 bar-g)
Fuel envelope, LHV	440-850	kJ/mol @ 25°C; equivalent to biogas compositions with 55 % - 100 %-mol CH ₄ with CO ₂ as a diluent
Tolerable fuel gas contaminant level	- Sulphur < 30ppb i.e. <0.04 mg(S)/m ³ ;	
	- Siloxanes < 0.06 mg (Si)/m ³ ;	
	- Halogens (e.g. Cl ₂ , HCl, halogenated hydrocarbons) <0.01 mg/m ³	

The size of the fuel cell to be installed have been decided in order to exploit the biogas flowrate calculated before. As fuel cell technology has the great advantage of being scalable, in order to build a power plant with a greater power potential it is sufficient to install more SOFC modules. The equivalent number of SOFC modules is found dividing the power to be installed, 10 MW in this case, by the power of the single module (60 kW for C60 SOFC). The resulting number of modules is 167.

Thermal and electric energy yearly produced can be found with the same steps used in the ICE CHP case.

Economics

As previously mentioned, the main obstacle for the affirmation of fuel cell technologies is their high costs. The capex for the installation of the SOFC CHP systems has been found considering offers for similar fuel cell types and sizes. Considering a reference value of unit price equal to 11 k€/kW, it has been scaled for a larger size, with a scaling factor of 0,95:

$$C_1 = C_0 \cdot \left(\frac{S_1}{S_0}\right)^n$$

Where

- S_1 is the power of the SOFC CHP to be installed;
- S_2 is the power of a SOFC module;
- $n= 0.95$ is the scaling factor.

As regards OPEX, in addition to biogas price, operation and maintenance costs have been estimated as 5 % of the total plant cost C_1 that has just been found.

With respect to savings, the same considerations as for the ICE CHP case are true. A higher number of white certificates are obtained in this scenario, the SOFC being a more efficient technology. Thus, white certificates number amounts to 11.430.

Table 27: costs and savings for Biogas in SOFC CHP case

	Useful effect		CAPEX	OPEX	Saving EE		Saving NG		Saving CO ₂		TEE	
	MW _{el} /y	MWh _t /h/y	K€	K€/y	MWh/y	K€/y	kSmc/y	K€/y	ton/y	K€/y	TEE/y	K€/y
Biogas in SOFC CHP	80.000	28.000	85.500	12.555	80.000	10.000	3.245	1.023	32.361	136	11.430	2.858

BIOGAS UPGRADING

Biogas upgrading is a valid alternative for biogas direct utilization as it allows not to convert the power production systems previously installed in the plant. For example, when considering an industrial plant powered by an NG-fed CHP, the production of biomethane on site, exploiting waste streams, would lead to a reduction in NG otherwise got from the grid.

However, for the present analysis, we are comparing all these scenarios as an alternative to the case “from the grid”, in which electric energy comes from the grid and thermal energy from the boiler. As a consequence, the installation of a new cogenerator is necessary. The final use chosen for the biomethane would be in an ICE CHP.

The power size of the CHP to be installed is in this case given by consideration on the total thermal and electric consumption of the industrial plant. By performing various simulations with different sizes of the CHP, the optimal electric power potential results to be 15 MW.

The choice of the optimal CHP size is based on the load-duration curves of thermal and electric power, which show on the x-axis the number of annual hours for which the load is kept greater than or equal to the value indicated on the ordinate. The key point in the dimensioning is that the lower the dissipated energy the higher the system efficiency. If a CHP size able to cover the maximum load is installed, the system would work at maximum load only for few hours, while the rest of the time, to cover the energy demand, it would work with low efficiency.

To avoid the problem of low overall efficiency, CHP dimensioning is thus performed in order to have a full load functioning for the most part of the time. Moreover, in order to

obtain white certificates, the system must be included in the definition of high-efficiency cogeneration.

On the opposite, when a too small size is installed, the system would work almost always at maximum load, but a large amount of integration would be needed.

On the basis of the mentioned criterium, a 15 MWe results to be the optimal size, as it is able to cover the greatest share of thermal and electric consumptions and guarantee maximum savings.

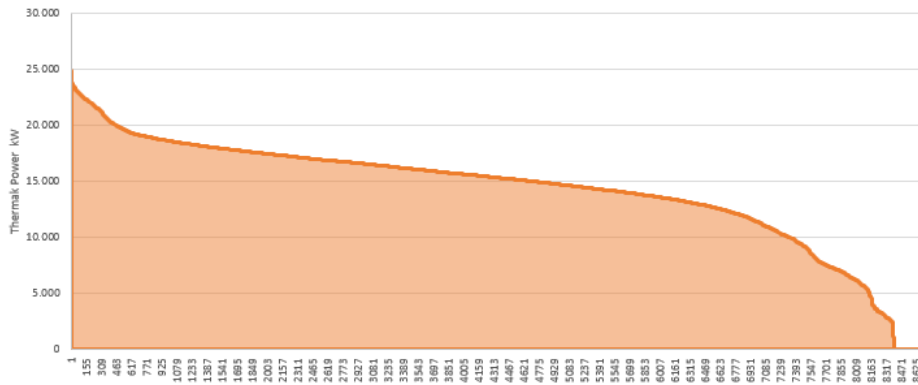


Figure 59: thermal load duration curve

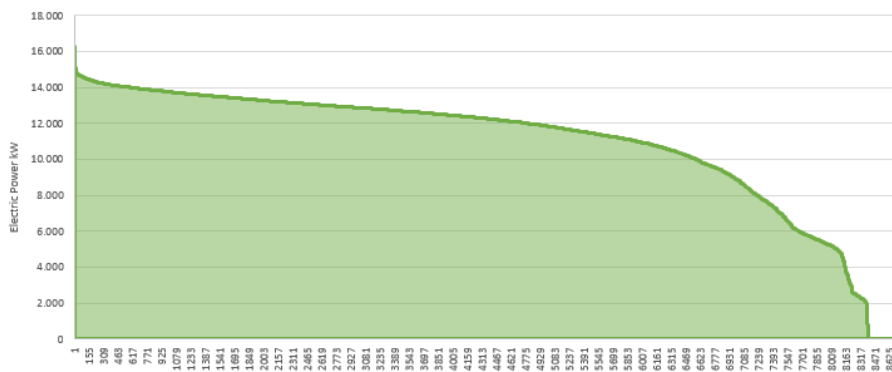


Figure 60: electric load duration curve

For this reason, three cogenerators Rolls Royce, model B36:45L9-AG, are being suggested, providing 5.270 kW of electric power each.

Table 28: CHP data from datasheet

Rolls Royce, model B36:45L9-AG		
Pel	5.270	kW
η_{el}	45,8	
Pth	4.254	kW
η_{th}	37%	
η_{tot}	82,8	

A membrane technology is selected for the upgrading process, as it does not need an additional amount of heat, and so the energy penalty for power production is reduced. However, such technology requires a high compression work as the biogas must be recirculated several times in the membranes in order to reach the quality requirements to fuel the CHP.

Similarly to previous cases, energy production is calculated from the total amount of biogas feeding the CHP.

Economics

The investment cost of the membrane separation system has been estimated on the basis of biomethane production potential and cost of equivalent systems. Thus, a CAPEX of 1.000 M€ has been considered for upgrading, based on Engie internal offers. This cost is added to the initial costs for AD system and for the cogeneration, from offers for similar engine types and sizes.

Table 29: CAPEX of biogas upgrading

CAPEX		
AD system	5.500	k€
Membrane upgrading	1.000	k€
CHP	13.736	k€
TOT	20.236	k€

The greatest share of the yearly cost is assumed to be linked to CHP operation and maintenance. OPEX of the Rolls Royce CHP are estimated as 1.720.000 €/y, including the ordinary maintenance and other cyclic maintenance costs. The found OPEX must be added to the waste streams cost for biogas production, as done before.

In order to perform a complete saving analysis, the total amount of energy required by the plant has been considered in the simulation. The greatest share of this energy would be covered by the CHP system, while the remaining part of electric energy is taken from the electric grid as well as the thermal energy comes from integration in boilers.

Table 30: 15 MW CHP scenario

NG-fed CHP scenario		
E_{el, CHP}	99.408	MWh,el
E_{th, CHP}	53.179	MWh,th
E_{el, boiler}	7.636	MWh,el
E_{th, boiler}	85.555	MWh,th

Referring to the scenario in which biogas is converted into biomethane, it is possible to substitute a large part of the CHP fuel consumption with the amount of biofuel on-site produced. The benefit of combining the two solutions is the strong reduction in emissions from the engine, the CO₂ coming from biomethane combustion being considered negligible. Moreover, in the case in which the biomass entering the AD has a low cost, as a consequence the produced biogas will be economically convenient with respect to NG from the grid. Therefore, the exploitation of fuel auto-produced instead of natural gas from the grid would result in economic convenience.

Nevertheless, starting from a biomass cost of 122 €/ton for the treated case, the final cost associated to biogas is much higher than the price of NG, thus leading to low economic benefit.

Cost for the electric energy from the grid has been included in the opex, as well as cost of fuel. The latter is found as the sum of the expenses for biogas and for Natural Gas, calculated as the difference between the fuel consumption and the available biofuel.

Table 31: OPEX of biomethane in CHP scenario

OPEX		
CHP maintenance	1.720	k€
Thermal duty for AD	8.000	MWh
NG for AD	926.891	Smc
biomethane	15.243.848	Smc
NG	20.336.712	Smc
biomethane cost	8.947	k€/y
NG cost	6.414	k€/y

Savings are evaluated as for the other “Waste to Energy” scenarios, and the incentives considered are white certificates, due to the high efficiency of the CHP, amounting to a number of 9.090.

As for emission reduction, when the emission rate of electricity from the grid is considered, CHP systems allow for a reduction of CO₂ tons released in atmosphere, even if a larger amount of fuel is burnt. On the contrary, for the counting in EU ETS scheme only the CO₂ released in combustion processes taking place in the plant is considered. Therefore, the CHP scenario results in increasing emission with respect to the base case, leading to an additional expense associated to CO₂.

Table 32: costs and savings for Biogas Upgrading case

	Useful effect		CAPEX	OPEX	Saving EE		Saving NG		Saving CO ₂		TEE	
	MW _{el} /y	MWh _t h/y	K€	K€/y	MWh/y	K€/y	kSmc/y	K€/y	ton/y	K€/y	TEE/y	K€/y
Biogas Upgrading	107.044	138.764	20.236	17.080	107.044	13.380	16.074	5.070	28.284	-140	9.090	2.490

The determining indexes for the described four alternatives in biogas utilization are shown in Table 33.

Table 33: Waste to Energy indexes

	PB	LCOC IRR=10%	€/MWh	€/tonCO ₂
Biogas in Boiler	-	191	71	150
Biogas in ICE CHP	5,9	14	111	-43
Biogas in SOFC CHP	58,5	2.434	214	272
Biogas Upgrading	5,4	87	114	-34

4.3.4 Power and Waste to Fuel

Power and Waste to Fuel scenario is obtained by combining a PV field installation, to be exploited for hydrogen production, and a CO₂ capture system. The final product, consisting of synthetic methane, is given by the chemical reaction of those two chemical flows resulting in CH₄ exiting the methanation unit.

Firstly, the renewable source to be assigned for this scope has been decided, selecting the PV field above the roof of the plant warehouse. Once an estimation of maximum electric power and yearly energy production values is made, there follows the dimensioning of the unit in which electrolysis would take place. In this case we have:

Table 34: Power and Waste to Fuel dimensioning

Electrolyser dimensioning		
P_{el,max PV}	2.458	kW
E_{el, year}	4.228	MWh
P_{electrolyzer}	2.500	kW

A second step is the evaluation of the H₂ production potential that strongly depends on the type of technology chosen, whether Alkaline or PEM (Proton Exchange Membrane). The values of H₂ production efficiencies are written in Table 35, with a clear distinction between efficiency at the beginning of life (BOF) and at end of life (EOF).

Table 35: Electrolyser efficiency

technology	H ₂ production efficiency	UM
Alk BOF	4,6	kWh _{ac} / Nm ³
Alk EOF	5,1	kWh _{ac} / Nm ³
PEM BOF	5	kWh _{ac} / Nm ³
PEM EOF	5,5	kWh _{ac} / Nm ³

PEM technology has been selected in this case, considering an average value of the efficiency of 5,25 kWh_{ac}/Nm³. Thus, H₂ production is found. Next step is the combination of the hydrogen flowrate with the CO₂, the latter coming from the upgrading system or from the carbon capture from flue gas exiting the combustion processes.

As shown in the formula of the chemical reaction written in Chapter 3, a mol of H₂ reacts with 0,5 moles of CO₂. As a consequence, a smaller amount of CO₂ is required in the methanation unit. Considering a methanation efficiency of 90%, the synthetic CH₄ production potential is given in Table 36.

Table 36: Synthetic CH₄ production

H ₂ produced	805.333	Nm ³ /y
CO ₂ valorised	402.667	Nm ³ /y
η _{methanation}	90 %	
Synthetic CH ₄	362.400	Nm ³ /y

This quantity is then added to the bio-methane production from membrane separation. In fact, by coupling the methanation unit and biogas upgrading system, the CO₂ capture in membranes has the twofold benefit of purifying biogas, thus producing bio-CH₄, and separating CO₂ to be converted into syn-CH₄.

Starting from biogas yearly amount from the AD process, the yearly flowrates given in Table 37: CH₄ on-site production are obtained.

Table 37: CH₄ on-site production

Bio CH ₄	362.400	Nm ³ /y
Syn CH ₄	15.243.667	Nm ³ /y
Tot CH ₄ produced on site	15.606.067	Nm ³ /y

For an economic feasibility evaluation of this scenario it has been decided to exploit the produced SNG in an ICE CHP. The same CHP system introduced before has been considered.

Therefore, the energy yearly produced is found considering to cover with the new set-up the whole energy consumption, where large part of the CHP fuel comes from biomethane and synthetic methane on-site produced.

Economics

For the appraisal of CAPEX and OPEX associated to the whole system, the reference is to the economic analysis of similar projects.

Considering that for an PEM electrolyser of 250 kW_{el} capacity the CAPEX is around 1500-2000 €/kW [38], this investment cost has been scaled to the capacity of 2.500 kW, with a scaling factor of 0.95.

$$C_1 = C_0 \cdot \left(\frac{S_1}{S_0}\right)^n$$

Where:

- C_1 is the investment cost of the 2.500 kW electrolyser to be installed;
- C_2 is the investment cost of the reference case with the 250-kW electrolyser, obtained by multiplying its capacity by an average unit cost of 1.750 €/kW;
- S_1 is the new electrolyser capacity of 2.500 kW;
- S_2 is the reference case electrolyser capacity of 250 kW;
- n is the scaling factor equal to 0.95.

A similar approach is followed for the membrane system, with a unit price of 1.200–1.600 €/kW [54], and for the Methanation Unit, with a unit cost of 1500 €/kW_{CH₄} [55].

For other components required for the synthetic methane production (buffer storage, gas cleaning system, etc.), we consider an additional cost of 30 to 35% of CAPEX of the main units (electrolyser and methanation Unit).

As regards the PV field, the investment cost is calculated from a unit price referring to the field peak power, equivalent to around 0.64 €/W_p. If we consider the field to be placed above the warehouse roof, a peak power of 3.740 kW_p is obtained, thus leading to a CAPEX of 2.964 k€.

The ICE CHP cost is assumed to be the same identified for the “Biogas Upgrading” case.

Table 34: Power and Waste to Fuel CAPEX

CAPEX		
AD	5.500.000	€
PV	2.394.112	€
electrolyser	3.937.500	€
MW	3.500.000	€
Methanation unit	651.641	€
BOP	1.376.742	€
CHP	13.736.000	€
TOT	31.095.995	€

In the yearly costs, electrolyser OPEX (accounting for 2 to 3% of CAPEX per year) and methanation unit OPEX (from 5 to 10% CAPEX per year) have been considered in addition to the cost of fuel, PV field maintenance and O&M for the CHP.

Table 38: Power and Waste to Fuel OPEX

OPEX		
fuel	15.775	k€/y
electrolyser	78	k€/y
PV	30	k€/y
CHP	1.720	k€/y
Methanation unit	48	k€/y
tot	17.652	k€/y

Savings associated to the electric and thermal energy yearly produced are calculated according to the same procedure as in the previous cases, and so are the white certificates, numbering 9.960 for the present case.

The main difference from the other solutions is in the evaluation of the emission reduction. In fact, in parallel to the exploitation of renewable fuels such as Bio-CH₄ and Syn-CH₄, whose emissions in the combustion process are not counted, the valorisation of a certain amount of CO₂ takes place. Such quantity of carbon dioxide is therefore not only excluded from the EU ETS emissions considered, but is also subtracted from the total amount of plant emissions.

Table 39: costs and savings for Power and Waste to Fuel case

	Useful effect		CAPEX	OPEX	Saving EE		Saving NG		Saving CO ₂		TEE	
	MW _{el} /y	MWh _{th} /y	K€	K€/y	MWh/y	K€/y	kSmc/y	K€/y	ton/y	K€/y	TEE/y	K€/y
Power and Waste to Fuel	107.04	138.734	31.096	17.652	107.04 4	13.380	16.073	5.070	27.618	-125	9.960	2.490

Determining indexes for this scenario are reported in Table 40: Power and Waste to Fuel indexes.

Table 40: Power and Waste to Fuel indexes

	PB	LCOC IRR=10%	€/MWh	€/tonCO ₂
Power and Waste to Fuel	9,8	-305	125	-1

4.3.5 Shifting Thermal towards electric

HIGH-TEMPERATURE HEAT PUMP

With respect to the studied industrial plant, two thermal flows have been identified from which thermal recovery can be performed: the oil cooling circuit of compressors and vacuum pumps, with temperatures around 70-80 °C, and the flow of hot air exiting the first drying phase, at a temperature at ~75 °C.

The thermal energy that it is possible to recover strictly depends on temperature levels, source and sink sides, and on the thermal potential of the source. Therefore, two simulations have been carried out, taking into account the two different thermal needs of the plant: hot water at 80°C and superheated water at 160°.

Depending on the delivery temperature to the primary circuit, a different COP is obtained.

1. $T_{\text{delivery}} = 90 \text{ °C} \rightarrow \text{COP} = 5.3$ approximately [56];
2. $T_{\text{delivery}} = 160 \text{ °C} \rightarrow \text{COP} = 2$ approximately;

Both cases can be considered when simulating recovery from the two sources. As previously described, the selected model of the heat pump is a Viking Heat Booster piston compressor heat pump [36].

1. CASE I: $T_{\text{delivery}} = 90 \text{ °C}$

The reference scheme for the 90° configuration exploiting waste heat from compressors and vacuum pumps is shown in Figure 61.

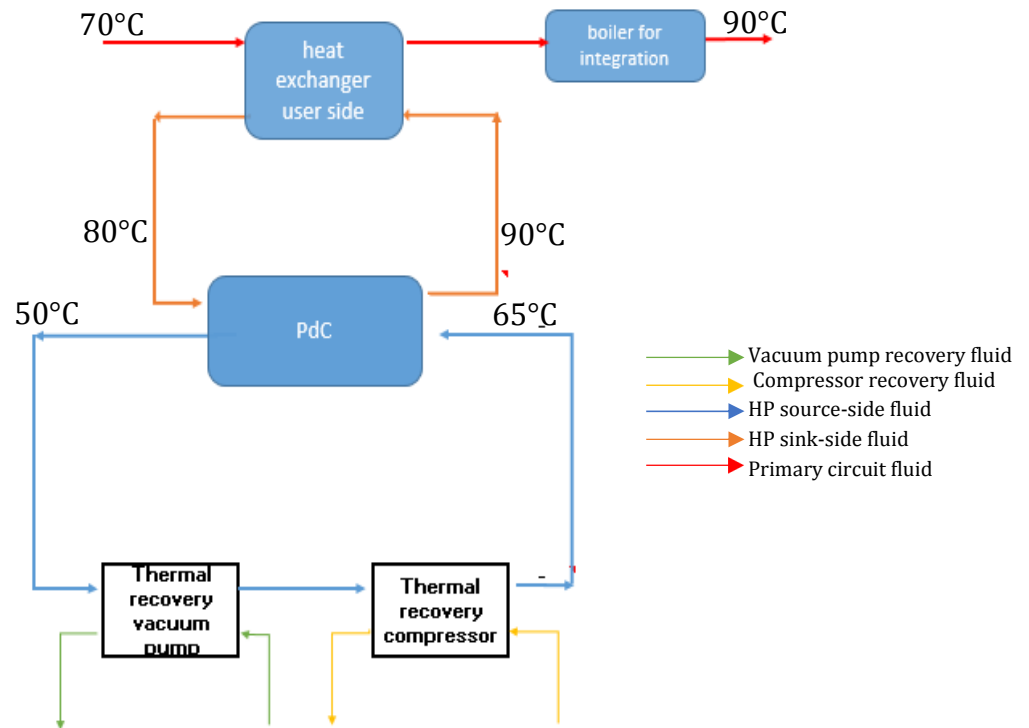


Figure 61: one stage Heat Pump configuration

Simulations have assumed the known value of thermal power recoverable to be the heat available source side of the heat pump. The procedure that follows refers to the case of recovery from vacuum pump and compressor cooling systems. A parallel analysis is performed in the case of recovery from dryers, so only final results are reported.

To calculate the useful thermal energy that can be obtained assumption on the following described quantities have been done:

- $T_{out, evap}=50^{\circ}\text{C}$ representing the temperature of working fluid exiting the heat pump evaporator at source side. Limits on temperature of the HP sink-side fluid are imposed by the mandatory ΔT that must be respected in the recovery heat exchanger. In fact, in order to make the heat transfer possible, the fluid temperature must be kept lower than temperatures of both vacuum pump and compressor recovery fluid;
- $\Delta T_{source}=15^{\circ}\text{C}$, the thermal gradient to be reached at recovery side;
- $T_{out, cond}=90^{\circ}\text{C}$. The same considerations on the ΔT at the heat exchanger are also valid for this temperature level. The thermodynamic conditions of the fluid coming back from the primary circuit are known, so the temperature of HP sink-side fluid must be higher than the temperature of primary fluid in the whole heat transfer process.
- $T_{in, cond}= 80^{\circ}\text{C}$;

By fixing those parameters the calculation of other main quantities is possible. Flowrate of the HP source and sink side fluids is given by the formula:

$$m_{HP} = \frac{P_{th}}{c_{p,fluid} \cdot \Delta T}$$

Where:

- P_{th} is the thermal power from recovery;
- $c_{p,fluid}$ is the specific heat of working fluid, water in this case, equal to 4.186 [kJ/kg/K];
- ΔT is different for the two fluids considered, equal to 15 °C at source-side, and to 10 °C at sink-side.

Regarding the primary circuit fluid, its flowrate has been found once the thermal needs at a temperature level of 80°C have been identified. Starting from the amount of thermal energy and the ΔT between delivery and return of the fluid, the flowrate is assessed.

Once the power at the recovery and the COP are known, the thermal power obtained at the primary circuit heat exchanger, as well as electric work absorbed can be calculated.

$$P_{el} = \frac{P_{recovery}}{1 - COP}$$

While

$$P_{th,user} = P_{el} \cdot COP$$

COP comes from a polynomial formula depending on $T_{out, evap}$ and $T_{out, cond}$ difference (Figure 62).

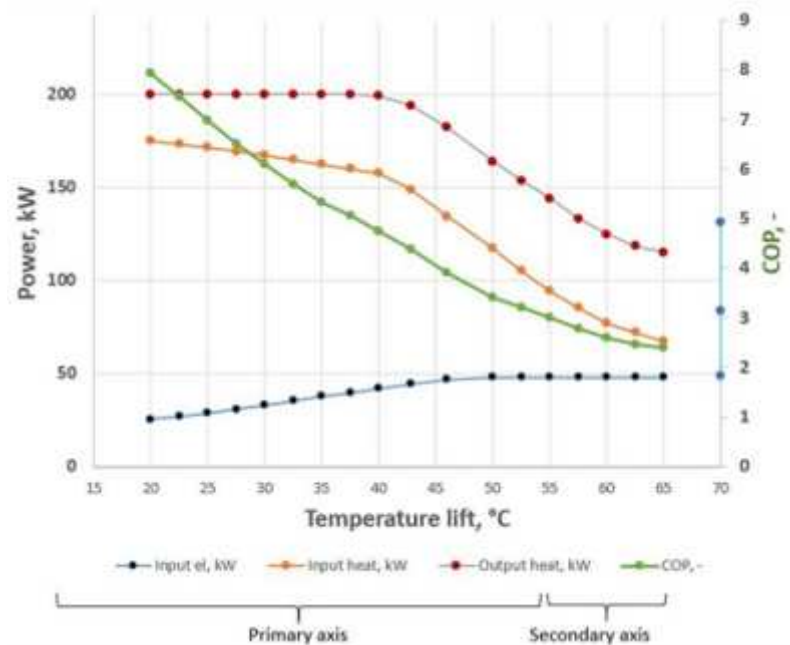


Figure 62: Heat Pump performance [56]

Electric energy expense and useful thermal energy gained in a year are found by multiplying the power values found above by the functioning hours of the recovery system, depending on the specific device considered. Moreover, in order to reach the thermal power calculated more than one heat pump has to be installed. That number is

found by dividing the electric power needed by the electric power that can be absorbed by a single device.

Since both cases are characterized by a small amount of recoverable thermal energy, the useful power produced is not enough to fulfill the total thermal need of the plant at 80°. Therefore, an integration in boilers is needed, to raise up the temperature of the primary fluid exiting the heat exchanger to 90°C.

Results of the simulation at 90°C for the two cases of recovery from vacuum pump and compressor and the one from dryers are reported in Table 41.

Table 41: 90°C simulation results

	recovery from vacuum pump and compressor	recovery from dryers	U.M.
$T_{out, evap}$	50	55	°C
n°of HP	4	2	
COP	5,1	5,3	
$P_{th, recovery}$	495	279	kW
$En_{th, user}$	3.244	2.749	MWh/y
$En_{el, ebsorbed}$	632	516	MWh/y
$En_{th, boiler}$	11508,83187	12.090	MWh/y

2. CASE II: $T_{delivery} = 160^{\circ} C$

This second case is based on the proposal of exploiting the waste thermal flows identified before to reach a final temperature of 160°C. In fact, the chosen heat pump device is designed to work also with a high temperature difference. As expected there are some limitations due to the fact that the higher the temperature lift the lower the COP. Thus, below minimum values of COP the system is no more efficient.

In the case we are considering, the too high temperature lift does not allow thermal recovery in a single stage. Therefore, the two-stage scheme shown below is adopted.

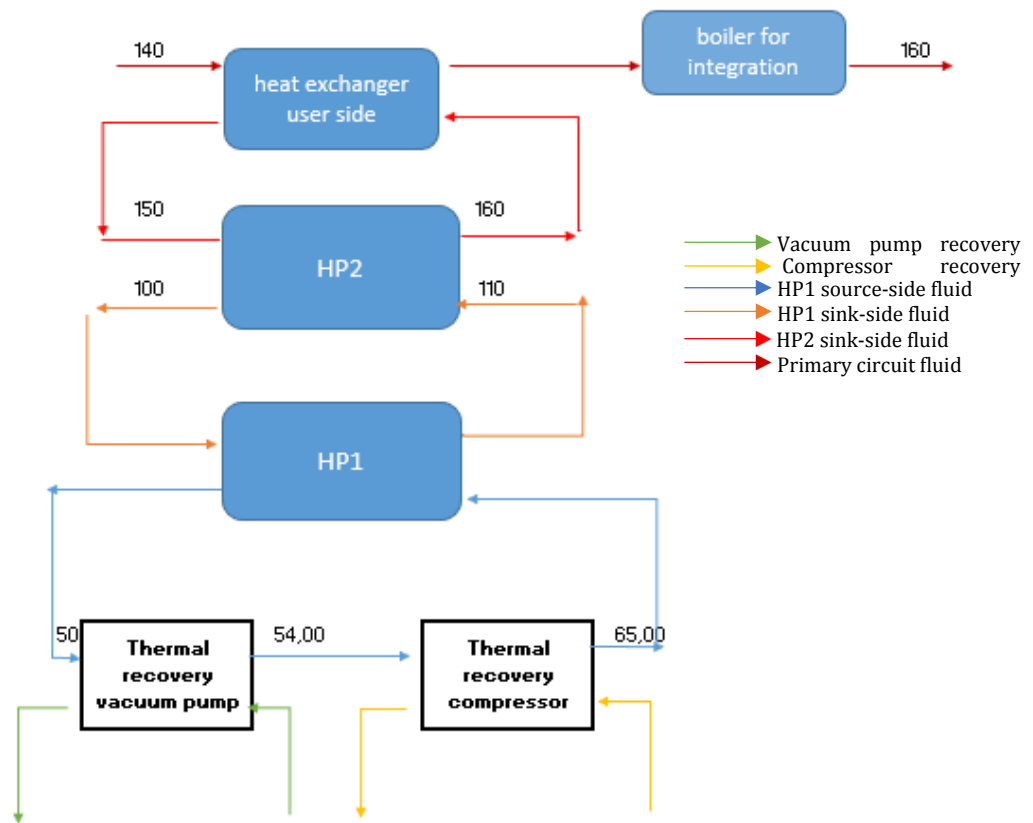


Figure 63: two stage Heat Pump configuration

A series configuration has been simulated, introducing one more fluid with respect to the simulation at 90°C. The temperature of this additional fluid is enhanced in the evaporator of HP1 and then taken back to its initial value in the condenser of HP2.

In this case there are more fixed parameters than in case 1.

The assumptions for the first heat pump (HP1) are:

- $T_{out, evap}=50$ °C for the case of recovery from vacuum pump and compressor;
- $T_{out, evap}=55$ °C for the case of recovery from dryers;
- $\Delta T_{source}=15$ °C;
- $T_{out, cond}=110$ °C;
- $T_{in, cond}= 100$ °C.

Instead, for the second heat pump (HP2) we supposed:

- $T_{out, evap}=160$ °C;
- $T_{in, evap}= 150$ °C.

Flowrate values for the various fluids can be calculated as explained before. Regarding the flowrate on the primary circuit, thermal needs are at 160 °C. Thus, once the energy required from the plant at this temperature level is evaluated and so is the difference between the delivery and the return, it is possible to find the flowrate too.

Results of the simulations are shown in Table 42.

Table 42: 160°C simulation results

	recovery from vacuum pump and compressor	recovery from dryers	U.M.
N° of HP1	8	13	
N° of HP2	4	7	
COP ₁	2,6	3,0	
COP ₂	2,6	2,6	
COP _{tot}	1,8	1,7	
P _{th, recovery}	495	279	kW
En _{th, user}	6.098	5.483	MWh/y
En _{el, ebsorbed}	5.580	3.250	MWh/y
En _{th, boiler}	88.955	85.586	MWh/y

As expected, the total COP of this series configuration has a very low value.

Economics

The CAPEX associated with the installation of heat pumps are evaluated considering a price per unit of 90 k€ for a single heat pump, referring to internal Engie offer. Additional costs are included in the Balance of Plant cost, assumed to be 20% of HP CAPEX.

For the considered technology, low maintenance costs are needed. Thus, it has been assumed that OPEX account for 5% of the heat pump CAPEX per year.

As for savings that can be obtained in the four described cases, the main benefit is that thermal energy is produced from a low temperature waste stream, and when a high COP is reached a small amount of electric energy is absorbed.

Table 43: costs and savings for Shifting Thermal to Electricity Technologies.

		Useful effect		CAPEX	OPEX	Saving EE		Saving NG		Saving CO ₂		TEE	
		MW _{el} /y	MWh _{th} /y	k€	k€/y	MWh/y	k€/y	kSmc/y	k€/y	ton/y	k€/y	TEE/y	k€/y
from vacuum pump and compressor	Heat Pump 90°C	-	3.244	361	15	-631	-79	375	119	530	16	192	48
	Heat Pump 160°C	-	6.098	2.152	89	-3.485	-436	706	222	248	29	-	-
From dryers	Heat Pump 90°C	-	2.749	169	7	-516	-65	319	100	455	13	166	42
	Heat Pump 160°C	-	5.483	1.070	45	-3.250	-406	635	200	186	27	-	-

MICROWAVE DRYING PROCESS

With regard to solutions aimed at shifting thermal consumption to electric, the Electro-Heat technologies described in Chapter IV are now dealt with. Among them, Microwave-based technology is considered the most suitable alternative to hot air-based pasta drying processes. In fact, compared to traditional drying processes, it is characterized by a much higher efficiency, with values around 70%.

Moreover, radiofrequency-based drying allows for a more uniform heat transfer in the product to be dried, as it is based on the volumetric generation of heat rather than conduction or convection methods.

Referring to hot air-based processes, the temperature must not exceed specific values, at which a barrier would be created on the surface product, preventing the leakage of the internal moisture. Therefore, the length of the drying phase depending essentially on dryer working temperature, a long stay of pasta in the dryer is necessary to obtain a high quality of the product.

This problem is overcome when microwave technology is used. As a consequence, the benefit of a shorter drying phase is obtained, with positive effect on the industrial plant production.

However, a preliminary estimation of the thermal and electric consumption as well as capex and opex would need more detailed information on the process, not available at the moment.

Table 44: Shifting Thermal towards Electric indexes

		PB	LCOC IRR=10%	€/MWh	€/tonCO ₂
from vacuum pump and compressor	Heat Pump 90°C	4,1	47	17	-312
	Heat Pump 160 °C	-	472	105	367
From dryers	Heat Pump 90°C	2,0	-68	10	-432
	Heat Pump 160 °C	-	342	90	279

4.3.6 Carbon Capture

In order to separate the CO₂ from the flue gas exiting the boilers now installed it has been chosen to use MEA solvent in a post-combustion capture process, with a capture rate of 90%.

Similar carbon dioxide capture systems are generally installed in power production plants with a capacity in the MW range, taken as a reference. For the evaluation of technical and

economic feasibility of this technology in the case under exam, a scale effect has been applied to account for its smaller size.

All the CO₂ post-combustion processes require a consistent amount of thermal and electric energy to work properly. In particular, to drive the separation process using MEA as solvent, a quantity of around 1,05 kg of steam per kg of CO₂ captured is necessary. Steam thermodynamic conditions are characterized by a pressure of 2 bar and a temperature of 140 °C. Considering to exploit the vapor enthalpy content from its starting value to the value of saturated water at 2 bar, the thermal energy required in the capture process becomes known once the vapor flowrate has been estimated.

Moreover, electric energy is needed within the system for the compression phase. Duty for CO₂ compression is ~ 0.33 MW/kg/s of CO₂ captured [57].

Economics

CAPEX and OPEX have been estimated on the basis of data from the latest DOE report on CO₂ capture from NGCC power plants [57]. Referring to a large-scale plant with 600 MW capacity, a unit price of 550 € per kW installed is considered: it includes the CO₂ absorption systems, consisting of an absorber, a stripper, an ancillary equipment and the CO₂ compression systems.

The CAPEX is scaled with the following formula, considering that the thermal capacity of the boilers is around 42 MW.

$$C_1 = C_0 \cdot \left(\frac{S_1}{S_0}\right)^n$$

Where:

- C_1 is the investment cost for the installation of the new capture system to the boilers;
- C_2 is the investment cost of the reference case, obtained by multiplying its capacity by the unit cost in €/kW;
- S_1 is the capacity of the boilers, expressed in primary energy to be compared to the capacity of the reference power plant;
- S_2 is the reference case power capacity, always in primary energy;
- n is the scaling factor equal to 0,85 [58].

Regarding OPEX, a cost of 17,8 €/MWh [57] has been considered.

Compared to the previously analysed scenarios, the installation of a carbon capture system does not involve benefits in terms of energy production, Natural Gas consumption reduction or white certificates achievement. Contrariwise, CCU leads to energy penalties, thus lowering the overall power production system of the industrial plant.

Despite the disadvantages mentioned and a very high investment cost, the main advantage of the carbon capture technology is its much higher emission reduction potential than it occurs in alternatives.

The same steps have been performed, considering that carbon capture is applied to the cases of NG-fed CHP (15 MW of electric power) and biogas-fed CHP (of 7,908 MWe).

Table 45: Carbon Capture results

	boiler	biogas-fed CHP	NG-fed CHP	
Primary energy	46,4	18,0	35,7	MW
P_el	-	7,9	15,0	MWe
P_th	41,8	7,2	8,0	MWth
CAPEX	18.759	7.259	14.425	k€
Equivalent hours	8.000	8.000	6.600	hours
OPEX	3.244	1.255	1.762	k€/y
thermal duty	19.587	17.275	26.048	MWh,th/y
Electric duty	2.743	2.419	3.648	MWhe/y
ton CO₂ captured	29.927	26.393	39.798	ton CO ₂ /y
Cost per ton of CO₂ captured	152	68	70	€/ton

Table 46: costs and savings for Carbon Capture shows the economic results in the case of carbon capture applied to installed boilers. The other two cases have been included in the calculation of benefits when combining the different solutions.

Table 46: costs and savings for Carbon Capture

	Useful effect		CAPEX	OPEX	Saving EE		Saving NG		Saving CO ₂		TEE	
	MW_el /y	MWh_th /y	k€	k€/y	MWh/y	k€/y	kSmc/y	k€/y	ton/y	k€/y	TEE/y	k€/y
CCU in boilers	-	-	18.759	3.244	-2.743	-343	-2-269	-715	29.927	643	-	-

Table 47: Carbon Capture indexes

	PB	LCOC IRR=10%	€/MWh	€/tonCO ₂
CCU	-	245	-	164

Chapter V: Optimal combinations and sensitivity analysis

5.1 Today optimal combination

5.1.1 Selection criteria

The optimal configuration has been selected taking into account the determining parameters previously described. The most interesting technical solutions are identified thanks to the parameter expressed in €/ton_{CO2}. Moreover, for each of the described options two key factors are considered: the amount of CO₂ emission reduction potential, given in ton/y, and the economic indicators showing whether a solution is economically convenient or not.

When an intervention is characterized by a negative value of €/ton_{CO2} this means that the energy produced has a lower cost than in traditional energy production processes. The lower its value the most convenient is the production of the energy vector through the considered solution instead of generating it in the “as is” case.

Table 48: cost per ton of CO₂ avoided

	ton/y	€/tonCO ₂
Heat Pump 90°C b	455	- 432
Heat Pump 90°C a	530	-312
PV	2.845	- 279
Solar thermal 90°C	2.959	- 207
Methane-fed CHP	488	-140
CSP	5.099	- 112
Solar Thermal 160°C	1.279	- 100
Biogas-fed CHP	31.872	- 43
Biomethane-fed CHP	28.284	-34
Synthetic methane-fed CHP	28.993	-17
Biogas-fed boiler	28.004	150
Carbon Capture	29.926	164
Heat Pump 160°C b	186	279
Biogas-fed SOFC	32.361	303
Heat Pump 160°C a	248	367

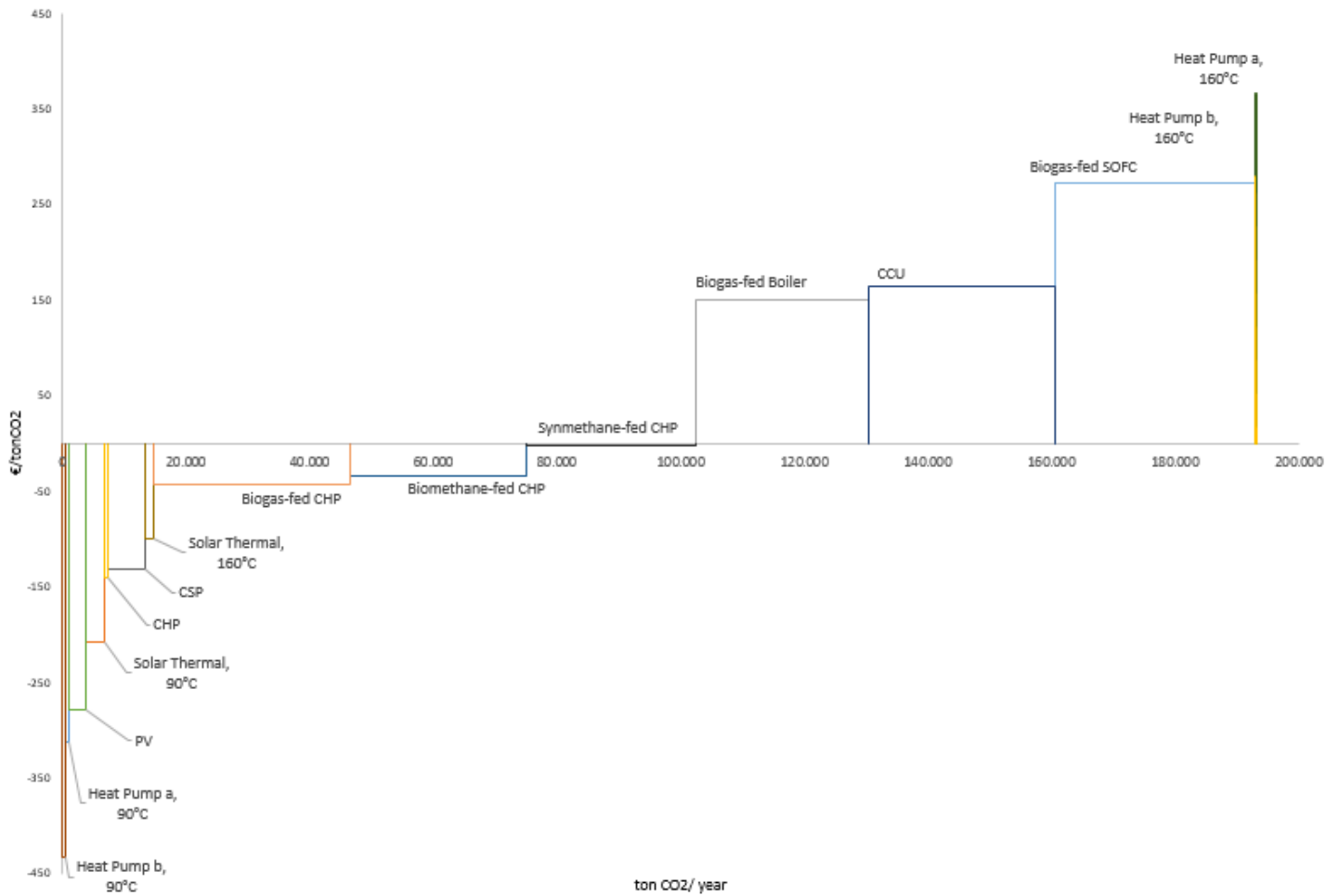


Figure 64: solutions ordered with ascending cost per ton of CO₂ avoided

The other criterion used for the choice of the solutions to be combined is the Pay-Back obtained if they were installed. Only interventions characterized by a PB shorter than 12 years have been considered.

The technical solutions are ordered in Table 49 in ascending order according to pay-back time.

Table 49: Technical solutions ordered with ascending PB

	ton/y	PB
Heat Pump 90°C b	455	2,0
CHP	488	2,1
Heat Pump 90°C a	530	4,1
Solar Thermal 90°C	2.959	4,6
PV	2.845	4,9
biomethane-fed CHP	28.284	5,4
biogas-fed CHP	31.872	5,9
CSP	6.225	7,8
synthetic methane-fed CHP	28.993	8,4
Solar Thermal 160°C	1.279	11,8
biogas-fed SOFC	32.361	58,5

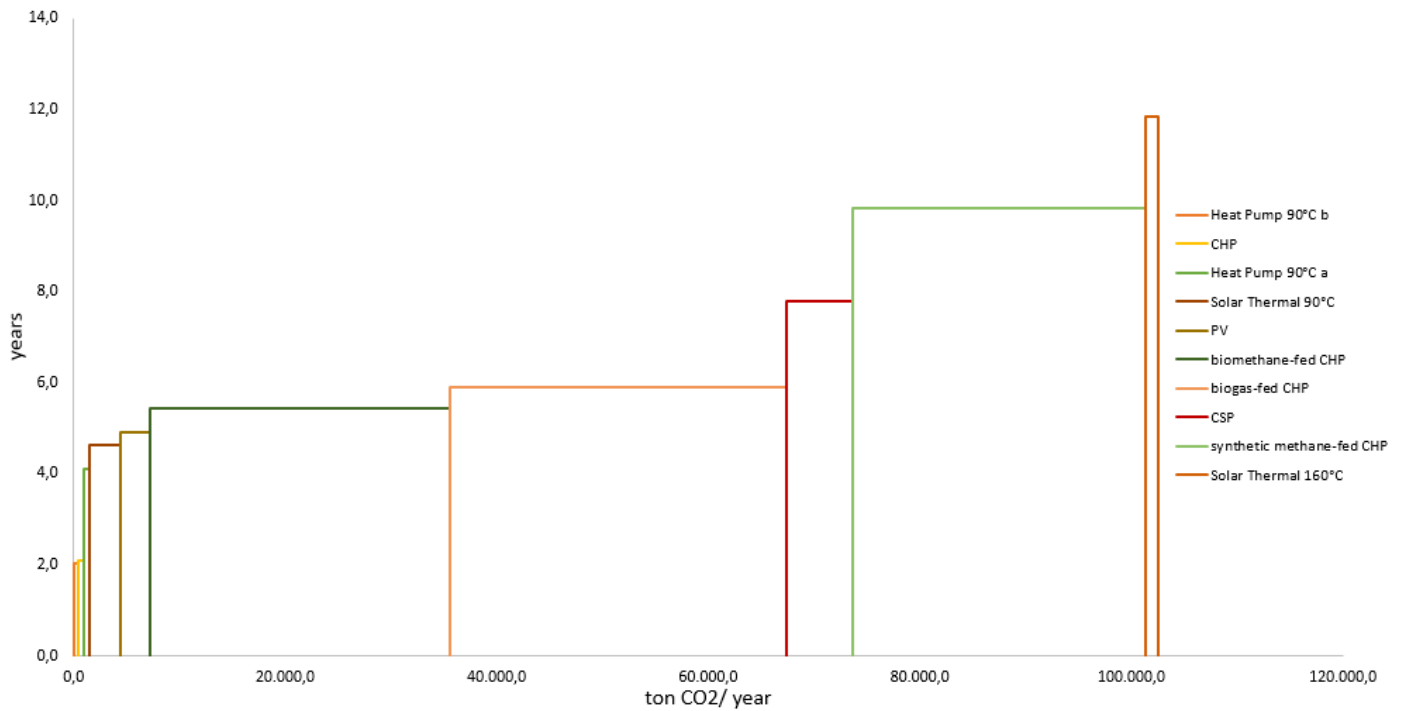


Figure 65: Technical solutions ordered with ascending PB

5.1.2 Survey of results

Cogeneration, the most efficient way to generate simultaneously electric and thermal power, turns out to be one of the best solutions in terms of payback, as it generates considerable economic savings. Nevertheless, as the traditional ICE CHP is supplied by NG and consumes a consistent amount of fuel to cover the industrial plant energy needs, its installation is associated to large CO₂ emissions. However, it must be underlined that electric energy from the grid is also based on combustion processes, bringing about CO₂ release, so in the end advantages from the CHP installation in terms of emissions are real. On the opposite, if we consider EU ETS counting method, CHP fuelled with Natural Gas would lead to an increase in CO₂ emissions with respect to the base case (electric energy from the grid and thermal energy from boilers) as a higher amount of fossil fuel is burnt, thus leading to an additional expense for the tons of CO₂ released in atmosphere. For this reason, this technical solution is excluded from the optimal configuration in the decarbonization pathway.

In terms of cost per ton of CO₂ avoided, the two most economically convenient solutions for thermal power production are the two heat pump systems (case a. describes the recovery from vacuum pump and compressor cooling circuits, while case b. derives from recovery from dryers). This result was quite predictable, as all interventions realizing an increase in efficiency or thermal recovery are generally characterized by a small investment cost with respect to new installations and allow for an optimal exploitation of primary energy. In the specific case of a heat pump providing hot water at a temperature level of 90°C, it produces heat starting from a waste energy stream. Moreover, the temperature lift from the considered sources to the primary circuit is small, which involves good COP values and low electric duty. Therefore, the two simulated heat pump

systems have been included in the combination, considering to exploit green electricity coming from RES on-site.

Research on the best solutions in terms of cost per ton of CO₂ avoided, in fact, also focuses on the PV installation. Since it is characterized by a PB time lower than 5, it results to be a feasible and economically convenient investment. The PV field would occupy the same field considered in simulations for CSP system. For this reason, the two solutions have been compared in order to select the optimal one both in economic terms and in terms of emissions reduction.

Even if CSP has a higher CO₂ emission avoiding potential with respect to the PV installation, it has a longer PB time and a lower cost per ton of CO₂ avoided. For this reason, the PV field has been chosen as a part of the optimal configuration.

Unlike CSP, excluded from the decarbonization scenario, solar thermal technology is included. It also exploits thermal power from RES but is characterized by a shorter PB compared to concentrated solar panels. This is due to the fact that, despite the higher thermal efficiency of CSP, solar thermal technology is less complex as far as installation is concerned, and therefore costs are much lower.

Between the two simulations carried out, the solution of producing hot water at 90°C results to be the optimal one, as generating superheated water at 160°C in traditional panels would lead to high thermal losses.

Referring to the various alternative for on-site produced biogas, the criteria used for the selection of the best option are the maximisation of emission reduction and acceptable values of economic indexes.

The economics of all the solutions analysed is strongly affected by the high cost of the waste streams making up the biomass from which the biogas is derived. This entails to a much higher cost of biogas compared to natural gas from the grid, determining operating expenses for some of the solutions higher than the economic saving. This is what happens in the biogas-fed boiler scenario, for which a time of return on investment cannot be calculated.

The high cost of biogas is partially compensated for by the high efficiency of biofuel-fed CHP, whether dealing with Internal combustion engine or with SOFC. In fact, as these combined systems allow for a simultaneous generation of electric and thermal power, they create savings associated to both energy vectors. However, since SOFC technology cost is still far more expensive than traditional CHP, the time for its investment cost to return is not acceptable.

A further selection is necessary in terms of choosing between biogas, biomethane or synthetic methane-fed ICE CHP. For the optimal solution, the economic aspects and maximisation of emission reduction have been taken into account. Since the solutions are characterized by similar amounts of CO₂ avoided, dealing with the same biomass starting quantity, the determining parameters are firstly the cost per ton of CO₂ avoided and secondly and PB time. The biogas-fed CHP being associated to a lower cost per ton reduced, it has been chosen to include this solution in the “best decarbonized scenario”.

In addition, the simulation of applying carbon capture to the CHP has been carried out, as this solution leads to a strong reduction in the plant emissions. However, as shown by the carbon capture LCOC index, to make the investment reasonable the price for CO₂ allowances should rise to around 200 €/ton_{CO2}. Therefore, considering the present framework, the scenario including CCU would bring more expenses than savings.

5.1.3 Best decarbonized-scenario

Considering the results for each of the solutions discussed above, an optimal combination has been put together, aimed at maximizing the emission reduction and the economic saving. The decarbonization pathway is made up of:

1. Solar Thermal installation, producing hot water at 90°C;
2. PV field;
3. Heat Pump recovery from dryers, producing hot water at 90°C;
4. Heat Pump recovery from vacuum pump and compressor, producing hot water at 90°C;
5. Biogas-fed CHP;
6. Carbon Capture;

Table 50: optimal decarbonization pathway results

	CAPEX [k€]	OPEX [k€/y]	saving [k€/y]	PB	Saving CO ₂ [ton/y]	Emission reduction
sol th	3.702	56	797	4,6	2.959	5,6%
sol th + PV	8.886	96	1.570	5,7	5.804	9,8%
sol th + PV + HP a	9.247	110	1.679	5,5	6.333	10,6%
sol th + PV + HP a + HP b	9.417	118	1.779	5.3	6.789	11,3%
sol th + PV + HP_a + HP_b + CHP biogas	22.317	9.910	1.938	11,5	38.661	58,1%
sol th + PV + HP_a + HP_b + CHP biogas+ CCU	29.577	11.163	- 174	-	65.054	90,0%

In Figure 66 the cumulative of capex is shown: x-coordinate identifies the total amount of CO₂ ton avoided with the optimal configuration. A red arrow indicates the “as is” case.

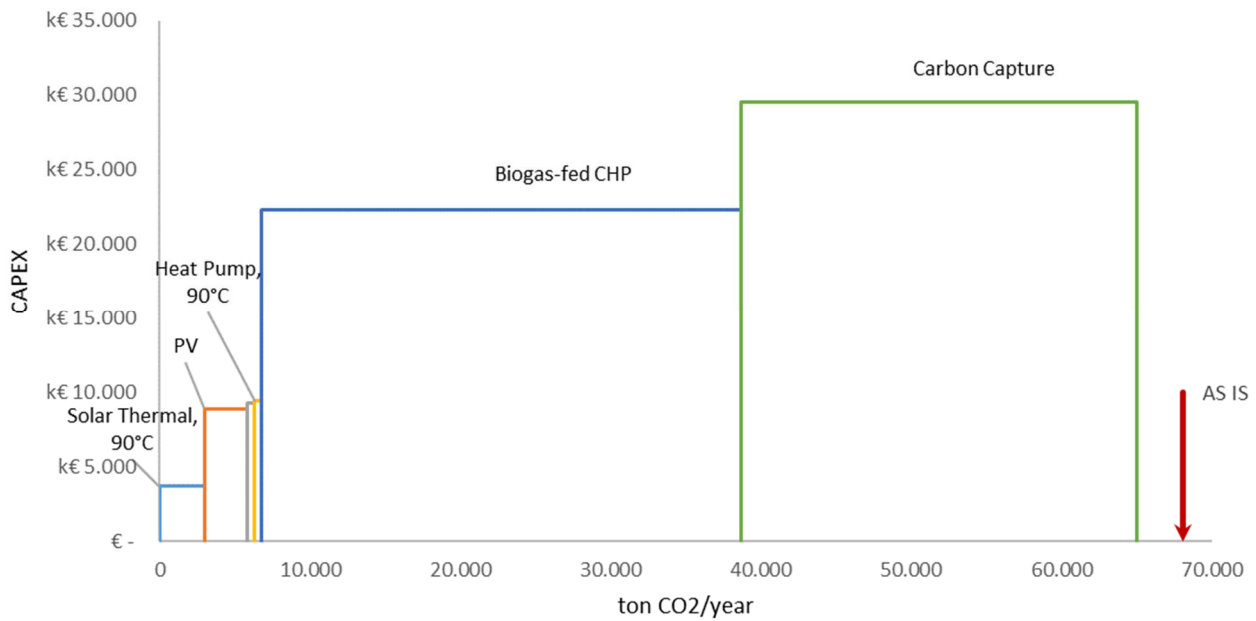


Figure 66: Cumulative of CAPEX for the optimal configuration

As it can be seen in the cumulative curve, the biogas-fed CHP and the Carbon capture are the two installations with the greatest impact on total CAPEX. At the same time, they largely contribute to emission reduction, leading the final combination to avoid emissions almost entirely, compared to the base case.

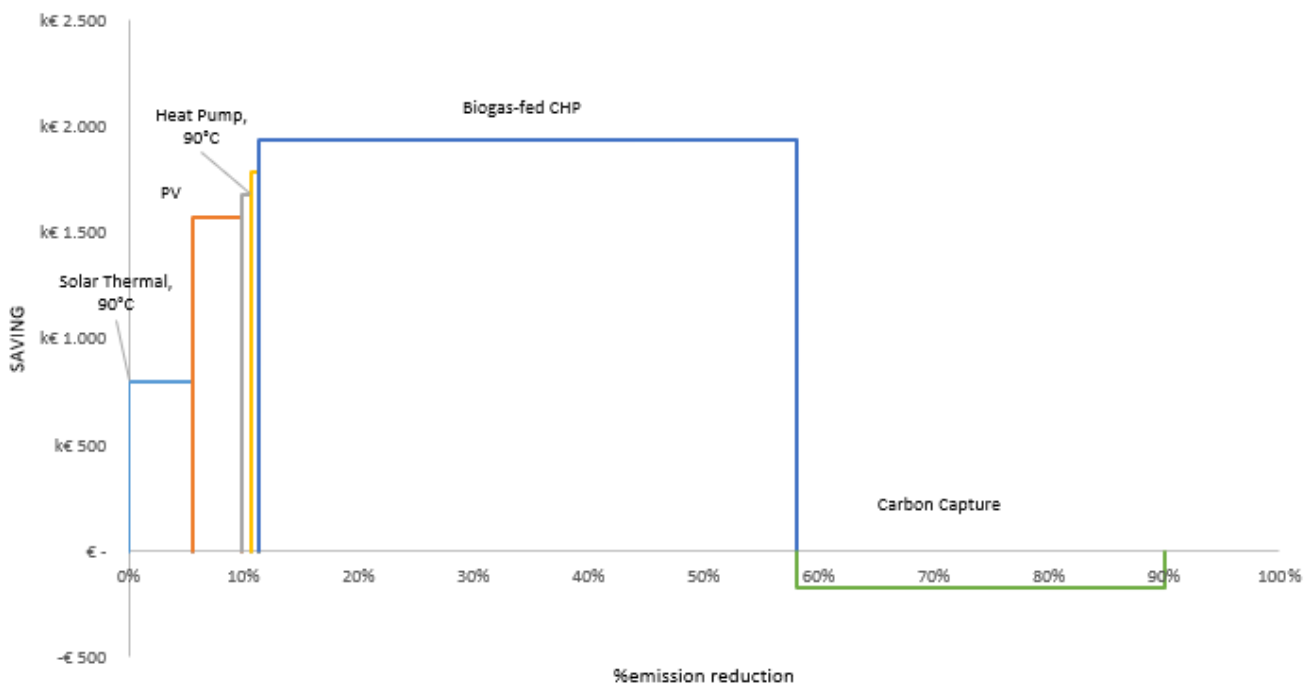


Figure 67: Saving and emission reduction potential of the best decarbonization pathway

Figure 67: Saving and emission reduction potential of the best decarbonization pathway displays economic savings for the optimal combination, making it clear that the very high cost of carbon capture forfeits the benefits previously gained.

In conclusion, referring to the studied case, the capture of CO₂ would help reducing the emissions almost entirely but at the same time would make the investment unacceptable.

Thus, the optimal combination for the decarbonization pathway is stopped at the stage of biogas-fed CHP, without going beyond to carbon capture, which has proved to be uneconomical.

Table 51: Best decarbonized scenario

Decarbonized scenario	
CAPEX	22 M€
Saving	2 M€
PB	11,5
Emission reduction	58 %

5.1.4 Alternative combinations

As for the second decarbonization scenario, biomethane-fed CHP has been included in the technical solutions to be combined.

In this case the decarbonization pathway is made up of:

1. Solar Thermal installation, producing hot water at 90°C;
2. PV field;
3. Heat Pump recovery from dryers, producing hot water at 90°C;
4. Heat Pump recovery from vacuum pump and compressor, producing hot water at 90°C;
5. NG-fed CHP;
6. Biomethane on-site production for CHP fuelling;
7. Carbon Capture;

Table 52: second decarbonization pathway results

	CAPEX [k€]	OPEX [k€/y]	saving [k€/y]	PB	Saving CO ₂ [ton/y]	Emission reduction
sol th	3.702	56	797	4,6	2.959	6%
sol th + PV	8.886	96	1.850	4,8	5.804	9,8%
sol th + PV + HP _a	9.247	110	1.939	4,8	6.333	10,6%
sol th + PV + HP _a + HP _b	9.417	118	2.023	4,7	6.789	11,3%
sol th + PV + HP _a + HP _b + NG CHP	23.153	12.519	8.178	2,8	4.805	0,7%
sol th + PV + HP _a + HP _b + biomethane in CHP + CCU	29.653	16.950	4.344	6,8	32.601	47,9%
sol th + PV + HP _a + HP _b + CHP + biomethane in CHP+ CCU	57.815	32.317	- 10.319	-	65.310	96,0%

As shown in Table 52, adding NG-based CHP to the cumulated decarbonization scenario, a decrease in the previously gained emission reduction occurs. This outcome is represented in the Figure 68 by a recession in the line of tons of CO₂ avoided.

If then the biogas upgrading system is integrated in the combination, despite an increase in the capex, and a subsequent decrease in savings, a much more consistent reduction of emissions can be reached.

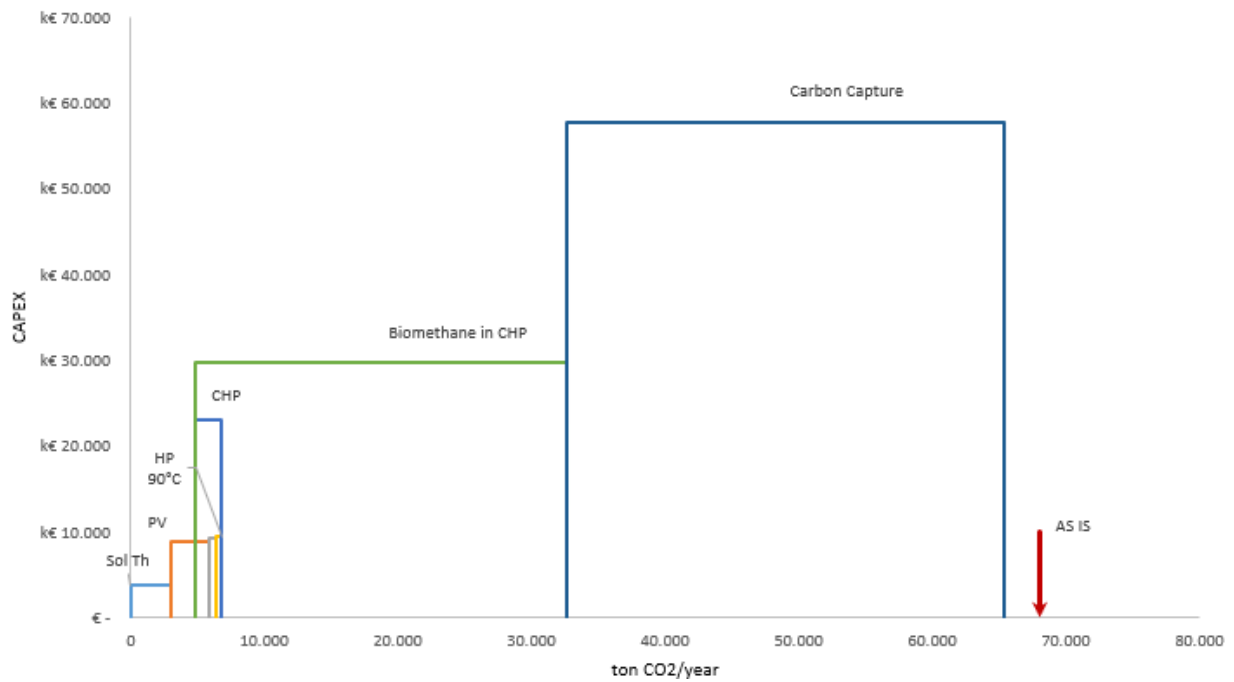


Figure 68: second decarbonization pathway

As for optimal decarbonized configuration, carbon capture is added to the combination to try to entirely avoid the emissions of the industrial plant and evaluate effects obtained from an economic point of view. It results that savings from all the solutions previously combined are nulled, because the economic benefits do not sufficiently account for the growth of yearly expenses.

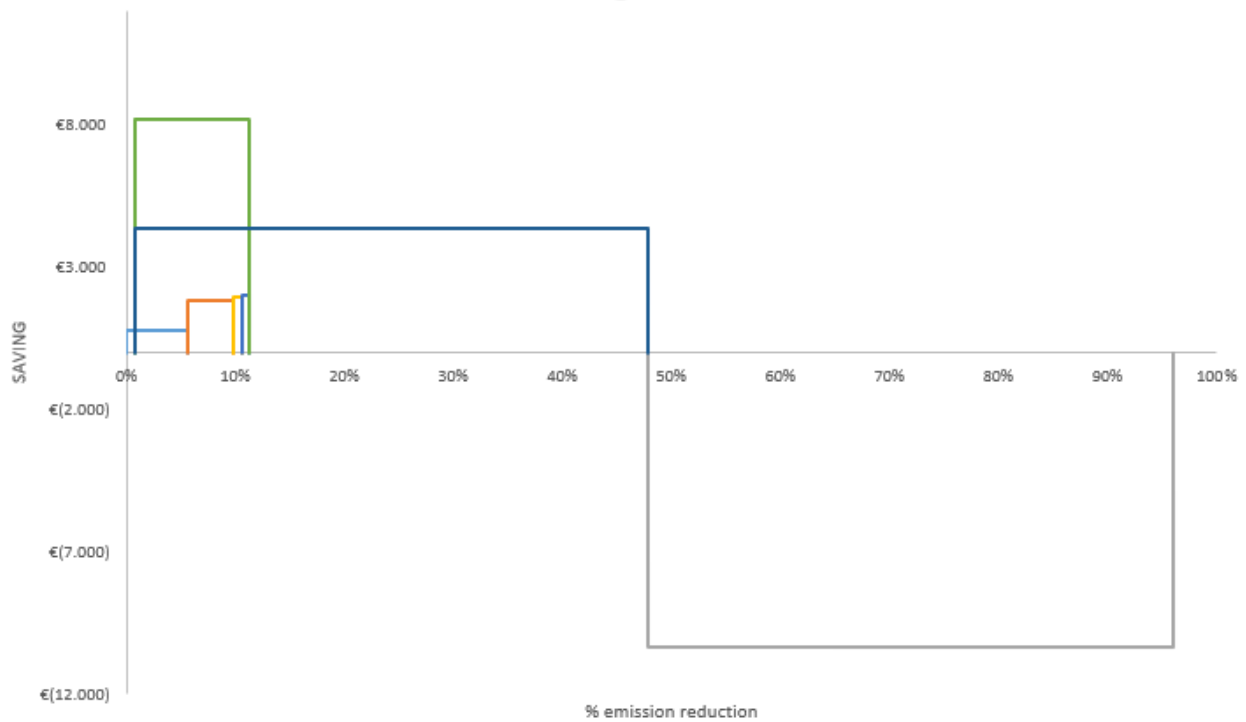


Figure 69: Saving and emission reduction potential of the best decarbonization pathway

Thus, according to the second configuration, what has been evaluated for the optimal scenario about carbon capture is still valid.

The results obtained in the configuration built, excluding carbon capture, are in Table 53.

Table 53: second decarbonized scenario

Second Decarbonized scenario	
CAPEX	30 M€
Saving	4,3 M€
PB	6,8
Emission reduction	48 %

Similar results are obtained in the scenario where biomethane and synthetic methane are produced on-site and are exploited in the NG-fed CHP. As expected, a longer payback time is necessary, due to the higher investment cost and operational expenses (Table 54).

Table 54: Third decarbonized scenario

Third Decarbonized scenario	
CAPEX	38 M€
Saving	3,2 M€
PB	11,8
Emission reduction	48 %

5.2 Future scenarios and sensitivity analysis

Future scenarios have been analysed in order to evaluate the economic feasibility of the decarbonized pathway even in a different framework of energy vectors and CO₂ prices. Thus, several simulations have been performed, on the basis of different prices trends:

1. Prices of electricity from the grid, NG and CO₂ increase of 20%;
2. Prices of electricity from the grid, NG and CO₂ decrease of 20%;
3. Only price of CO₂ changes according Engie forecast trend;

5.2.1 Uniform increase in prices

The scenario in which energy vectors and CO₂ prices increase uniformly is simulated, considering that they rise up of 20%.

Table 55: +20% scenario

	scenario	PB	Saving k€
optimal configuration	to date	11,5	1.938
	+20%	3,8	5.851
second configuration	to date	6,8	4.344
	+20%	4,4	6.791
third configuration	to date	11,8	3.219
	+20%	7,0	5.442

In Table 55: +20% scenario the “+20%” scenario is compared to the scenario with today prices. As expected, economic benefits associated to the decarbonized scenarios strongly increase. This positive result is due to the fact that the scenarios discussed above not only allow for a generation on-site of energy vectors at a lower price with respect to the grid, but also produce energy with a much lower carbon footprint. Thus, when considering an increase in the price of energy from the grid as well as in the price of CO₂, the economic convenience of decarbonized scenarios becomes evident. Consequently, the PB of the various combination is reduced.

5.2.2 Uniform decrease in prices

As opposed to the previous case, here a uniform decrease in prices is simulated. Results are shown in Table 56: -20% scenario.

Table 56: -20% scenario

	saving	PB	Saving k€
optimal configuration	to date	11,5	1.938
	-20%	455,6	49
second configuration	to date	6,8	4.344
	-20%	15,6	1.897
third configuration	to date	11,8	3.219
	-20%	38,2	997

5.2.3 CO₂ price increase

A final simulation is performed, considering the actual prices for electric energy and NG and a varying cost per ton of CO₂.

Based on Engie forecast until 2022, the CO₂ price that has been taken into account is 24,38 €/ton_{CO2}.



Figure 70: CO₂ trend according to ENGIE forecast

Extending the trend proposed by Engie's forecast, in 2040 a price for CO₂ of 67,39 €/ton_{CO2} is obtained.

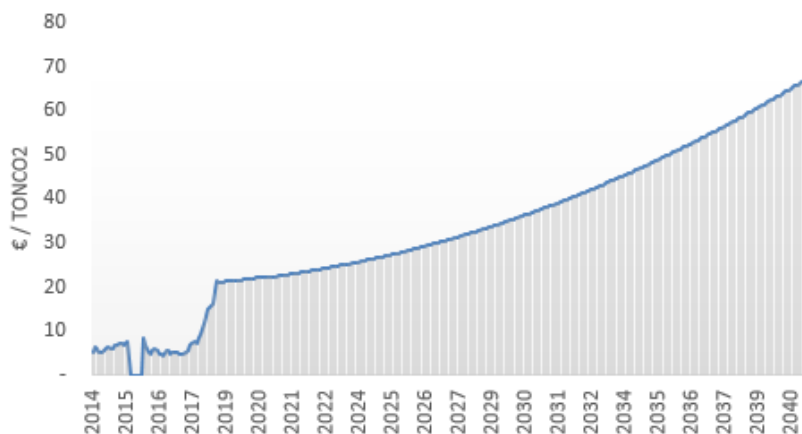


Figure 71: extended EU ETS trend from ENGIE forecast

The final results of the sensitivity analysis are reported below.

Table 57: 2022 and 2040 scenario according to Engie's forecast for CO₂

	scenario	PB	Saving k€
optimal configuration	to date	11,5	1.938
	2022	11,3	1.983
	2040	8,4	2.655
second configuration	to date	6,8	4.344
	2022	6,8	4.338
	2040	7,0	4.242
third configuration	to date	11,8	3.219
	2022	11,9	3.210
	2040	12,3	3.087

As shown by data in Table 57: 2022 and 2040 scenario according to Engie's forecast for CO₂, an increase in carbon dioxide price in EU ETS market would further the scenario including biogas-fed CHP, identified as the optimal one. In fact, compared to the other possible options, best decarbonized configuration allows to reach a much stronger impact on emission reduction. Thus, the important savings associated to the amount of CO₂ avoided and with an increasing CO₂ cost, make this combination more and more convenient also from an economic point of view.

On the contrary the second and third configurations would be considerably affected by the higher CO₂ price. This is due to the fact that the NG-fed cogeneration included in those two combinations brings about greater fossil fuel consumption with respect to the base case, which causes an additional cost for emission increase.

Chapter VI: Conclusions

In the present study a technological scouting has been performed and an optimal decarbonization scenario for a real industrial plant has been finally identified, with the best technical solutions both in economic terms and in terms of maximization of emission reduction.

Among the three possible combinations suggested, the optimal one has been selected following the criterium of the largest emission reduction in the decarbonized scenario compared to the base case, in which thermal energy comes from boilers and electric energy comes from the grid.

Hence, the best decarbonized scenario includes:

1. Solar thermal technology providing hot water at 90°C;
2. PV field;
3. Heat Pumps for thermal recovery of two different plant waste streams, supplying heat to the user at 90°C;
4. Biogas-fed cogeneration system;

Considering current prices for electricity, Natural Gas and CO₂ allowances, economic analysis for the decarbonization pathway has led to an overall CAPEX of around 22 M€ to get an emission reduction of 58%.

In the actual economic framework, annual savings for about 2 M€ would be gained, thus reaching a PayBack time of 11,5 years for the total investment.

Then, a sensitivity analysis on the energy vectors and CO₂ prices has showed that, even in a future scenario with a rising CO₂ price, as it is expected to be according to Engie's forecasts, the optimal combination mentioned above is likely to be the best one. Moreover, the economic convenience of the decarbonized scenario grows rapidly, being responsible for a reduction of PB to 8,4 years, considering an estimated price of CO₂ in 2040 with an economic valorization per ton tripled compared to today.

The results obtained therefore suggest that not only is a decarbonization pathway possible, but it is also increasingly convenient from an economic point of view when a rise of prices of CO₂ allowances is expected.

It might be objected that an estimated PB longer than 10 years requires companies to take too great a risk in making the investment. However, a growing commitment for environmental safeguards from industrial parties would have a positive impact on customers, because the sensibility towards environmental issues is becoming more and more widespread. In other words, economic considerations should also take into account important benefits associated to the brand image.

Moreover, the industrial sector being largely responsible for most CO₂ emissions, firm actions towards carbon neutrality and the reduction of plant emissions would strongly contribute to take a decisive step forward in fighting climate change.

Bibliography

- [1] NOAA National Centers for Environmental Information, "State of the Climate: Global Climate Report for Annual 2017," 2017. [Online]. Available: <https://www.ncdc.noaa.gov/sotc/global/201713>.
- [2] NOAA National Centers for Environmental, "Climate at a Glance: Global Time Series." [Online]. Available: <https://www.ncdc.noaa.gov/cag/>.
- [3] A. M. Society, "STATE OF THE CLIMATE IN 2017," vol. 99, no. 8, 2018.
- [4] J. Huang, B. Mendoza, J. S. Daniel, C. J. Nielsen, L. Rotstayn, and O. Wild, "Anthropogenic and Natural Radiative Forcing."
- [5] NOAA, "trends CO2." [Online]. Available: <http://www.esrl.noaa.gov/gmd/ccgg/trends>.
- [6] NOAA, "trends CH4." [Online]. Available: http://www.esrl.noaa.gov/gmd/ccgg/trends_ch4/.
- [7] C. Change, *CLIMATE CHANGE 2014 Mitigation of Climate Change Summary for Policymakers and Technical Summary Mitigation of Climate Change*. 2014.
- [8] IEA, *Energy Technology perspective*. 2010.
- [9] "UNITED NATIONS FRAMEWORK CONVENTION," vol. 62220, 1992.
- [10] "KYOTO PROTOCOL TO THE UNITED NATIONS FRAMEWORK KYOTO PROTOCOL TO THE UNITED NATIONS FRAMEWORK," 1998.
- [11] F. C. P. L. Rev, "ADOPTION OF THE PARIS AGREEMENT Proposal by the President," vol. 21932, no. December, pp. 1–32, 2015.
- [12] T. H. E. E. Parliament, T. H. E. Council, O. F. The, and E. Union, "European Parliament (2003) Art. 1, Directive EC/87/2003," pp. 32–46, 2003.
- [13] C. From, T. H. E. Commission, T. O. The, T. H. E. Council, T. H. E. E. Economic, T. H. E. Committee, and O. F. The, "A policy framework for climate and energy in the period from 2020 to 2030," pp. 1–18, 2014.
- [14] O. F. T. H. E. Council, *DIRECTIVE (EU) 2018/410 OF THE EUROPEAN PARLIAMENT AND OF THE COUNCIL*. 2018.
- [15] T. H. E. E. Parliament, T. H. E. Council, O. F. The, and E. Union, *DIRECTIVE 2006/32/EC on energy end-use efficiency*. 2006, pp. 64–85.
- [16] Gazzetta Ufficiale della Repubblica Italiana, *D.M. correttivo 10 maggio 2018*. 2017, pp. 48–62.
- [17] GSE, "Rapporto annuale sulle aste di quote europee di emissione 2017," 2017.
- [18] GSE, "Rapporto aste di quote europee di emissione 2018, III trimestre," 2018.
- [19] European Parliament, "Directive on the promotion of the use of energy from renewable sources," pp. 16–62, 2009.
- [20] GSE, "Monitoraggio FER nazionale, obiettivo complessivo." [Online]. Available: <https://www.gse.it/dati-e-scenari/monitoraggio-fer/monitoraggio-nazionale/obiettivo-complessivo>. [Accessed: 12-Sep-2018].
- [21] "RE 100: The world's most influential companies, committed to 100% renewable power." [Online]. Available: <http://there100.org/>. [Accessed: 10-Jul-2018].
- [22] L. Ruini, M. Marino, S. Pignatelli, F. Laio, and L. Ridol, "Water footprint of a large-sized food company : The case of Barilla pasta production \$," vol. 2, pp. 7–24, 2013.
- [23] Europeran Commission, *Integrated Pollution Prevention and Controlin: Food , Drink and Milk*

Industries. 2006.

- [24] ISPRA, “Fattori di emissione per la produzione ed il consumo di energia elettrica in Italia,” 2017. [Online]. Available: <http://www.sinanet.isprambiente.it/it/sia-ispra/serie-storiche-emissioni/fattori-di-emissione-per-la-produzione-ed-il-consumo-di-energia-elettrica-in-italia/view>. [Accessed: 14-Oct-2018].
- [25] IEA, “Heating without global warming,” 2014.
- [26] IEA, “World: Electricity and heat for 2016,” 2016. [Online]. Available: <https://www.iea.org/statistics/?country=WORLD&year=2016&category=Key indicators&indicator=HeatGenByFuel&mode=chart&categoryBrowse=false&dataTable=ELECTRICITYANDHEAT&showDataTable=true>.
- [27] Euroheat & Power, “The European Heat Market,” 2006.
- [28] TVP Solar, “PRODUCT DATASHEET : MT-Power,” 2015.
- [29] IEA Renewable Energy Division, “Technology Roadmap Concentrating Solar Power,” 2012.
- [30] GSE, “determinazione del mix energetico nazionale 2017,” 2017. [Online]. Available: <https://www.gse.it/servizi-per-te/fuel-mix-determinazione-del-mix-energetico-per-gli-anni-2016-2017>. [Accessed: 14-Oct-2018].
- [31] IEA, “Technology Roadmap Solar PV Energy,” 2014.
- [32] Eurostat, “European Statistics, 2017.” [Online]. Available: <http://ec.europa.eu/eurostat> (accessed. [Accessed: 01-Jul-2017]).
- [33] N. Scarlat, J. Dallemand, and F. Fahl, “Biogas : Developments and perspectives in Europe,” *Renew. Energy*, vol. 129, pp. 457–472, 2018.
- [34] General Electric, “Data sheet JMS 612 GS-N.L.” pp. 1–12, 2017.
- [35] Convion, “Datasheet: CONVION C60,” 2018.
- [36] European Biogas Association, “STATISTICAL REPORT 2017,” 2017.
- [37] A. Petersson, J. B. Holm-nielsen, and D. Baxter, “Biogas upgrading technologies – developments and innovations,” 2009.
- [38] Storengy, “METHYCENTRE: Unité de Power - to - Gas (hydrogène et méthane de synthèse) couplée à une unité de méthanisation.”
- [39] U.S. Department of Energy, “Heat Pumps for Steam and Fuel Saving,” 2003.
- [40] S. S. Bertsch, “High temperature heat pumps : Market overview , state of the art , research status , refrigerants , and application potentials de,” vol. 152, 2018.
- [41] Viking Heat Engines, “HeatBooster HBS 4.”
- [42] C. M. Galanakis, *Sustainable Food Systems from Agriculture to Industry*. 2018.
- [43] Zero Emission Platform, “Capture, transport and safe storage of CO2.” [Online]. Available: <http://www.zeroemissionsplatform.eu/ccs-technology/capture.html>. [Accessed: 28-Oct-2018].
- [44] D. Y. C. Leung, G. Caramanna, and M. M. Maroto-valer, “An overview of current status of carbon dioxide capture and storage technologies,” *Renew. Sustain. Energy Rev.*, vol. 39, pp. 426–443, 2014.
- [45] O. X. Y. Combustion and W. Co, “CO 2 CAPTURE TECHNOLOGIES OXY COMBUSTION WITH CO 2 CAPTURE,” no. January, 2012.
- [46] “CO2 absorption performance of aqueous alkanolamines in packed columns,” vol. 47, no. 2002,

p. 2018, 2018.

- [47] Zero.co2, "Post-combustion carbon capture." [Online]. Available: <http://www.zero.co2.no/introduction/what-is-ccs>. [Accessed: 28-Oct-2018].
- [48] T. Iea, G. Gas, I. E. A. Ghg, I. E. A. Ghg, M. Macdonald, C. Cycle, G. Turbine, C. U. Supercritical, P. Fuel, I. Gasification, C. Cycle, C. Uscpf, I. E. A. Ghg, T. Igcc, I. E. A. Ghg, I. E. A. Ghg, I. E. A. Ghg, M. Macdonald, G. J. Lhv, I. E. A. Ghg, U. S. Dollar, U. S. Dollars, and I. E. A. Ghg, "CO 2 CAPTURE AS A FACTOR IN POWER STATION INVESTMENT DECISIONS Background to the Study," vol. 19, 2005.
- [49] Minambiente, "tabella coefficienti standard nazionali." 2017.
- [50] Gazzetta Ufficiale della Repubblica Italiana, "tabella di conversione tep," vol. 3, p. 2014, 2014.
- [51] Canadian Solar, "PRODUCT DATASHEET: Cs6k- 270 | 275 | 280 p," 2001.
- [52] N. E. L. Comune, D. I. Castiglione, and D. E. L. Lago, "Studio di fattibilità di un impianto di digestione anaerobica nel comune di castiglione del lago."
- [53] General Eletric, "Datasheet JMS 620 GS-N.L."
- [54] F. Bauer, C. Hulteberg, T. Persson, and D. Tamm, "Biogas upgrading – Review of commercial," 2013.
- [55] L. D. Christian Wix and Ib Dybkjær, Haldor Topsøe A/S and H. T. and Niels R. Udengaard, Haldor Topsoe Inc., "Coal to SNG – The Methanation Process," 2007.
- [56] Viking Heat Engines, "HeatBooster."
- [57] NETL, "Cost and Performance Baseline for Fossil Energy Plants Volume 1a: Bituminous Coal (PC) and Natural Gas to Electricity," vol. 1, 2015.
- [58] ENEA, "Tecnologie di cattura e sequestrazione della CO2," 2011.